

# CHAPTER 4

---

## Ozone Variability and Trends

**Lead Authors:**

R.D. Bojkov  
R.D. Hudson

**Coauthors:**

L. Bishop  
V. Fioletov  
J.M. Russell III  
R.S. Stolarski  
O. Uchino  
C.S. Zerefos

**Contributors:**

R. Atkinson  
D.S. Balis  
P.K. Bhartia  
H. Claude  
L. Flynn  
R. Guicherit  
F. Hasebe  
G. Labow  
J.A. Logan  
R.D. McPeters  
A.J. Miller  
R. Müller  
R. Piacenti  
W.J. Randel  
H. Smit  
B.H. Subbaraya  
K. Tourpali  
P. von der Gathen  
A. Zand

Members of the SPARC/IOC Profile Trends Panel

# CHAPTER 4

## OZONE VARIABILITY AND TRENDS

### Contents

SCIENTIFIC SUMMARY .....	4.1
4.1 INTRODUCTION .....	4.5
4.2 DATA SOURCES .....	4.5
4.2.1 Total Ozone .....	4.5
4.2.1.1 Ground-Based Total Ozone Measurements .....	4.5
4.2.1.2 Satellite Total Ozone Measurements .....	4.7
Total Ozone Mapping Spectrometer (TOMS) .....	4.7
Solar Backscatter Ultraviolet (SBUV), SBUV/2 BUV .....	4.7
TOVS .....	4.8
4.2.1.3 Comparison between Ground-Based and Satellite Ozone Data .....	4.8
4.2.2 Vertical Ozone Distribution .....	4.9
4.2.2.1 Data Availability .....	4.9
4.2.2.2 Data Limitations for Use in Trend Determinations .....	4.10
4.2.2.3 Intercomparisons .....	4.11
SAGE Versus Ozonesondes .....	4.11
SAGE Versus Lidar .....	4.12
SAGE Versus Umkehr .....	4.12
SAGE Versus SBUV .....	4.13
SAGE II Versus HALOE .....	4.13
SAGE II Versus MLS and HALOE .....	4.14
SAGE II Versus Ozonesonde .....	4.14
4.2.2.4 Summary .....	4.15
4.3 OZONE NATURAL VARIABILITY .....	4.16
4.3.1 Short-Term Variations .....	4.16
4.3.2 Longer Term Variations .....	4.17
4.3.2.1 The Annual Cycle .....	4.17
4.3.2.2 The QBO .....	4.17
4.3.2.3 The ENSO .....	4.18
4.3.2.4 The Solar Activity Cycle .....	4.18
4.3.2.5 Transient Large Volcanic Effects .....	4.19
4.4 STATISTICAL CALCULATIONS OF TRENDS .....	4.19
4.4.1 Introduction .....	4.19
4.4.2 Total Ozone Trend Statistical Model .....	4.21
4.4.3 SPARC/IOC Statistical Model Intercomparison .....	4.22

4.5	LONG-TERM CHANGES IN TOTAL OZONE .....	4.22
4.5.1	Global, Latitudinal, and Longitudinal Trends .....	4.22
4.5.2	Changes in the Northern Hemisphere: Middle and Polar Latitudes .....	4.31
4.5.2.1	Trends and Variability .....	4.34
4.5.2.2	Estimating the Ozone Mass Deficiency .....	4.36
4.5.2.3	Comparisons with O <sub>3</sub> MD in the Southern Hemisphere .....	4.37
4.5.3	Changes in Antarctica .....	4.38
4.6	LONG-TERM CHANGES IN VERTICAL PROFILES .....	4.40
4.6.1	Upper Stratosphere .....	4.40
4.6.2	Lower Stratosphere .....	4.43
4.6.3	Combined Trends .....	4.46
4.6.4	Consistency between Total Ozone and Vertical Profile Trends .....	4.47
	REFERENCES .....	4.48

## SCIENTIFIC SUMMARY

### Non-Polar Ozone

#### TOTAL COLUMN OZONE

- The 1994 Assessment noted large negative trends in midlatitude total ozone in the 1980s, with an additional marked decrease in Northern Hemisphere midlatitude ozone following the large enhancement of stratospheric aerosol caused by the eruption of Mt. Pinatubo in 1991. By 1994, the transient effect on total ozone of the Mt. Pinatubo aerosols had largely disappeared. Since 1994, non-polar total ozone, while variable, has not shown an overall negative trend, and total ozone levels are now at a higher level than would be predicted by a linear extrapolation of the pre-Pinatubo trend. Extrapolation of the pre-Pinatubo trend of -2.9%/decade in Northern Hemisphere midlatitudes (25°-60°) would predict an ozone depletion relative to 1979 of -5.5% at the end of 1997, whereas instead the deviations have averaged about -4% in the last 2 or 3 years. Seasonally, the corresponding winter/spring (December-May) and summer/fall (June-November) changes averaged about -5.5% and -2.8%, respectively, whereas a linear extrapolation of the pre-Pinatubo trend would predict -7.6% and -3.4%, respectively. In the Southern Hemisphere (25°-60°), trend extrapolation would predict -7.2% depletion at the end of 1997, whereas the smoothed data indicate a 1997 value of about -4% (satellite) or -5% (ground).
- As shown in Table 4-1, trends in total ozone from January 1979 updated through the end of 1997 exhibit the now-familiar pattern of negative trends with the following features:
  - Trends in both hemispheres in mid and high latitudes in all seasons are negative, large, and statistically significant.
  - Trends in the equatorial regions (20°S to 20°N) are statistically nonsignificant.

**Table 4-1. Total ozone trends in percent per decade and uncertainties (two standard errors) from Total Ozone Mapping Spectrometer (TOMS) data\*.**

Latitudes		Trend (%/decade)		
		Annual	Dec-May <sup>1</sup>	Jun-Nov <sup>2</sup>
North	50°-65°	-3.7 ± 1.6	-4.4 ± 2.6	-2.8 ± 1.3
North	30°-50°	-2.8 ± 1.7	-3.8 ± 2.4	-1.7 ± 1.3
Equatorial	20°-20°	-0.5 ± 1.3	-0.3 ± 1.6	-0.7 ± 1.3
South	30°-50°	-1.9 ± 1.3	-2.4 ± 1.2	-1.4 ± 1.9
South	50°-65°	-4.4 ± 1.8	-3.4 ± 1.6	-5.2 ± 2.6

\* Values in table are averages from Total Ozone Mapping Spectrometer (TOMS) trends in Table 4-5. Ground-based trends are shown in Table 4-4 for somewhat different latitude bands.

<sup>1</sup> North winter/spring and south summer/fall.

<sup>2</sup> North summer/fall and south winter/spring.

## OZONE TRENDS

- In the middle and high latitudes, the overall ozone amount has declined during all months of the year, and the amplitude of the annual cycle for stations has decreased by about 15% mainly as a result of a decline in the maximum. In the Northern Hemisphere, the trends are much larger (more negative) in the winter and spring seasons (December-January-February, March-April-May) about -3 to -6%/decade, than in summer and fall (June-July-August, September-October-November), about -1 to -3%/decade.
- Regional trends in total ozone show some systematic differences among continental-scale regions at the same latitudes, e.g., Siberia, Europe, and North America. The longitudinal trend calculations using gridded data from TOMS show the strongest negative trends over Siberia in spring and large negative trends over Europe in winter and spring. North America shows relatively smaller trends in winter/spring.
- Total ozone levels at 60°N-60°S were at their lowest in 1993 in the aftermath of the Mt. Pinatubo eruption. Since that time, ground-based ozone values have remained fairly constant, whereas the Earth Probe (EP)-TOMS record, which began in 1996, shows global ozone to be about 2% higher. This discrepancy, which is not seen in the northern midlatitudes (the region where we have most confidence in the observational record) has not been resolved.
- New scientific understanding shows that quasi-decadal ozone oscillations have been induced by major volcanic eruptions in the past 20 years. The confounding influences of solar and volcanic effects on ozone time-series analyses could affect the interpretation of recent changes.

## VERTICAL OZONE DISTRIBUTION

- Based on the Stratospheric Aerosol and Gas Experiment (SAGE I/II) Version 5.96 data, there is no significant inter-hemispheric difference in upper stratospheric trends for data extended through 1996.
- Combined trends and uncertainties (including both statistical and systemic errors) have been estimated from all available measurement systems. This was done only for the northern midlatitudes. The combined trends are negative at all altitudes between 10 and 50 km and are statistically significant at the 2-sigma level. The combined trend has two local maxima,  $-7.4 \pm 2.0\%/decade$  at 40 km and  $-7.6 \pm 4.6\%/decade$  at 15 km. The smallest trend deduced,  $-2.0 \pm 1.8\%/decade$ , occurred at 30 km. This combined trend, representing the results from all the independent data sources, is an indicator of the robustness of the trend results.
- Statistically significant trends of -6 to -8%/decade have been found at 40-50 km altitude for the midlatitudes. There is good agreement between SAGE I/II and Umkehr. The Solar Backscatter Ultraviolet (SBUV/SBUV2) spectrometer combined record shows less-negative trends. There is a factor of 2 seasonal variation in the trends, with the maximum value in winter.
- Trends in the column amount of ozone above 20 km deduced from SAGE I/II are much less than the column trends deduced from TOMS. However, the TOMS-SAGE differences are consistent with the sonde trends below 20 km. There is also a consistent seasonal variation for the satellite and sonde data.
- There is good agreement between SAGE I/II trends and sonde trends over the altitude region from 15 to 27 km at northern latitudes for the time period 1980 to 1996. This is a significant improvement compared with previous comparisons due principally to the revision of the SAGE dataset. The agreement in the derived trends from SAGE II-only and the sondes is excellent for the period 1984-1996.
- Both sonde and SAGE data show that most of the column ozone loss at midlatitudes occurs between 10 and 25 km altitude, with peak loss between 15 and 20 km. The seasonal variation of the trend occurs primarily between 10 and 20 km, with largest trends in winter and spring.

## Polar Ozone

### ARCTIC OZONE

- In the Arctic vortex, extremely low ozone values were deduced in late-winter/spring (a loss of about 100 Dobson units (DU; m-atm cm) with extremes exceeding ~200 DU below the 1964-1976 averages) in 6 out of the last 9 years. They are comparable with the values recorded (episodically) in the areas adjacent to the vortex. The ozone deficiencies are observed mostly in the layer a few kilometers above the tropopause.
- In the spring seasons of 1993, 1995, 1996, and 1997, the difference in total ozone from the pre-1976 level was comparable with differences observed in the austral spring.

### ANTARCTIC OZONE

- The large ozone losses continued at high latitudes in the Southern Hemisphere. The trends from 1979 in winter (June-July-August) are up to -6%/decade, and especially, in spring (September-October-November), up to -10%/decade, due to the influence of the Antarctic ozone hole. Trends in the summer months are smaller (-2 to -5%).
- Since the last Assessment, the monthly total ozone in September and October in Antarctica continued at a level of 40 to 55% below the pre-ozone-hole values, with up to a 70% decrease for periods of a week or so.
- At maximum expansion, the size of the ozone hole (defined as the area containing ozone values less than 220 DU) was nearly the same as during the early 1990s ( $>20 \times 10^6 \text{ km}^2$ ).
- In the lower stratosphere, between 12 and 20 km, over the September-November period, the monthly-mean ozone content was, on the average, between 60 and 90% below the pre-ozone-hole values and at times nearly completely destroyed.

## 4.1 INTRODUCTION

Several techniques, both satellite and ground based, have been developed to measure ozone in the atmosphere; some detect the absorption and emission of solar and atmospheric radiation, and others use chemical titration. While it has been relatively easy to measure total column ozone at a particular time and place, it has not proved easy to detect changes in total column ozone or the profile of a few percent over periods exceeding a decade. To do this one must know how the absolute calibration of the instrument (or instruments) and any information (a priori, viewing geometry, etc.) used in the retrieval algorithms change with time. One way of verifying that the drifts in these quantities are properly understood is by comparing the trends obtained by independent instruments. Thus, for example, the reason that one has confidence in the total ozone trends is that data from the satellite-based Nimbus-7 Total Ozone Mapping Spectrometer (TOMS) and the ground-based Dobson network both give the same trend within their assigned errors.

In Section 4.2 the sources of the data used in this Assessment are discussed. Detailed descriptions of many of the major techniques and instruments can be found in two reports. The report of the International Ozone Trends Panel (WMO, 1990a) contains descriptions of the instruments used in the total ozone studies. Since the 1994 Assessment (WMO, 1995), scientists from the World Climate Research Programme (WCRP) project on Stratospheric Processes and their Role in Climate (SPARC) and the International Ozone Commission (IOC) have performed a similar study of the trends in the vertical distribution of ozone (WMO, 1998). The reader is referred to those documents for details of the instruments and the associated algorithms.

The various sources of the variability in the ozone fields are discussed in Section 4.3. It is this variability that often sets the upper limit on the ability to make estimates of the long-term trends. Section 4.4 gives an account of the statistical methods used in estimating ozone trends, including a comparison of the different techniques that are currently used. Sections 4.5 and 4.6 describe the long-term changes in total ozone and vertical profiles, respectively. The data used in this analysis extend to December 1997 for the total ozone and to January 1997 for the ozone profiles.

## 4.2 DATA SOURCES

### 4.2.1 Total Ozone

#### 4.2.1.1 GROUND-BASED TOTAL OZONE MEASUREMENTS

Three types of ground-based total ozone instruments have been used in this Assessment: the Dobson spectrophotometer, the Brewer spectrophotometer, and the filter ozonometer. The error in the most accurate direct-sun ozone observations by the Dobson spectrophotometer for a well-calibrated and operated instrument is about 1% ( $1\sigma$ ) (Basher, 1995). For zenith sky measurements it is about 3%. The potential long-term stability of the Dobson instrument is about  $\pm 0.5\%$  ( $1\sigma$ ) for annual means (WMO, 1980). Details on Dobson instrument accuracy and error sources can be found in a number of publications (e.g., WMO, 1990a, 1992, 1993). More than 90 Dobson stations are operated continuously. These are periodically calibrated against the World Primary Standard Dobson no. 83. WMO traveling standard lamp tests show that more than 75% of the Dobson instruments differ with the standard lamp by less than  $\pm 1.5\%$  (Basher, 1995).

The Brewer spectrophotometers demonstrate performances similar to those of the Dobson instruments (Kerr *et al.*, 1988). Most Brewer instruments are calibrated by the traveling standard, with the traveling standard itself calibrated against the Brewer reference "triad" in Toronto (Kerr *et al.*, 1998). Observed long-term trends between the different Brewer instruments of the triad, with Toronto Dobson instrument no. 77 and TOMS, do not exceed 1%/decade (Kerr *et al.*, 1998).

The M-83 filter ozonometer and its later modification, the M-124, have been used for total ozone observations, mostly in the former USSR, since the early 1960s. The filter ozonometer data have recently been reevaluated (Bojkov *et al.*, 1994). Data prior to the modernization of the M-83 instruments in 1972 were found to be largely unreliable. The filter instruments tend to be less accurate than the Dobson and Brewer spectrophotometers. Unlike the Dobson and Brewer stations, filter instrument stations have used several different instruments over their period of operation. Typically, the former-USSR network filter instruments were replaced every 2-3 years. The errors reported by the

## OZONE TRENDS

instrument developers for well-calibrated and maintained filter instruments (M-124) are about 3% for direct sun and 5% for zenith sky observations (Gustin *et al.*, 1985). The reevaluated dataset is consistent with these numbers. More than 40 stations using filter instruments had long enough records for use in this Assessment.

All ground-based total ozone data deposited in the World Ozone and Ultraviolet Data Centre (WOUDC) were examined for possible inclusion in this Assessment, but for a variety of reasons a number were rejected. In general, the quality criteria as defined by Bojkov *et al.* (1995b) were used and are summarized here. First, only records starting before 1984 and having data after 1992 were considered sufficiently long for meaningful analyses. Second, a minimum of 10 days of data was required for a monthly mean to be included. Exceptions were made only for Buenos Aires for a few years in the 1970s and for Nairobi. In these cases the limit was decreased to 6 days if distributed evenly throughout the month. Third, some data records show large variations and deviations against nearby stations and satellite overpasses that could not be explained in terms of any natural phenomena and for which calibration data were not available. For a few stations it was obvious that the data were in error, but information on their correction or reevaluation was lacking (e.g., Casablanca, Manila). These data were not used. For this Assessment, the period of analysis was selected as January 1964 to December 1997, because before 1964 a sufficiently dense network was operating only in Europe, Japan, Australia, and North America.

The necessity for data reevaluation has been described before (e.g., Bojkov *et al.*, 1990), and the recommended procedures (WMO, 1993) for data reevaluation have been followed. For 34 stations from Brazil, Germany, Japan, United Kingdom, United States, and other countries the records were reevaluated by the national operating agencies (Angreji, 1989; Lapworth 1991; Lehmann *et al.*, 1992; Komhyr *et al.*, 1994; Kohler and Claude, 1998; Sahai *et al.*, 1998; Staehelin *et al.*, 1998a) and the reevaluated data submitted to the WOUDC. The present Assessment is based on the dataset currently available from the WOUDC. However, in some cases, some additional considerations have been applied:

- Data from three Indian stations were used, but only those starting from 1975, coinciding with their participation with their national standard Dobson in the World Meteorological Organization (WMO) intercomparison in Belsk (1974).
- Dobson instrument no. 97 operated at Buenos Aires before the calibration in March 1977 had readings 5.4% too low, and these data were not corrected or redeposited with the WOUDC. Based on this calibration, all data before March 1977 were increased by 5.4%.
- The Macquarie Island record was verified and revised back to 1979 (Lehmann *et al.*, 1992) and these data were used in the analysis. Lehmann *et al.* (1992) also show some problems with the data in the early 1980s, and for the period 1979-1986 a provisionally reevaluated dataset (WMO, 1990a) was used.
- Major problems with the Brisbane record in the early 1980s have been reported by Bojkov (1986). Provisionally reevaluated data prior to May 1985, as shown in WMO (1996), were used for Brisbane.
- Following a recommendation from the Japan Meteorological Agency (T. Ito, Japan Meteorological Agency, Japan, personal communication, 1998), the data for Kagoshima from November 1963 to July 1967 and January 1970 to March 1987 data have been increased by 9 Dobson units (DU; m-atm cm).
- On the basis of an instrument intercomparison in Arosa, in 1995, and comparisons with nearby stations and satellite data, all Sestola data from 1981-1994 have been reduced by 2%.
- Based on a few calibrations of the Nairobi Dobson instrument, the zenith sky data were not used, and the direct sun data prior to 1 May 1995 were increased by 2.6%.
- To obtain a longer record, data from nearby stations were combined for two cases. The record from the New Zealand station at Invercargill was added to the Lauder record up to 1985 with a small (1-2%) correction for the annual cycle. Also, the earlier Bracknell data were incorporated in the record of the U.K. station at Camborne.

The main dataset used in the present analysis is composed of monthly means of total ozone from 44 Dobson stations, some of which (Edmonton, Goose Bay, Churchill, Kodaikanal) were equipped with Brewer instruments during the last 10 years. The differences between Dobson and Brewer data for overlapping periods are within  $\pm 1\%$ . Brewer data were also used to fill short gaps in Dobson records at Hohenpeissenberg and Vigna Di Valle. (The stations and their latitude, data availabil-

ity, and seasonal and annual trends since 1979 are listed in Table 4-4.) Data from 21 ground-based stations north of 60°N were used for calculating Arctic trends, and from four Dobson stations south of 60°S for Antarctic trends. All total ozone data used in this Assessment are based on the Bass-Paur absorption coefficients.

#### 4.2.1.2 SATELLITE TOTAL OZONE MEASUREMENTS

##### *Total Ozone Mapping Spectrometer (TOMS)*

Data from three TOMS instruments were considered in this Assessment: Nimbus-7, Meteor-3, and Earth Probe (EP). The Nimbus-7 spacecraft operated from October 1978 to May 1993. Meteor-3 TOMS was in operation from August 1991 to December 1994. EP TOMS was launched in August 1996 and, at the time of the writing of this report, is still operating. All TOMS data were processed with the Version 7 TOMS algorithm. Nimbus-7 TOMS total ozone has an absolute error of  $\pm 3\%$ , a random error of  $\pm 2\%$  ( $1\sigma$ ), and the uncertainty in the drift for 14 years is  $\pm 1.5\%$  (though somewhat higher at higher latitudes) (McPeters *et al.*, 1996). For Meteor-3 TOMS these numbers are  $\pm 3\%$ ,  $\pm 3\%$ , and  $\pm 1\%$  for 3 years, respectively (Herman *et al.*, 1996).

Nimbus-7 TOMS data were used for the period November 1978 through April 1993, and Meteor-3 data for May 1993 until October 1994. The Meteor-3 data have gaps due to high solar zenith angle conditions because of the precessing orbit. During periods when the solar zenith angle is greater than 80°, the data are considered unreliable and were not used in this Assessment. Preliminary Earth Probe data from August 1996 to March 1998 were used. Following the recommendation by MCPeters and Labow (1996), only TOMS data taken at solar zenith angles less than 80° were used.

##### *Solar Backscatter Ultraviolet (SBUV), SBUV/2, BUV*

The SBUV instrument on board the Nimbus-7 spacecraft and the SBUV/2 instruments on board the National Oceanic and Atmospheric Administration (NOAA) spacecraft NOAA-9, NOAA-11, and NOAA-14 measure both total ozone and the vertical distributions of ozone (reported as ozone profiles in DU for 12 Umkehr layers (~5 km thick each), although the actual vertical resolution is poorer). The uncertainties are: absolute error, 3%; random error, 2%; and time-dependent

drift error, 3% (Fleig *et al.*, 1990). The SBUV data are available from November 1978 to May 1990. The data after February 1987 are affected by an out-of-synchronization condition and have been corrected by a “scene-stabilization” method described by Gleason and McPeters (1995).

The NOAA-11 SBUV/2 data are available from January 1989 to October 1994, with decreasing coverage of the Southern Hemisphere over the instrument lifetime due to precession of the NOAA-11 equator crossing times. The NOAA-11 SBUV/2 data have recently been reprocessed using updated calibrations and instrument behavior characterizations and an algorithm change to correct for grating position errors in the latter part of the record to produce the Version 6.1.2 dataset. The NOAA-11 absolute calibration was adjusted to match the Shuttle SBUV (SSBUV) calibration (Hilsenrath *et al.*, 1993), while the time-dependent calibration was maintained using an onboard calibration lamp system and verified through comparisons with SSBUV measurements. NOAA-9 SBUV/2 data have also been reprocessed with an adjustment to SSBUV and an updated calibration. Version 6.1.2 data are available for April 1985 to December 1996. The precession of the NOAA-9 orbit led to a period of poor viewing conditions from 1989 to 1992 (e.g., Fioletov *et al.*, 1998b).

All datasets have been processed with the Version 6 Backscatter Ultraviolet (BUV) algorithm described in Chapter 1 of the SPARC/IOC report (WMO, 1998) and Bhartia *et al.* (1996). Nimbus-7 SBUV data were used from November 1978 through December 1988, and NOAA-11 SBUV/2 data were used from January 1989 through January 1994. The NOAA-9 data for February 1994 to December 1996 were used. The NOAA-14 data have not been used in this Assessment.

The BUV instrument was launched on the Nimbus-4 satellite in April 1970. The satellite was placed in a sun-synchronous orbit with a near-noon local crossing time. The instrument was similar in design to the SBUV instruments (Heath *et al.*, 1975). The Nimbus-4 satellite had a series of power array failures that limited the instrument’s data coverage. The first and most serious power failure occurred in May 1972, causing the data coverage to be sporadic throughout the rest of the mission (May 1977). Details on the BUV instrument and algorithm can be found in Dave and Mateer (1967), Heath *et al.* (1973), and Krueger *et al.* (1973).

## OZONE TRENDS

### TOVS

The Television Infrared and Observational Satellite (TIROS)-N Operational Vertical Sounder (TOVS) units on NOAA polar-orbiting satellites can provide estimates of stratospheric ozone. The 9.7- $\mu\text{m}$  High Resolution Infrared Sounder (HIIRS) ozone channel is well suited for monitoring lower stratospheric ozone. Data using a two-layer physical retrieval to determine the lower stratospheric ozone and to estimate the total column ozone (Neuendorffer, 1996) are available for February 1979 to the present. Full global coverage is obtained even in the polar night (except over the cold Antarctic Plateau). The measurements in the 9.7- $\mu\text{m}$  channel are insensitive to middle-stratospheric and tropospheric ozone changes. TOVS ozone retrievals are sometimes complicated locally by cloud effects, water vapor absorption, and surface emissivity.

TOVS total ozone estimates agree with Dobson and Brewer station estimates to within 25 DU (on average) (Neuendorffer, 1993; Chesters and Neuendorffer, 1991). Zonal and global TOVS ozone averages are considerably more accurate than this; however, all such values must be treated with caution. TOVS total ozone estimates are really only sensitive to variations in the lower stratosphere, and long-term TOVS total ozone trends are, at best, only indicative of lower stratospheric ozone trends. Actual total ozone trends over the last 19 years are probably slightly (i.e., 5% to 25%) stronger than the corresponding trends observed in TOVS total ozone. Inter-satellite instrument differences complicate the use of this record for long-term trends. In this Assessment, only 60°S-60°N integrated ozone values from TOVS have been used.

#### 4.2.1.3 COMPARISON BETWEEN GROUND-BASED AND SATELLITE OZONE DATA

Figure 4-1 shows the percentage difference between total ozone from three satellite instruments and total ozone from 30 northern midlatitude Dobson and Brewer stations. The relative trend between Nimbus-7 TOMS and the ground-based network is near zero for the 14.5-year interval; however, there are some long-term fluctuations in the TOMS-Dobson/Brewer differences. Because of those fluctuations, the trend relative to ground-based stations can be higher for shorter time intervals (from +1%/decade for the 1978-1988 period to -1.4%/decade for the 1985-1993 period). There is about

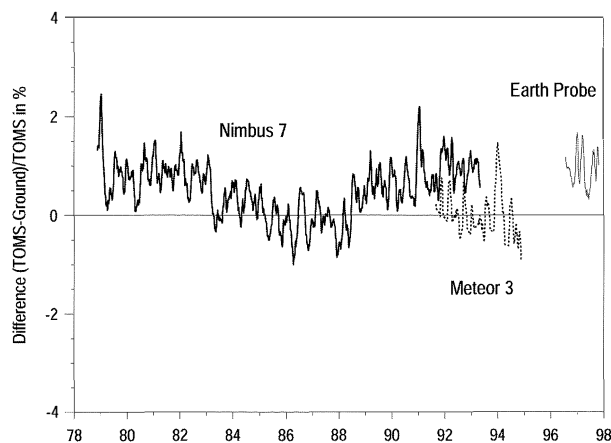


**Figure 4-1.** Weekly averages smoothed by four-point running means of the percentage difference between total ozone from three TOMS instruments and from 30 northern midlatitude ground-based stations (G. Labow, Raytheon STX Corporation, and R. McPeters, NASA Goddard Space Flight Center, U.S., personal communication, 1998).

a 1% systematic difference between Nimbus-7 TOMS and Meteor-3 TOMS. The year-and-a-half data record from Earth Probe TOMS appears to be approximately 1% higher than that of the ensemble of Dobson stations. Currently, EP TOMS data must be considered preliminary until the instrument's calibration can be better characterized.

The differences between the total ozone from 30 northern midlatitude Dobson stations and from the three BUV/SBUV satellite instruments were also compared. The early SBUV record is 1% higher on average than the Dobson ensemble. This difference drops to close to zero after 1983. The NOAA-11 SBUV/2 comparisons are more variable but are about 1% higher than the Dobson. The NOAA-9 SBUV/2 comparisons show little difference in 1994 but increase to 2% by the end of 1996.

Bojkov *et al.* (1988) found that, for the period 1978-1985, 50% of all Dobson stations showed less than 2% monthly standard deviations when compared with TOMS. For the period 1986-1993, standard deviations of less than 2% were found for 72% of the stations (Fioletov *et al.*, 1998a). These uncertainties in the TOMS and the ground-based data typically result in less than 2% differences for the ozone trends. However they show that agreement better than 1-2% between ground-based

**Table 4-2. Inventory of the most “reliable” datasets with time records longer than 5 years.**

Platform	Middle/Upper Stratosphere $Z > 25$ km	Low Stratosphere $Z < 25$ km	Troposphere
<b>Satellites</b>			
SAGE I	February 1979–November 1981	February 1979–November 1981	
SAGE II	October 1984–present	October 1984–present	
SBUV+SBUV/2	1978–present		
HALOE	October 1991–present	October 1991–present	
MLS	October 1991–present	October 1991–present	
<b>Ground-based</b>			
Microwave	1989–present	1989–present	
Umkehr/Dobson	1957–present		
Lidar	1990–present	1985–present	1990–present
Balloonborne sondes		1965–present	1965–present

and satellites probably cannot be reached. Conditions such as high zenith angles, very high total ozone, or heavy clouds are potential sources of errors for both systems. These effects are evident at several high-latitude stations in wintertime. Thus when comparing these systems, some differences are to be expected.

## 4.2.2 Vertical Ozone Distribution

### 4.2.2.1 DATA AVAILABILITY

The quality of vertical ozone profile data and their suitability for use in long-term trend investigations were recently evaluated by a team of international experts as part of the SPARC-IOC (WMO, 1998). The data available for trend studies come from different ozone-measuring platforms using different sensing techniques with different spatial and temporal coverage. A summary of the most reliable datasets with time records longer than 5 to 10 years is provided in Table 4-2.

Only four measurement systems have records long enough to assess long-term ozone trends: SAGE (I and II), SBUV and SBUV/2, Umkehr/Dobson, and ozonesondes. SAGE I and II, SBUV and SBUV/2, and the Umkehr/Dobson-network provide the major data sources to derive global ozone trends in the middle and upper stratosphere. Because of the length of the time record of SAGE and the high vertical resolution it provides, the focus of the SPARC/IOC study was on validation of SAGE trend capability. The good spatial cover-

age of the SBUV and SBUV/2 data can be used to examine the effect of the poorer spatial coverage of SAGE on the derived trends. In addition, the Halogen Occultation Experiment (HALOE) and Microwave Limb Sounder (MLS) data can be compared with SAGE II data to determine if there are any seasonal or latitudinal dependencies in SAGE II trends. Umkehr/Dobson, lidar, and microwave data can be used to verify the accuracy of individual profiles measured by the SAGE I and II satellite instruments and to further assess the validity of trends. Further, the ozonesonde network, starting in the early 1960s has generated a dataset for examining lower stratospheric and tropospheric ozone trends, although mainly in the northern midlatitudes.

An important issue from the previous Assessment (WMO, 1995) is the derivation of global ozone trends between the tropopause and 25 km. Ozonesondes provide data to derive long-term trends in this altitude range, but with very poor spatial coverage at a limited number of stations, mainly located on the continents in the Northern Hemisphere (NH). Therefore they cannot provide global trends. They do, however, provide valuable datasets for intercomparison with satellite results to investigate any instrument biases and drifts in indicated trends. SBUV and SBUV/2 and Umkehr/Dobson are not sensitive enough to provide useful information in the lower stratosphere, which leaves SAGE I/II as the only global dataset with temporal and spatial coverage sufficient to meet the global objective. The coverage of SAGE I and II, however, is still limited to between 60°S

## OZONE TRENDS

and 60°N. The 1994 Assessment (WMO, 1995) showed some significant differences between SAGE- and ozonesonde-derived trends in the lower stratosphere, with SAGE trends being larger. These differences were a major focus of the SPARC/IOC study (WMO, 1998). The validity of SAGE measurements for altitude ( $Z$ )  $\leq$  25 km was carefully scrutinized due to possible errors in the data caused, for example, by high aerosol loading resulting from volcanic eruptions (e.g., Mt. Pinatubo) or by ice crystal absorption due to high cirrus clouds (Cunnold *et al.*, 1996).

During the pre-satellite period, before 1978/1979, ozonesonde and Umkehr/Dobson measurements provided the only datasets for study of ozone change in any altitude region. Therefore, it is important to characterize the quality of the sonde and Umkehr time series during that period (i.e., 1965-1979). There are indications from the SPARC/IOC study (WMO, 1998) that in the tropopause region up to 17-20 km, ozonesonde results are more reliable than satellite measurements. That study used the newest, latest, and revised versions of the different ozone ground-based, in situ, and satellite datasets available before the end of June 1997. Those data were either linked to or stored on a dedicated temporary database. Once the report is released in the fall of 1998, all the data will be made publicly available at the SPARC/Ozone Trend Assessment World Wide Web site, and additionally the sonde data will be placed in the WOUDC in Toronto.

### 4.2.2.2 DATA LIMITATIONS FOR USE IN TREND DETERMINATIONS

The upper altitude limit for applying SAGE II data to determine trends is on the order of 50 km, based on noise in SAGE II and intercomparisons with HALOE data. The lower limit is less determinate, most likely because of atmospheric variability at low altitudes and aerosol effects both in SAGE II measurements and the data used for comparisons. In most instances, the differences in trends between SAGE II and correlative data start to increase below about 20 km and they become much more variable, thus limiting the lower altitude at which derived trends can be validated. This is not to say that trends from the different measurement systems are invalid in this range, but only that for the systems used in the intercomparisons, a less definitive statement can be made about trend validity. The low-altitude prob-

lems represent one of the most serious limitations for using the data because they affect the region that is most in need of improved understanding. Even though great attempts were made to reduce or eliminate aerosol effects in the latest SAGE II algorithm (Version 5.96), it is clear that the effects remain and are prominent.

Various screening approaches for the SAGE II data were evaluated by the SPARC/IOC study team, including eliminating values based on the aerosol extinction value, eliminating values based on the magnitude of the SAGE II error bars for ozone, or eliminating specific time periods. The latter approach was chosen and the time and altitude screening guide is included in Table 2-2 of the report (WMO, 1998).

There are some obvious sunrise-sunset differences in the SAGE II data that are important only above approximately 45 km. The data show a difference of ~10% between sunrise and sunset ozone values at 1 mb (sunset higher). This is not physical and is much greater, for example, than the difference between HALOE sunrise-sunset values, which is approximately 2%. There is no reason to prefer SAGE II sunrise measurements over sunset (or vice versa). The SPARC/IOC study recommends combining sunrise and sunset for doing trend studies, but because the reason for the sunrise-sunset differences is unknown, the error bars for derived trends will be increased above 45 km.

Another possible limitation is the effect of any SAGE I/II data offsets. While some evidence exists from Hohenpeissenberg, Payerne, and Uccle ozonesonde-SAGE comparisons to suggest that SAGE I and SAGE II overlapping measurements are inconsistent, the results are not statistically significant. It is known, however, that there is a latitude-dependent altitude registration difference between the two datasets that should be corrected before combining them. The correction scheme developed by Wang *et al.* (1996) was adopted as a satisfactory correction, leading to approximately a 300-m adjustment. The uncertainty in this correction for each latitude is about 100 m. Below 20-km altitude, the simple upward shift of the SAGE I profiles may be incorrect because of the large Rayleigh scattering contribution to the 0.6-nm extinction at these altitudes. A rigorous inversion of the SAGE I data to correct the altitude registration problem would be preferable. It is recommended that if the SAGE I data are used for trend calculations at altitudes below 20 km, they be used with caution. More intercomparisons and further study are needed to draw

firm conclusions about the offset, its errors, and any latitudinal dependence in the uncertainties.

The SBUV measurement system is believed to provide good information over layers 5 to 9 (25 km to 45 km). The upper altitude limit is driven by the coarse vertical resolution of the SBUV (~8 km) coupled with the declining ozone levels with increasing altitude. The lower limit is a result of reduced sensitivity due to poor vertical resolution, declining ozone values, and low information content below the ozone peak. The Umkehr has similar limitations (layers 4 to 8, or 20 km to 40 km) for comparable reasons. The ozonesonde measurements are generally limited to an upper altitude of about 27 km due to pump correction errors and sensing solution changes. Also, both the Brewer-Mast (BM) and electrochemical concentration cell (ECC) sondes are affected by the presence of sulfur dioxide (SO<sub>2</sub>) in the atmosphere, and when this is enhanced by a volcanic event, for example, there could be false short-term changes in measured ozone as the SO<sub>2</sub> layer decays. There are still important differences observed between results from different sounding stations using the same type of ozonesonde, and this is believed to be due to differences in the preparation and correction procedures applied at the various launch sites. Although much progress has been made to improve the quality and homogeneity of the ozonesonde data since the last Assessment (WMO, 1995), there is still an urgent need to investigate and intercompare the instrumental performance of the different sonde types as well as a need to revise and agree on procedures for preparation and data processing. Until this happens and methods are uniformly applied, the differences will persist.

#### 4.2.2.3 INTERCOMPARISONS

Coincidence criteria used for all comparisons shown are  $\pm 2^\circ$  latitude,  $\pm 12.5^\circ$  longitude, and 2 days time, unless otherwise noted. It was found, however, when validating the Nimbus-7 Limb Infrared Monitor of the Stratosphere (LIMS) data, that even 3 hours could make an important difference in the temperature agreement; but because SAGE II uses the solar occultation experiment approach, the number of coincidence opportunities are limited, requiring adoption of the criteria used. When comparisons are done against SAGE II, SAGE II is usually the reference for calculating percentages. Also unless otherwise noted, the error bars shown are the 2

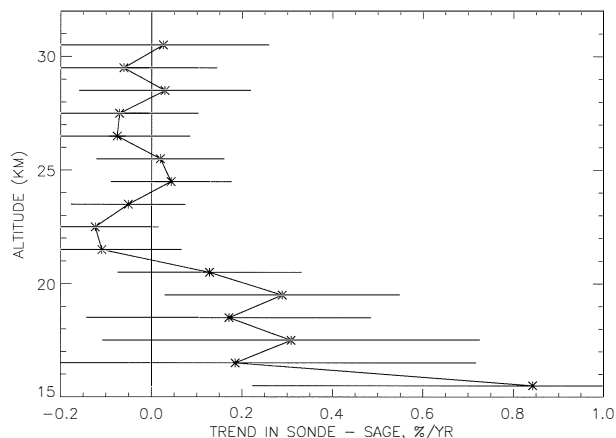


**Figure 4-2.** The altitude dependence of the trend in the sonde-SAGE II differences for the combined coincidences of the eight sonde sites. (From WMO, 1998.)

standard error mean bars (or 2 sem), calculated by dividing twice the standard deviation by the square root of the number of samples used in the comparison.

#### *SAGE Versus Ozonesondes*

The drift of SAGE II versus the sondes was determined by developing a single combined time series, at each altitude, of the coincident differences between the sondes and SAGE II for eight sounding sites ranging from 36°N to 52°N (Hohenpeissenberg, Payerne, Uccle, Boulder, Goose Bay, Sapporo, Edmonton, and Toronto) and then finding the slope of a least-squares straight-line fit through the points. Because each point in the time series is a difference between the sonde and SAGE II data, latitudinal, annual and semiannual oscillation, the quasi-biennial oscillation (QBO), and other effects are inconsequential to first order because the differencing would tend to cancel them out. If there is no drift in one measurement system relative to the other, the differences will remain constant with time. Measurements from the eight stations were combined to reduce geophysical and sampling noise caused by the fairly loose coincidence criteria used. The result is shown in Figure 4-2.

Note that a statistically significant indicated drift at the  $2\sigma$  level occurs at 19.5 km and it is only 0.28%/yr. Above about 20 km, the differences are on the order of -0.1%/yr and below 20 km, in the mean they are about 0.25%/yr, except at 15.5 km where the difference is 0.85%/yr.

## OZONE TRENDS

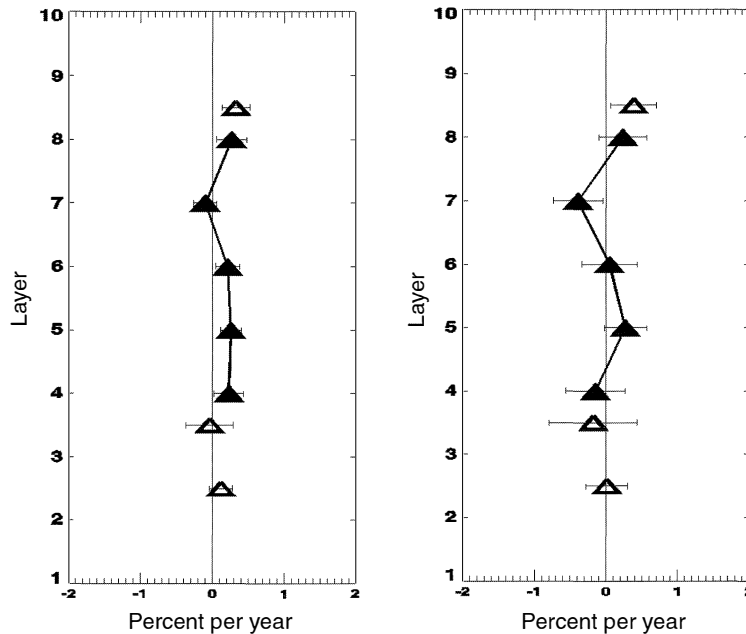


**Figure 4-3.** Hemispheric average regression slopes (% per year) of the layer-ozone time series of Umkehr-SAGE coincident-pair differences for the northern midlatitudes (left panel) and the southern midlatitudes (right panel). All error bars shown are  $\pm 2$  standard errors of the mean. Panels show the variance-weighted average slopes  $\pm 95\%$  confidence intervals associated with the variance-weighted means of the coincident-pair differences. The disconnected open triangles represent layers 2 through 10 plotted at layer 2.5, layers 2+3+4 plotted at layer 3.5, and layers 8+9+10 plotted at layer 8.5. The solid triangles represent individual levels. All Umkehr observations are individually corrected for aerosol interferences by using the Mateer and DeLuisi (1992) aerosol correction factors. (Modified from a figure in WMO, 1998.)

### *SAGE Versus Lidar*

In most cases, the lidar-SAGE difference time series show generally no trend significant at the two sigma standard error confidence level. Due to the higher variability of ozone at altitudes below 20 km, the standard deviation is higher in this range and the trend of the difference can be larger than  $1\% \text{ yr}^{-1}$ . At 17.5 km, the only record exceeding 100 coincidences (Hohenpeissenberg) shows a nonsignificant trend of  $(0.5 \pm 0.6)\% \text{ yr}^{-1}$ . The trends are also higher above 40 km, due to the decrease in the signal-to-noise ratio of the lidar measurements. In these regions, the trends can exceed  $1\% \text{ yr}^{-1}$ . The average trend for the records exceeding 100 coincidences in the range 40-50 km is  $(0.6 \pm 1.4)\% \text{ yr}^{-1}$ . Over the 20-35 km interval, the trend does not exceed  $(0.5 \pm 1)\% \text{ yr}^{-1}$ . On average in this range, values of about  $0.3\% \text{ yr}^{-1}$  with standard errors not exceeding 0.4% are found.

### *SAGE Versus Umkehr*

Average regression slopes and 95% confidence intervals of the SAGE-Umkehr coincident-pair-difference time series for the northern and southern midlatitudes (NML, SML) are shown versus altitude in Figure 4-3. The largest discrepancy between Umkehr and SAGE regression slopes occurs in layers 8 and 9, where the slope of the coincident-pair differences is  $(0.3 \pm 0.2)\%/ \text{ yr}$ , significantly different from zero at the 95% confidence level. In all other layers and layer combinations, the absolute slope of the differences is less than or equal to  $(0.2 \pm 0.2)\%/ \text{ yr}$ . The southern midlatitude averages show marginally significant discrepancies between Umkehr and SAGE only in layers 7 and 8<sup>+</sup>. The vertical structure of the Umkehr-SAGE differences in the variance-weighted SML averages is similar to the NML results. Primarily due to the smaller sample size,

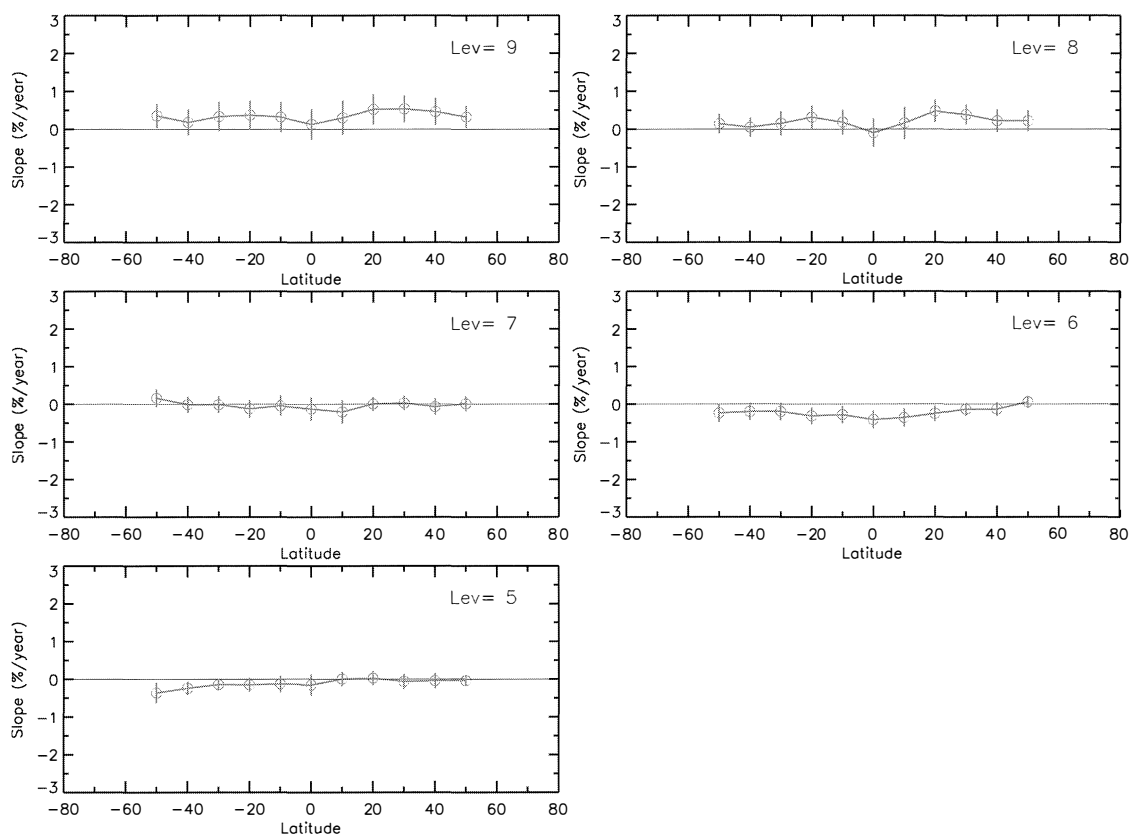


**Figure 4-4.** Linear slopes of the differences (SBUV-SAGE) between SAGE and coincident SBUV ozone observations from 1979 to 1990 expressed as a percentage of the SAGE Umkehr layer. Mean values were binned by month and placed in 10°-wide latitude bins. Error bars are twice the standard errors of the differences in slopes. (From WMO, 1998.)

the uncertainties in the SML are somewhat larger ( $\sim 0.3\%/yr$ ) than the uncertainties in the NML averages. Overall Umkehr-SAGE drift rates relative to each other are verified in a statistically significant sense to be no worse than  $\pm 0.2\%/yr$  in the NML and  $\pm 0.3\%/yr$  in the SML.

#### **SAGE Versus SBUV**

A comparison of the linear slopes of the coincident-pair differences between SBUV and combined SAGE I/II measurements is shown in Figure 4-4. SAGE data possess a more positive slope in layers 5 and 6 and a less positive slope in layers 8 and 9. The most significant difference is  $(+0.4 \pm 0.2)\% yr^{-1}$  in layer 9. However because of the offsetting differences in layers 5 to 7, it is concluded that overall there is no evidence of a drift in the SAGE (and overall SBUV) calibration of greater than

$0.2\% yr^{-1}$ , based on comparisons over the period 1979-1990. This is perhaps the longest period over which comparisons can be made between coincident ozone measurements obtained by essentially two separate instruments. It is likely to provide the strongest constraint possible on the absence of a drift in the SAGE ozone calibration. Additional details of SBUV-SAGE comparisons are provided in the SPARC report (WMO, 1998).

#### **SAGE II Versus HALOE**

Because SAGE II and HALOE (Russell *et al.*, 1993) are both solar occultation experiments, there are not enough coincidences to examine the trends of coincident differences. Instead, the entire data records for each experiment were used and the linear slopes of each experiment were compared. Down to 30 km, the

## OZONE TRENDS

**Table 4-3. Seasonal mean ozone values and the standard deviation (in ppbv) of the mean in the mid-troposphere (4.5-5.5 km height) at the Observatoire de Haute Provence (OHP).** The number of profiles is denoted by *n*.

Time	ECC Measurements 1991-1995		Lidar Measurements 1990-1995	
	mean O <sub>3</sub>	<i>n</i>	mean O <sub>3</sub>	<i>n</i>
November–February	49.0 ± 0.8	66	47.2 ± 1.2	96
March	53.5 ± 2.7	18	53.8 ± 2.7	23
April–June	65.2 ± 1.5	52	63.2 ± 2.3	56
July–September	63.0 ± 1.5	54	60.7 ± 1.8	74
October	53.1 ± 2.1	52	55.2 ± 3.0	14
All	54.3 ± 0.6	207	53.8 ± 1.2	263

differences in the annual change (i.e., the indicated drift rate) are  $\leq 0.5\%$  at all latitudes except  $55^\circ\text{S}$ , where they are  $\sim 1\%$ . This is also true for 25 km at many latitudes, but there are two latitude bands, i.e.,  $15^\circ\text{N}$  and  $55^\circ\text{S}$ , where the differences are 1.5 to  $2\% \text{ yr}^{-1}$ . At 20 km, the differences are on the order of 2 to  $4\% \text{ yr}^{-1}$ . When latitudinal averages of the indicated drift rates at a given altitude are taken, the mean indicated drift rate for the  $60^\circ\text{S}$  to  $60^\circ\text{N}$  range and for 50 km down to 25 km, while not statistically significant, are less than  $0.2\% \text{ yr}^{-1}$  at all altitudes except 30 km, where the value is  $(0.4 \pm 0.25)\% \text{ yr}^{-1}$ . At 20 km, the latitudinally averaged differences are barely significant at the  $(1.4 \pm 1.2)\% \text{ yr}^{-1}$  level. Below 20 km, the differences are large, and no useful results are obtained in the tropics because of poor sampling.

### *SAGE II Versus MLS and HALOE*

Because MLS uses limb emission, there are many coincidences with SAGE II and, at different times, with HALOE. Therefore, MLS can be used as a transfer standard to, in effect, examine the linear slopes of coincident differences, i.e., the indicated drift rates between MLS and SAGE II or MLS and HALOE. The overlap period is less than 6 years (and is only half this at altitudes below 40 mb because of the prescribed time filtering of SAGE II data to remove aerosol effects). SAGE II slopes equal or exceed MLS slopes in the latitudinal mean at all levels from 1 to 46 mb, but there is no recognizable pattern in the differences and only at 22 mb is the difference barely significant at the 95% confidence level. The mean of the indicated drift rates between 1 and 46 mb is  $(-0.4 \pm 0.8)\% /$

yr. SAGE ozone slopes can be related to HALOE ozone slopes based on a comparison of slopes in coincident HALOE and MLS measurements. The only significant MLS-HALOE slope difference at the 95% confidence level between 1 and 22 mb occurs at 22 mb, where the HALOE slope is  $0.9\% \text{ yr}^{-1}$  less than the MLS slope. The differences in the 1 to 22 mb region are latitude and altitude dependent and average  $(-0.1 \pm 0.8)\% / \text{yr}$ . It is concluded that HALOE, MLS, and SAGE II do not drift relative to each other by more than  $0.5\% / \text{yr}$ , which is within the measurement uncertainties.

### *SAGE II Versus Ozonesonde*

The SPARC/IOC study (WMO, 1998) carried out an extensive analysis of the three different types of ozonesondes in use today (electrochemical concentration cell (ECC), Brewer-Mast (BM), and the Japanese KC68/79) including evaluation of the Joint Ozone Sonde Intercomparison Experiment (JOSIE) laboratory intercomparison study and field intercomparisons. Comparisons of ozonesondes in the stratosphere with other ozone-profiling techniques show consistent results, with agreement of about  $\pm(3-5)\%$  at altitudes between the tropopause and 28 km. The precision of the different sonde types is better than  $\pm 3\%$ . Above 27 km the results are not consistent due to instrumental uncertainties (e.g., pump corrections and sensing solution changes) and caution must be used, at least for the non-ECC types of sondes, when applying the data for long-term trend determinations.

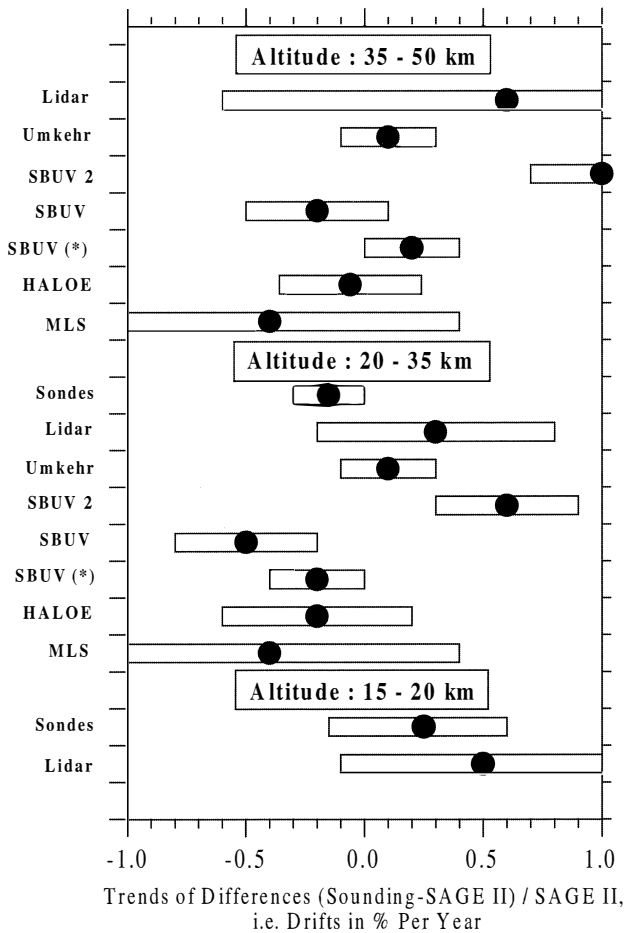


**Figure 4-5.** Trends of differences (i.e., drifts) between ozone measurements made by various ozone profiling instruments and SAGE II, in percent per year [(Sounding-SAGE II)/SAGE II]. Trends of ozonesondes, lidar, and Umkehr differences are presented as averages for eight northern midlatitude sounding stations. Trends of satellite differences are presented as global means. The average differences are indicated by the dots, and the bars represent the 99% confidence interval of the drift estimation. The entries for SBUV are for SBUV/SAGE II comparison; entries for SBUV\* are for SBUV/combined SAGE I and SAGE II comparison. (From WMO, 1998.)

In general, ECC sondes provide more consistent results than the other two types of sondes. The precision of the ECC sonde is better than  $\pm(5-10)\%$  and shows a small positive bias of about 3%. BM and KC79 sondes are less precise,  $\pm(10-20)\%$ , but there are no indications of any bias larger than  $\pm 5\%$ . It appears that large relative changes in accuracy between BM sondes and ECC sondes may have occurred between 1970 and 1991. A recent study done by Ancellet and Beekmann (1997), however, shows some encouraging results for future long-term tropospheric observations. These authors evaluated the ozone-profiling capability of the ECC sonde by performing comparisons with routine lidar measurements made at the Observatoire de Haute Provence (OHP) during the 1990-1995 period.

The seasonal means of mid-tropospheric ozone (4.4-4.5 km altitude) obtained by the ECC sonde and lidar are summarized in Table 4-3. ECC values are not corrected by total ozone normalization. Both datasets show excellent agreement in the annual mean (54.3 ppbv for ECC, 53.8 ppbv for lidar) and in seasonal variations in the mid-troposphere. Differences in particular periods are generally in the range of 2 ppbv (5%). For 15 simultaneous ECC versus lidar profiles, the mean of the differences observed between 4 and 7 km was  $2.5 \pm 1.8$  ppbv ( $4 \pm 3\%$ ). Although there is a dearth of comparative studies to evaluate the performance of ozonesondes in the troposphere, this present study under regular field operations together with the studies under controlled laboratory conditions show that there is sufficient confidence in the performance of the ECC sondes to use them for future tropospheric trend assessment studies.

**4.2.2.4 SUMMARY**

The regression slopes for time series of coincident differences between SAGE II and other measurements, for individual stations or latitudes, are summarized in Figure 4-5. Values range from  $\sim(-0.3 \pm 0.15)\% \text{ yr}^{-1}$  to  $\sim(0.5 \pm 0.7)\% \text{ yr}^{-1}$  (sondes, lidar, Umkehr, HALOE) for altitudes between 20 km and 35 km and  $\sim(-0.5 \pm 0.5)\% \text{ yr}^{-1}$  to  $\sim(1 \pm 1)\% \text{ yr}^{-1}$  for altitudes between 35 and 50 km. Only two systems (sondes and lidar) provide useful trend comparison data for the altitude range between 15 and 20 km. The best-matched SAGE-sonde agreement was obtained when the eight midlatitude sonde stations covering from 36°N to 52°N were combined into a single time series to calculate the regression slope of the differences. No statistically significant differences were

## OZONE TRENDS

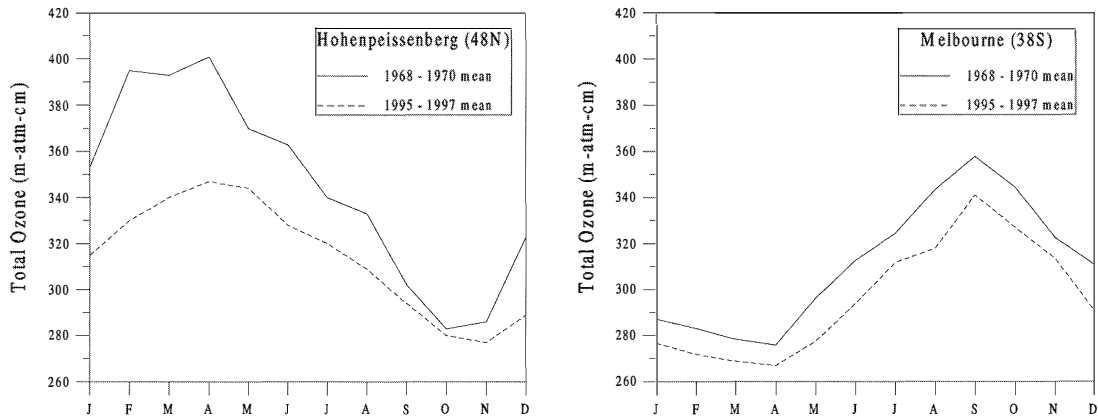


**Figure 4-6.** Changes in the annual cycle as seen at Hohenpeissenberg (48°N) and Melbourne (38°S).

obtained for the combined time series, but the mean difference was  $\sim 0.25\%$  with an error of from  $\pm(0.3 \text{ to } 0.4)\%/yr$  above  $\sim 15$  km altitude. This represents a significant improvement in SAGE versus sonde agreement since the 1994 Assessment report (WMO, 1995).

Examination of latitudinally averaged trends of differences (i.e., global trends) shows negative drifts of  $(-0.06 \text{ to } -0.4\%) \pm \sim 0.6\%/yr$  for comparisons of SBUV, HALOE, and MLS with SAGE II (i.e., the SAGE II trend is larger than other measurements). These differences, although statistically insignificant, give a slight indication of a SAGE II drift with time (the SAGE II trend is larger). SBUV/2 differences with SAGE II are of opposite sign to SBUV, HALOE, and MLS, but this is most likely due to algorithm effects brought on by a drifting orbit. Globally averaged analyses of the longest satellite time series, SBUV compared with the composite time series of SAGE I/II (1979 to 1997), show agreement to  $(-0.2 \text{ to } 0.2)\% \pm 0.2\%/yr$  in the altitude region between 20 and 50 km. All of these results show a remarkable degree of consistency and add confidence to the use of SAGE II and other satellite data in calculating long-term ozone trends.

Ozonesonde studies show good consistency throughout the stratosphere for the three ozonesonde types currently in use, and they generally agree to within about 3 to 5% from the tropopause to about 28 km. Recent analyses of a 5-year record of ozonesonde and lidar soundings in the troposphere give an encouraging indication of the ability of the sondes and the lidars to provide useful data for assessing long-term tropospheric ozone trends.

### 4.3 OZONE NATURAL VARIABILITY

The natural variability of atmospheric ozone occurs in a broad spectrum of time scales, ranging from day to day, month to month, interseasonal to interannual, and decadal. Atmospheric circulation, chemistry, and radiative processes all play important roles in the variability of ozone, as described in the previous assessments (e.g., WMO, 1990a, 1995). Natural fluctuations in total ozone include subsynoptic- and synoptic-scale variations, semiannual and annual variations, and those variations associated with the quasi-biennial oscillation (QBO), regional El Niño/La Niña effects, volcanic effects, and the solar activity cycle. The amplitude of synoptic-scale variations can be about 30% of the monthly mean over middle and polar latitudes, while the peak-to-peak amplitude of the annual cycle ranges from less than 6% in the equatorial and tropical belts to about 30% at 60°N or 60°S latitude. The amplitude of the QBO ranges from 4% to about 7-8%, and the solar activity amplitude is between 1 and 2% in the total ozone and up to 5-7% in the upper stratospheric ozone. The large transient El Niño/La Niña events produce localized regional fluctuations of up to about 5%. Large volcanic eruptions reaching the stratosphere could cause significant temporary changes that range from 2% at low latitudes up to 5% over high latitudes in winter.

#### 4.3.1 Short-Term Variations

Subsynoptic and synoptic fluctuations in ozone amounts of about 10% in the tropics, increasing to  $\sim 30\%$  over middle and high latitudes, are known from the

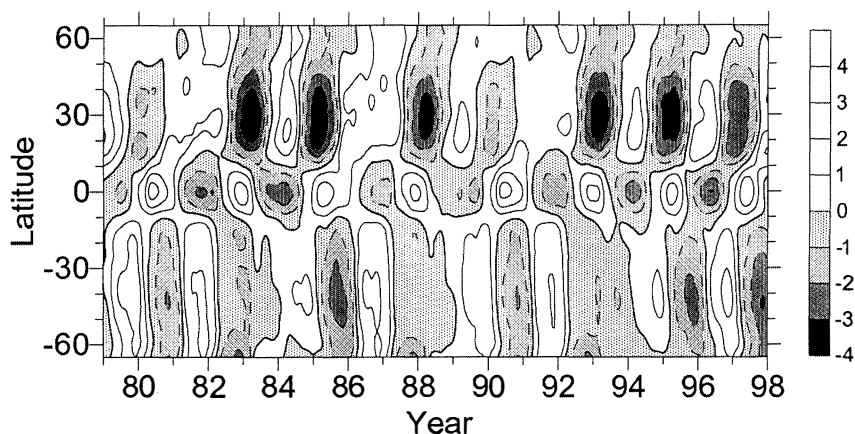


**Figure 4-7.** Time-latitude cross section of the amplitude of the QBO (in %) of the zonal-mean total ozone. (Updated from Zerefos *et al.*, 1994.)

pioneering work of Dobson *et al.* (1946) and Meetham (1937) and from more recent studies (e.g., WMO, 1995; Atkinson, 1997). Springtime tropopause folding events are accompanied by intrusion of stratospheric ozone air in the troposphere. During such events total column ozone increases by 10% or more for a day or two. In the polar winter/spring, during stratospheric warming events, large ozone increases exceeding 100-130 DU for a few days are observed.

## 4.3.2 Longer Term Variations

### 4.3.2.1 THE ANNUAL CYCLE

Total ozone in the polar and middle latitudes reaches its annual maximum in the winter/spring months and its minimum in the fall months. The annual peak-to-trough differences were, respectively,  $\sim 180$  and  $\sim 145$  DU in the pre-1976 period. Comparing these numbers with those of the most recent years (1985-1997) strongly affected by the ozone decline, it is clear that not only has the annual average ozone in the middle and polar latitudes declined by 4-7% (up to 20% over Antarctica), but also changes have occurred in the annual course. The annual peak-to-trough differences decreased by 15-20% from those of the 1964-1976 period. The changes in the annual cycle are caused mainly by the decline of the total ozone during the period of the ozone maximum (e.g., late winter/spring). An illustration of this change is shown on Figure 4-6 based on data from Hohenpeissenberg ( $48^\circ\text{N}$ ) and Melbourne ( $38^\circ\text{S}$ ).

For the global ozone annual cycle, the existence of a double maximum in the pre-ozone-hole years, re-

lated to the seasonal spring maxima in northern and southern mid and polar latitudes, is well pronounced. The ozone decline in the last two decades, particularly over Antarctica, has resulted in nearly complete disappearance of the secondary maximum of the global total ozone in September-October (e.g., Bojkov *et al.*, 1995a).

### 4.3.2.2 THE QBO

The QBO signal in total ozone is in phase with equatorial zonal winds within  $\sim 10^\circ\text{N}$  to  $\sim 10^\circ\text{S}$ , changing phase as one moves poleward. The amplitude of QBO zonal ozone anomalies is 2-4% of the long-term mean (see Figure 4-7); this is smaller than at individual stations, where it can be up to 7-8%. The effect of the QBO over middle and high latitudes is more pronounced if the transition from easterlies to westerlies happens just prior to the winter/spring season in each hemisphere. In general, during the westerly phase of the QBO the negative ozone anomalies are more pronounced over the middle and polar latitudes than the positive anomalies during the easterly phase (e.g., Bojkov, 1987; Zerefos *et al.*, 1992; Randel and Cobb, 1994; Yang and Tung, 1995; Hollandsworth *et al.*, 1995a).

The vertical profile of ozone associated with the QBO signal has been analyzed by a number of recent studies, using either SAGE II data (e.g., Hasebe, 1994; Randel and Wu, 1996) or long-term ozonesonde records over the European and Canadian regions (e.g., Bojkov and Fioletov, 1998). The analyses of the vertical structure of the QBO (Hasebe, 1994; Randel and Wu, 1996) indicate that there are two cells over the tropics and middle latitudes with peak amplitudes between 20 and

## OZONE TRENDS

27 km and 30 and 38 km altitude. This two-cell structure is separated at a “nodal” height of about 28 km. The two maxima are in phase over middle latitudes but in quadrature over the tropics. The rate of the phase descent of the QBO-related changes in ozone varies from 0.5 to 1 km/month, being greater over the polar region.

At high latitudes it is possible to isolate the QBO effect on column ozone using regression analysis linked to the equatorial zonal winds, including seasonal dependency, to account for the seasonally synchronized extratropical QBO. Seasonally-dependent regression coefficients can be used for the statistical modeling of the QBO in the vertical ozone profile (WMO, 1998). The conventional theory of the QBO signal associated with the equatorial lower stratospheric ozone considers the vertical ozone advection due to the secondary mean meridional circulation described by Reed (1965), Plumb and Bell (1982), and Trepte and Hitchman (1992) as the primary driving process (Hasebe, 1994). In spite of many sophisticated numerical model simulations, full understanding of the QBO effect on equatorial ozone has not yet been achieved (see Chapter 7 of this Assessment).

### 4.3.2.3 THE ENSO

The El Niño-Southern Oscillation (ENSO) phenomenon is aperiodic, and its effect on total ozone does not show zonal symmetry but rather follows a wave-train propagation, known over the Northern Hemisphere as the Pacific-North American (PNA) teleconnection pattern (Wallace and Gutzler, 1981), as discussed by Zerefos *et al.* (1994) and Kayano (1997). Major ENSO warm events have been suggested as partly responsible for the observed negative ozone departures in 1982-1983 (Bojkov, 1987), and indeed at the “centers of action” of ENSO (defined by Wallace and Gutzler, 1981), total ozone deficiencies as large as -4% can be expected.

Zonal averages of ozone departures during ENSO events are small and may not be important in regression models for zonal ozone. Regionally, the departures are negative and large (up to 5%) but longitudinally located in the teleconnection pattern (e.g., North Pacific, North Atlantic). Results from earlier and from the 1997-1998 ENSO event show that negative ozone anomalies were associated with regions of horizontal wind divergence in the upper troposphere over the eastern equatorial Pacific and East Africa. Positive ozone anomalies are found over regions of wind convergence in the upper troposphere over the western equatorial Pacific and east-

ern part of the Indian Ocean (Chernikov *et al.*, 1998). It should be noted here that during La Niña events these anomaly patterns are reversed (Shiotani, 1992; Zerefos *et al.*, 1994; Randel and Cobb, 1994; Kayano, 1997). Stronger uplifting and the higher tropopause associated with the convective cloud activity have been suggested as an explanation of the ozone reduction during these events.

### 4.3.2.4 THE SOLAR ACTIVITY CYCLE

Recent discussions of the influence of solar activity on stratospheric ozone can be found in Chandra and McPeters, 1994; Jackman *et al.*, 1996; Bojkov and Fioletov, 1998; Zerefos *et al.*, 1997, 1998; McCormack *et al.*, 1997; McCormack and Hood, 1997; Hood, 1997; Labitzke and van Loon, 1997; and Staehelin *et al.*, 1998b. These studies confirm that the long-term (quasi-decadal) solar activity effect on total ozone shows a total variation of ~2% from the 1964-1994 mean. The 27-day solar rotation signal in ozone is seen well in the upper stratosphere, with peak-to-trough differences of ~4-6%, which are statistically significant (Chandra and McPeters, 1994; Zerefos *et al.*, 1997). Indeed theory predicts that in the upper stratosphere the solar activity signal should be enhanced (e.g., Brasseur, 1993). Although the decadal variation in the upper stratospheric ozone observed in satellite data is similar in spatial pattern to model calculations, most model predictions are somewhat lower than observations.

The solar effect on the vertical ozone profiles, over Canada and Europe, is significant in the altitude range of 18-28 km, with an amplitude up to 4 nb per 100 units of F10.7 (10.7-cm) solar flux. This is shown in Figure 4-8 (Bojkov and Fioletov, 1998). The solar activity signal in total ozone exceeds the noise level only over the tropics; at high latitudes the solar activity components are not statistically significant when compared with the higher ozone fluctuations that prevail there.

The coincidence in recent years of the volcanic eruptions of El Chichón (1982) and Mt. Pinatubo (1991) with the beginning of the declining phase of the solar cycles 21 and 22 may well have depressed total ozone levels, thus increasing the variance in decadal time scales (Solomon *et al.*, 1996). The complications that arise have been addressed by McCormack *et al.* (1997), who calculate a solar cycle effect of ~2.5% and show that the 11-year solar signal in total ozone can be approximately separated from volcanic aerosol effects and that solar

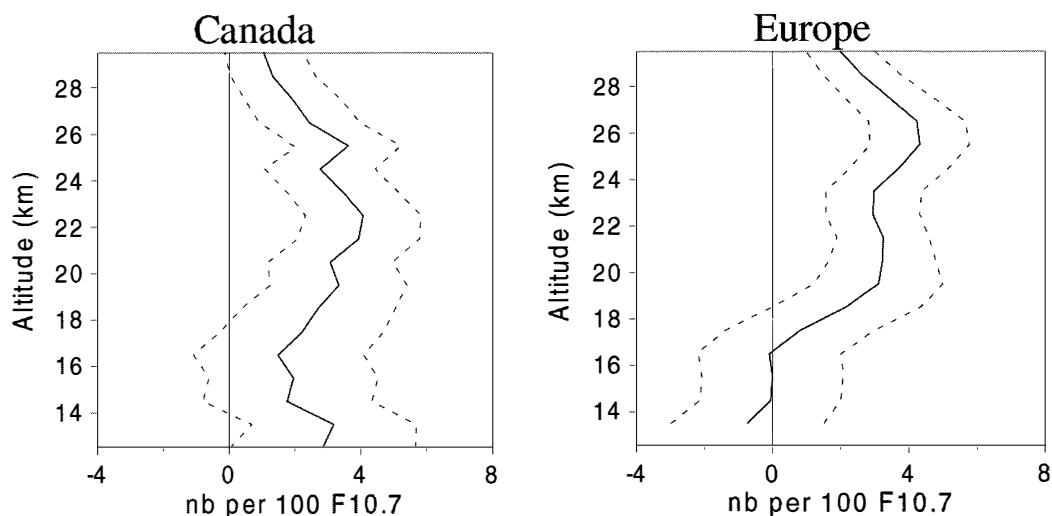


**Figure 4-8.** Solar effect in nanobars per 100 units of 10.7-cm solar flux for stratospheric ozone over Canada and Europe using ozone soundings for the period 1973-1994. (From Bojkov and Fioletov, 1998.)

activity peaks around 30 degrees of latitude. However, in the lower stratosphere, short records are indeed unlikely to allow reliable separation of volcanic and solar signals (WMO, 1998).

#### 4.3.2.5 TRANSIENT LARGE VOLCANIC EFFECTS

Large volcanic eruptions capable of injecting gases in the stratosphere can cause increases of sulfate aerosol levels with significant radiative/chemical and dynamical results (Hofmann and Solomon, 1989; Brasseur and Granier, 1992; Solomon *et al.*, 1996; Portmann *et al.*, 1996). The occurrence of a strong El Niño, combined with the El Chichón eruption, has shown the need to separate these effects from the additional variability caused by both the QBO and solar activity (e.g., Bojkov, 1987; Randel *et al.*, 1995; Solomon *et al.*, 1996; Angell, 1997; McCormack *et al.*, 1997; Zerefos *et al.*, 1992, 1994, 1997). Angell (1997) compared the impact of three major volcanic eruptions on global and regional total ozone after adjustments had been made for the QBO. He reported that the magnitude of the observed ozone deficiency, which can be attributed to the volcanic effect, ranges between 2 and 4% at the equatorial latitudes, lasting for several months after the eruption. This is similar to the results obtained by Zerefos *et al.* (1994, 1996). Larger negative ozone anomalies following the Mt. Pinatubo eruption (up to 5%) are found over the Northern Hemisphere in winter; however, it is difficult to separate the volcanic aerosol effect from the transport influ-

enced by the westerly phase of the QBO. McCormack *et al.* (1997) reached similar conclusions when estimating the volcanic effect on total ozone and introduced a term linked to the atmospheric aerosol content in a multiple regression model, in an attempt to statistically model the volcanic aerosol influence on ozone. They found that the aerosol component peaks at high latitudes, and they have attempted to separate it from the solar component.

## 4.4 STATISTICAL CALCULATIONS OF TRENDS

### 4.4.1 Introduction

Derivation of trends in ozone over time implies the use of statistical regression techniques. Some of these regression models are very complex, attempting to account for a number of sources of variation in ozone levels in order to improve the estimates of the trends in ozone over time. The regression models have also been used, of course, to investigate the effect on ozone of these other ancillary variables themselves.

A wide variety of statistical models have been used by different researchers, although most of these have evolved to have a number of similar features. The 1989 Assessment (WMO, 1990b, Chapter 2) contained brief intercomparison results of a few of these statistical models, where it was found that variations in the statistical model or the ancillary variables used had relatively

## OZONE TRENDS

minor effects on total ozone trends. The SPARC/IOC Report (WMO, 1998, Chapter 3) contains a discussion of the statistical and ancillary variable issues involved, and presents the results of an intercomparison study in which 10 researchers (or research teams) used their standard statistical models to derive ozone trends on three test datasets. Section 4.4.3 summarizes the findings.

The typical necessary or desirable terms in the statistical model include the following:

- *Seasonal means:* Some form of seasonality in ozone mean level must be accounted for; for example, with a monthly trend model it is common to fit monthly means, although sometimes a sum of seasonal harmonic terms is used, often with fewer than the 12 degrees of freedom used with monthly means. With weekly data, harmonic seasonal terms are the norm.
- *Seasonal trends:* We now know that ozone trends vary by season and that this must be allowed for by use of seasonal trend terms such as monthly or seasonal trends (sometimes also incorporated as harmonics). Figure 4-9 shows for Northern Hemisphere Dobson stations the monthly dependence of ozone jointly with the monthly dependence of ozone trends calculated from the model used for Table 4-4 in Section 4.5.1. The largest trends in ozone occur at the times of the highest ozone, in the winter-spring.
- *Ancillary variables:* Other variables are known to affect ozone levels; accounting for them can reduce noise levels, thereby improving trend detection capability, and in some cases can remove bias. An example of the latter would be accounting for a solar effect when the trend period does not cover several solar cycles. The most common ancillary variables accounted for are the solar effect (the 10.7-cm radio flux or the sunspot number are used as proxies) or the quasi-biennial oscillation (QBO) in equatorial stratospheric winds. Failure to account for the QBO, especially in the tropics, can aggravate autoregression in the residuals from the regression and lead to larger uncertainty (standard errors) in the trends.
- *Autoregression:* Even when all of the above effects are taken into account, monthly ozone residuals remain correlated with the previous month's residuals, especially when noise levels are lower, such as for total ozone or zonal means; this effect is known as

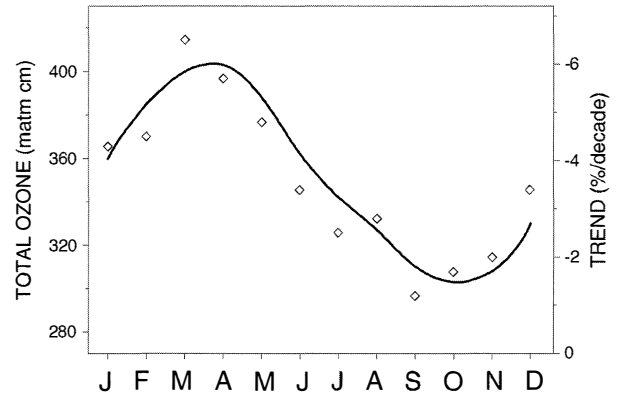


**Figure 4-9.** The seasonal dependence of total ozone levels (solid line) and total ozone trends (symbols) for January 1979 to December 1997 over Dobson stations in the band 35°-60°N (average of station trends). (From Bojkov *et al.*, 1995a, and updated by the authors.)

autocorrelation. This is usually accounted for by permitting the residual series,  $N_t$  to depend on its previous values, often as an order-1 autoregressive (AR(1)) series,  $N_t = \phi \cdot N_{t-1} + e_t$ , where the  $e_t$  series is uncorrelated (Box *et al.*, 1994; Bojkov *et al.*, 1990). Allowing for this in the regression model does not usually change the calculated trends by much, but it increases the reported standard errors to reflect an increased uncertainty in the trend estimate. Some authors use ordinary least-squares techniques for the regression estimates but obtain the standard errors of the trend estimates through bootstrap or jackknife (resampling) techniques; these techniques have been found to lead to standard errors similar to those of methods using autoregressive models.

- *Seasonal weighting:* Ozone is more variable in winter/spring and many researchers take this into account by statistical weighting of the observations according to some estimate of seasonal variance, for example, using the reciprocals of the monthly variances of the residuals from the fit. Although this has little effect on the calculated trends themselves, it increases the uncertainty estimates of the winter/spring trends while decreasing those of the summer/fall trends.
- *Dynamical variables:* Several authors (e.g., Ziemke *et al.*, 1997; Wege and Claude, 1997) have investigated

the effects of dynamical/meteorological variables on ozone and on ozone time trends. These dynamical variables can be associated with a substantial fraction of the variance in ozone. Nevertheless, use of these variables in regression models where the primary purpose is to estimate ozone time trends leads to difficulties in interpretation of the resulting trends in ozone. As an example, long-term changes in ozone will themselves lead to changes in stratospheric temperatures; regression of ozone on both time and temperature will lead to ozone time trends (usually of lesser magnitude), trends which do not represent changes in ozone due to any particular external influence. Dynamical variables are not included in any of the trend regression models considered in this chapter.

- *Standard errors for seasonal trends:* Proper calculation of the trend standard errors for seasonal trends when monthly trends are fitted, or for a year-round trend when monthly or seasonal trends are fitted, requires use of the covariance matrix of the trend estimates. This is particularly important when the autoregression coefficient is large, because then, for example, the January trend is highly correlated with the February and December trends, and the December-January-February average trend will have larger uncertainty than one would calculate if it were assumed that these trends had statistically independent errors.
- *Model variations:* A number of model variations have been considered, usually for purposes of more detailed analysis of ancillary variables. For example, possible seasonal effects of solar or QBO variations or in the autoregression coefficient have been considered, either in magnitude or time lag. These variations typically have little effect on reported ozone time trends, although inflation of the standard errors can occur if the model is seriously over-parameterized.

The above model aspects are discussed in more detail in the SPARC/IOC trends report (WMO, 1998), and specific features of the models of 10 research groups are tabulated. Intercomparison results on three test datasets for these groups are summarized in Section 4.4.3 below.

The total ozone trend results in Section 4.5 are calculated from statistical models identical (or nearly so) to those used in the last Assessment (WMO, 1995). This model is described in more detail in Section 4.4.2. The

ozone vertical profile trends in Section 4.6 were calculated by a variety of researchers, depending on instrument system; the SPARC/IOC report (WMO, 1998) contains the details of these statistical models.

#### 4.4.2 Total Ozone Trend Statistical Model

This section describes the core statistical model used in deriving the total ozone trends in Section 4.5 (see Bojkov *et al.*, 1990). Let  $y_t$  represent monthly total ozone values for a particular series, for example, a Dobson station or a TOMS zonal mean. The statistical model for  $y_t$  is of the form

$$y_t = (\text{Monthly mean}) + (\text{Monthly trend}) + (\text{Solar effect}) + (\text{QBO effect}) + \text{Noise}$$

or more precisely,

$$y_t = \sum_{i=1}^{12} \mu_i I_{i;t} + \sum_{i=1}^{12} \beta_i I_{i;t} R_t + \gamma_1 Z_{1;t} + \gamma_2 Z_{2;t} + N_t \tag{4-1}$$

with the following definitions:

- $\mu_i$  = Ozone mean in month  $i$ ,  $i = 1 \dots 12$ .
- $I_{i;t}$  = Indicator series for month  $i$  of the year, i.e., 1 if the month corresponds to month  $i$  of the year, and 0 otherwise.
- $\beta_i$  = Trend in Dobson units/yr in month  $i$  of the year.
- $R_t$  = Linear ramp function measuring years from the first month of the series; equal to  $(t - t_0)/12$ . For series beginning before 1970, it is often taken to be a ramp function equal to zero for  $t < t_0$ , where  $t_0$  corresponds to 12/69, and then  $(t - t_0)/12$  for  $t \geq t_0$ .
- $Z_{1;t}$  = Solar 10.7-cm flux series, with  $\gamma_1$  the associated coefficient.
- $Z_{2;t}$  = QBO 50-mb wind series lagged some appropriate number of months (latitude dependent), with  $\gamma_2$  the associated coefficient (TOMS analyses). These terms are sometimes represented as two terms (50-mb and 30-mb winds) (Dobson analyses).
- $N_t$  = Residual noise series.

The residual noise series  $N_t$  is modeled as an autoregressive AR(1) series, with weights inversely proportional to the monthly residual variances.

## OZONE TRENDS

### 4.4.3 SPARC/IOC Statistical Model Intercomparison

As part of the SPARC/IOC trends report (WMO, 1998), an intercomparison of trend models was done, in which each research group was asked to analyze the same three datasets. The purpose of the exercise was to determine to what extent the differences in the statistical trend models commonly in use would affect ozone trend estimates and their uncertainties (standard errors). The three datasets used were (a) Nimbus-7 TOMS 40°-50°N zonal-mean ozone from November 1978-April 1993; (b) Uccle sondes monthly-mean ozone at 13 km from January 1969-December 1996; (c) SAGE I and II monthly-mean ozone at 40.5 km, 35°-45°N, from February 1979-December 1996. The test sets differed in the amount of missing data, with the TOMS dataset having a complete series, and at the other extreme, the SAGE combination dataset having serious missing-data issues with a monthly pattern that caused some researchers to obtain somewhat different results when calculating seasonal trends.

The following are the main conclusions of the model intercomparison (taken from the SPARC/IOC report), which are also illustrated in Figure 4-10 (also from the SPARC/IOC report); this is the comparison for the SAGE I/II test data, in which inter-researcher differences were the most extreme. For the test data (TOMS) with no missing monthly values, all researchers obtained similar results for trends. There were variations in standard errors, however, that were large enough to give some concern, as they affect the statistical significance of the trends. For example, long-term total ozone trends from SBUV near the equator border on statistical significance (WMO, 1995). Lack of proper calculation of standard errors in such a situation may result in non-significant trends being declared statistically significant, or vice versa.

For the test datasets with missing values, particularly the SAGE set with large numbers of missing values in a strong pattern form, some researchers' results deviated substantially from the average, with respect to both trend estimate and, especially, standard error. Some researchers feel that in such situations, it is better to fit a simpler model to maintain stability; for example, by fitting seasonal trends directly or by use of reduced numbers of harmonic terms for the seasonal trends and possibly also the seasonal cycle.

Based on these intercomparisons, there seems reason to suggest that researchers provide good documen-

tation for the features of their statistical model. Particularly, when any patterns of missing data exist that have strong time-dependent features, the methods of handling the missing data should be discussed in detail.

## 4.5 LONG-TERM CHANGES IN TOTAL OZONE

### 4.5.1 Global, Latitudinal, and Longitudinal Trends

The last Assessment (WMO, 1995) reported trend results for total ozone for observations through February 1994 for ground-based stations and through 5/94 for satellite (SBUV + SBUV/2) instruments. This section updates those trends through 12/97 for ground-based stations and satellite data (TOMS). Additional TOMS data through 6/98 (indicated by different symbols) are included in the time series plots of total ozone in order to show the most recent data; however, these months are not included in the trend calculations, in order that the ground-based and satellite data time periods be identical.

Prior Assessments (WMO, 1992, 1995) have documented substantial declines in mid- to high-latitude total ozone amounts, while indicating little if any change over equatorial latitudes. Percentage changes have been found to be higher in the winter/spring seasons than in the summer/fall seasons; the larger percentage changes follow the higher levels of ozone in the winter/spring seasons (see Figure 4-9). Figure 4-11 shows contour plots of mean ozone by month and latitude for a baseline period (1964-1976) compared to recent years. The left panels show mean ozone from ground-based stations for the period 1964-1976 (upper panel) and 1985-1997 (lower panel). The right panels show satellite data, using SBUV data 1970-1972 in the upper panel with Nimbus-7 TOMS (1985-1993) and Earth Probe TOMS (1996-1997) data in the lower. Ground and satellite data are in good agreement, with ozone field differences within  $\pm 2\%$  except over the polar regions. The decline between the two periods in southern midlatitudes is 6.1%, with monthly contributions of more than 10% coming from September-November (ozone-hole months). Over northern latitudes the decline is 3.5%, with monthly contributions of more than 5.5% coming from December-April.

The most recent available data indicate a lessening of the large negative trends in total ozone seen in the 1980s and early 1990s. Figure 4-12 shows monthly deviations from (non-polar) total ozone (area weighted,

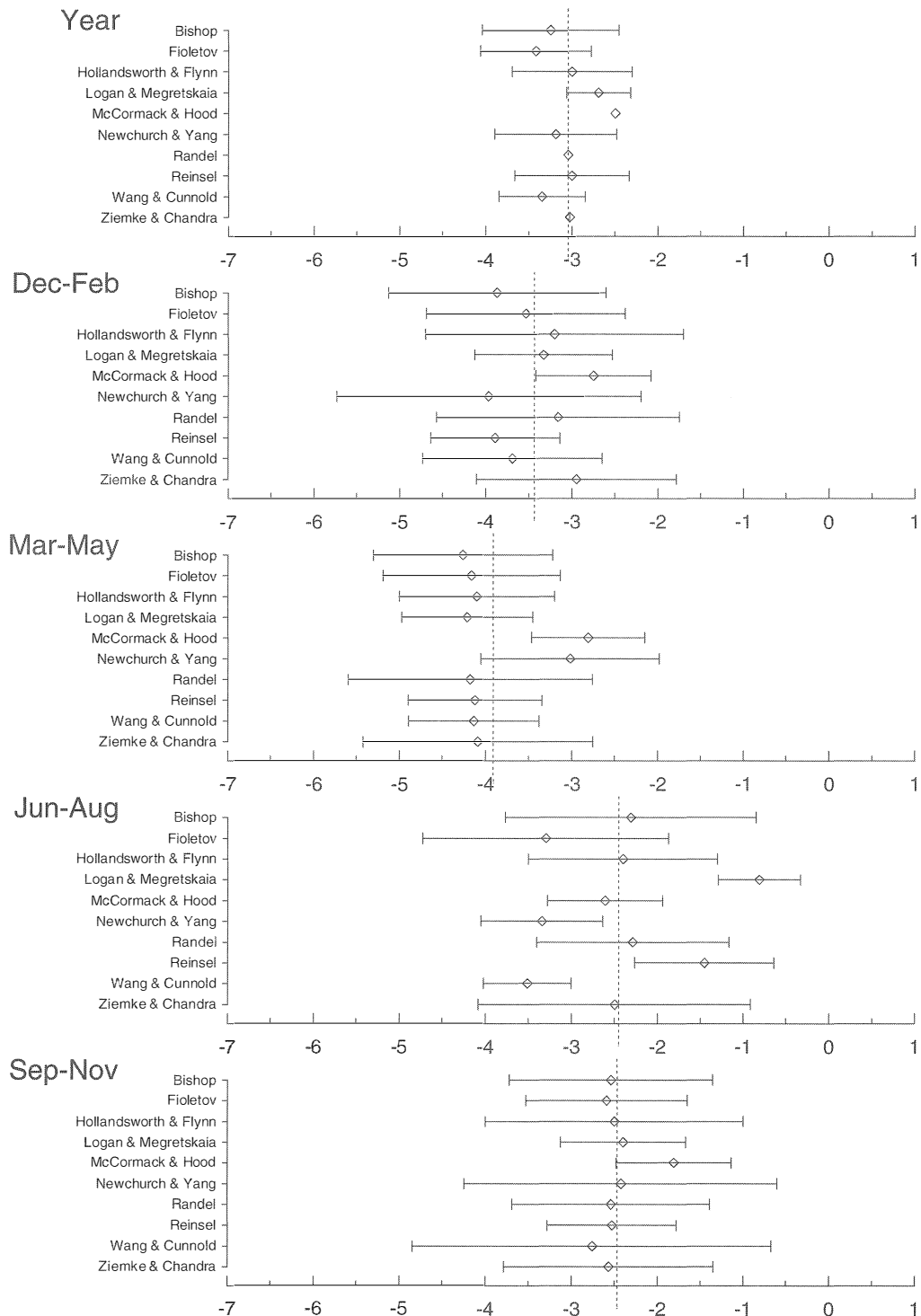


**Figure 4-10.** Ozone trend estimates by researchers for SPARC/IOC Test Set 3, SAGE I/II 40.5-km ozone at 35°-45°N for February 1979-December 1996. Trends are in  $10^9 \text{ cm}^{-3}/\text{yr}$ . Uncertainty intervals are one standard error. Year-round trends (average over all months) were calculated where possible if not given directly by the researcher, but in some cases not enough information was given to calculate the corresponding standard error. The vertical dotted line is the mean of all researchers' trend estimates. (From WMO, 1998.)

## OZONE TRENDS

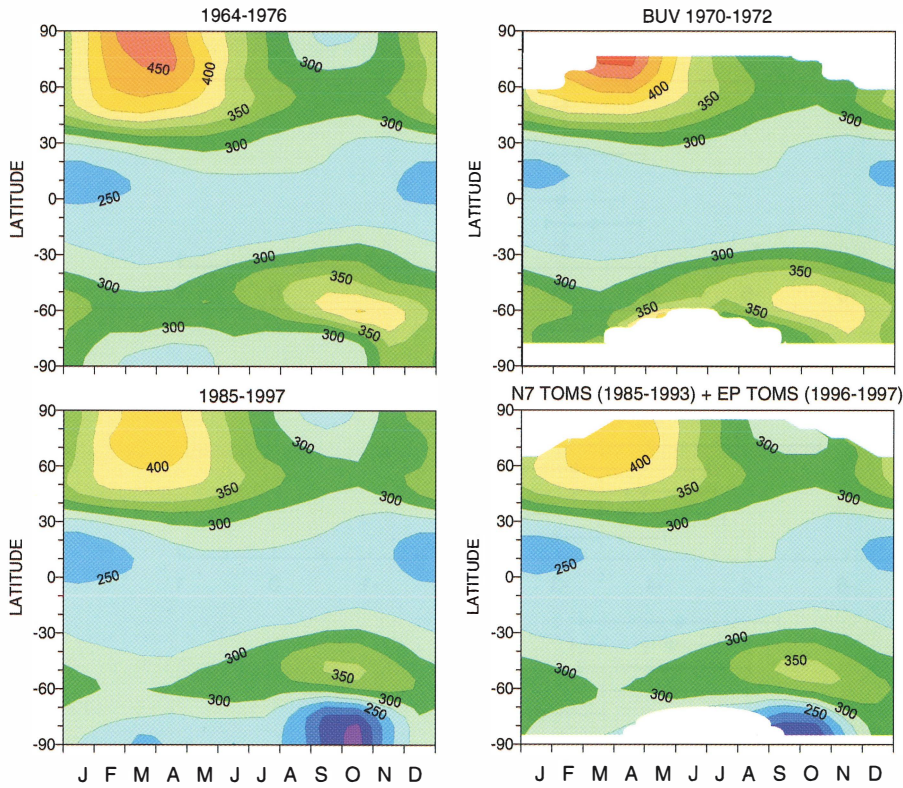


**Figure 4-11.** Contour plots of levels of total ozone by latitude and month. Left plots: Ground-based data for the periods 1964-1976 (upper panel) and 1985-1997 (lower panel). Right plots: Satellite data for the periods 1970-1972 (BUV, upper panel) and 1985-1997 (Nimbus-7 and Earth Probe TOMS, lower panel).

60°S - 60°N Total Ozone Adjusted for Seasonal, Solar and QBO Effects

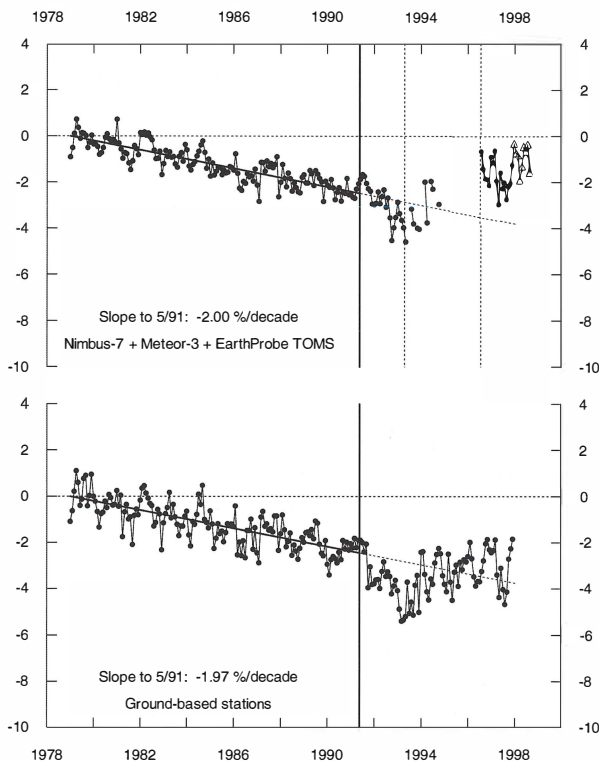


**Figure 4-12.** Deviations in total ozone, area weighted over 60°S-60°N. A seasonal trend model, including solar and QBO effects, was fit to ozone over the period 1/79 to 5/91. Deviations represent ozone adjusted for baseline monthly means (1/79 intercepts), solar and QBO effects, and seasonal differences in the trend, while the year-round average trend is not removed; then deviations are expressed in percentage of baseline monthly mean. The upper panel shows TMS deviations and the lower panel represents a ground-based series constructed from average ozone at stations in 5° latitude zones. Trend models are fit independently to TMS and ground-based ozone. The solid straight line represents the least squares fit to the deviations up to 5/91, and is extended as a dotted line through 12/97. The bold vertical line is at the time of the Mt. Pinatubo eruption, 5/91. Dotted vertical lines represent switches from one TMS satellite to another. Open triangles distinguish TMS data for the months 1/98 through 6/98.

60°S-60°N) over time for two instrument systems: (a) Nimbus-7 (11/78-4/93) + Meteor-3 (5/93-10/94) + Earth Probe (8/96-9/98) TOMS; and (b) ground-based stations (1/64-12/97). For this figure, no further adjustments were made over the most recently revised data for any possible calibration differences between different satellites (see Section 4.2 for discussion of the instrument data quality). The deviations shown in Figure 4-12, obtained from monthly total ozone using a least-squares fit of the data up to 5/91, are adjusted for seasonal cycle (1/79 monthly intercepts), solar and QBO effects, and monthly differences in the trend while leaving in the average trend, and are expressed as a percentage of the 1/79 monthly intercepts. Satellite and ground-based data are fit separately, but have nearly identical trends of about -2%/decade up to 5/91.

Both data systems show the same features. There is a strong, nearly linear, decrease in total ozone throughout the 1980s, followed by a sudden decrease in 1992-1993 due to effects of the Mt. Pinatubo eruption. There is a recovery from the Mt. Pinatubo effect in 1994, and subsequent total ozone levels (through 9/98 for Earth Probe TOMS) show no evidence of further decreases. It must be kept in mind that the 1996-1998 Earth Probe data are considered preliminary, but current overpass intercomparisons with the ground-based network indicate only about a 1%-level difference (Earth Probe higher) and perhaps 0 to 0.5% difference between Earth Probe TOMS and Nimbus-7 TOMS (Earth Probe higher). The ground-based data in the post-1994 period are slightly lower than the Earth Probe TOMS data, even if one were to consider that the Earth Probe data might be biased high relative to Nimbus-7 TOMS by perhaps 0.5%. However, it should be noted that the ground-based stations are very scarce in the tropics and Southern Hemisphere; the ground-based series in Figure 4-12 is constructed from average ozone for stations in 5° latitude zones, and for a few zones in the Southern Hemisphere, the zonal average had to be interpolated from adjacent zones.

One reason why the pre-Pinatubo trend does not extrapolate well to the present time is that a reduction in the slope of the downward trend in total ozone is to be expected from the leveling off of the stratospheric equivalent chlorine loading. Figure 4-13 shows a plot of the equivalent effective stratospheric chlorine (EESC) from Chapter 11 (A1 scenario) on the expanded time scale of 11/78-6/98, indicating a flattening of the equivalent chlorine concentration over the years 1995-1998, so that the

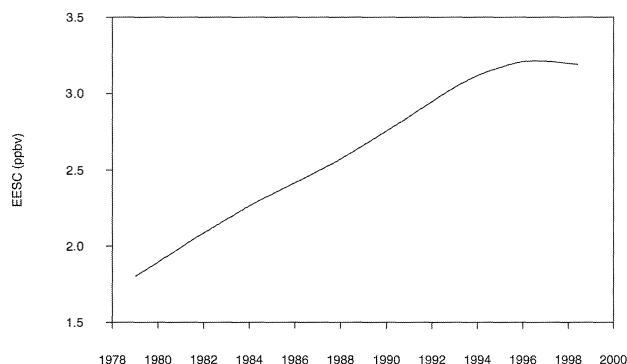


**Figure 4-13.** Equivalent effective stratospheric chlorine (scenario A1) from Chapter 11, on an expanded time scale of 1/79 to 6/98.

pre-Pinatubo trend in chlorine loading has not been maintained. Furthermore, enhanced stratospheric aerosols were present throughout much of the decade of the 1980s due to earlier volcanic eruptions, likely enhancing the downward trend in ozone observed before the eruption of Mt. Pinatubo. It is also possible that long-term variations such as the solar effect are not represented well enough in the statistical model and may account for some of the leveling off. Figure 4-14 shows the 25°N-60°N deviations when the seasonal, solar, and QBO effects are adjusted for by the linear regression, and Figure 4-15 for the same latitude range, but where the seasonal effect only is adjusted for. The long-term ozone variations are larger on Figure 4-15 than on Figure 4-14 because the solar effect is not removed, and as a result the recent data do not appear to show as much of a significant deviation from the long-term trend; furthermore, the recent data are for a solar minimum, and adjustment for the solar effect in Figure 4-14 results in a relative raising of the data compared to Figure 4-15. It seems likely that even if the recent decline of the 1980s midlatitude trends is primarily due to a leveling of the stratospheric equivalent chlorine concentration, it may be several more years before we can make this attribution. It should also be noted that this reduction of downward trend should *not* be interpreted as a recovery of ozone (see Chapter 12).

Figure 4-14 shows the consistency of the TOMS and ground-based records where the ground-based data are plentiful. Though much more variable than the near-global data, the satellite and ground-based Northern Hemisphere data show nearly identical deviations on a month-to-month basis. Again, there is a leveling of the

## OZONE TRENDS

25°N - 60°N Total Ozone Adjusted for Seasonal, Solar and QBO Effects

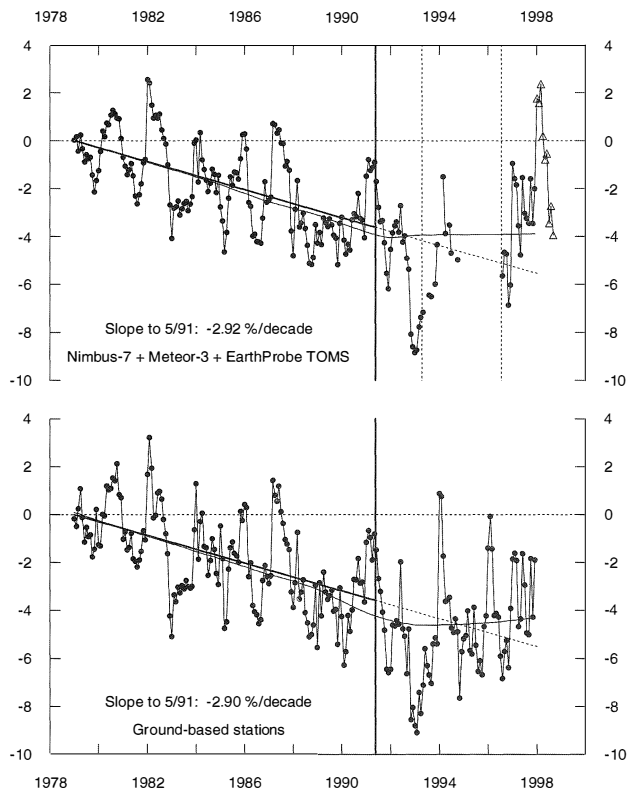


**Figure 4-14.** Deviations in total ozone, area weighted over 25°N-60°N. Calculations of deviations were done as in Figure 4-12. The solid straight line represents the least squares fit to the deviations up to 5/91, and is extended as a dotted line through 12/97. The thin smoother lines are from a lowess local regression fit; the fit does not include the 1/98-6/98 TOMS data (triangles).

ozone trend in the post-1994 period. Extrapolation of the pre-Pinatubo trend of  $-2.9\%/decade$  would predict an ozone deviation of  $-5.5\%$  at the end of 1997, while the lowess smoother on the plot indicates the deviations have instead averaged about  $-4\%$  in the last 2 or 3 years. When the same calculations are performed on a seasonal basis, the corresponding winter/spring (December-May) and summer/fall (June-November) changes average about  $-5.5\%$  and  $-2.8\%$ , respectively, while a linear extrapolation of the pre-Pinatubo trend would predict  $-7.6\%$  and  $-3.4\%$ , respectively.

The Southern Hemisphere midlatitudes also exhibit a leveling off of the trend, as indicated in Figure 4-16,

25°N - 60°N Total Ozone Adjusted for Seasonal Effects Only

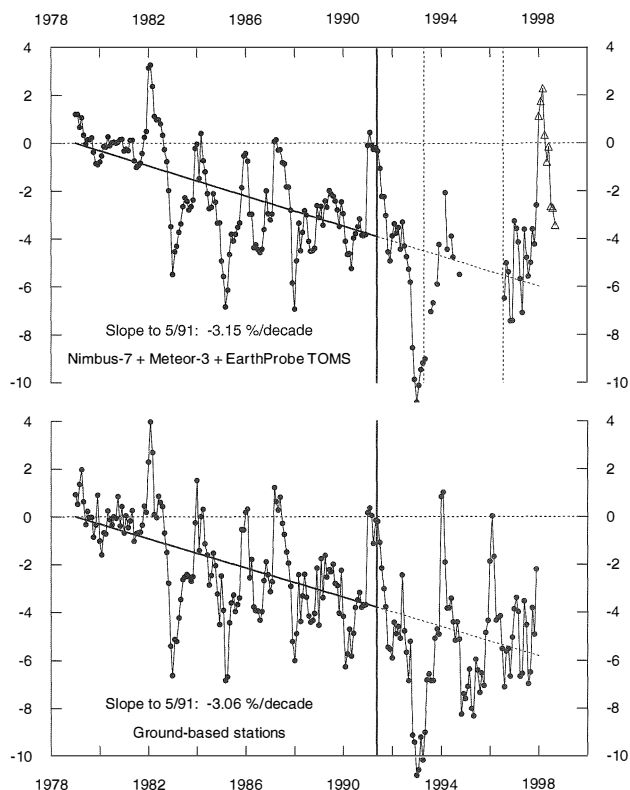


**Figure 4-15.** Deviations in total ozone, area weighted over 25°N-60°N. Calculations of deviations were done as in Figure 4-12, except that the solar and QBO effects were not fit and not adjusted for. The solid straight line represents the least squares fit to the deviations up to 5/91, and is extended as a dotted line through 12/97.

although 1997 shows some extremely low values that would be yet lower if the plot had not been adjusted for the solar effect. Nevertheless, the pre-Pinatubo trend is not maintained after 1994; trend extrapolation would predict  $-7.2\%$  depletion at the end of 1997, while the lowess fit indicates a smoothed 1997 value of about  $-4\%$  (satellite) or  $-5\%$  (ground).

As an update to previous assessments, trends in total ozone have been calculated for ground-based stations using data through December 1997 at most stations. Table 4-4 shows the list of stations used, and seasonal trends and standard errors at each station over the period 1/79 through 12/97. The data used are discussed

## 25°S - 60°S Total Ozone Adjusted for Seasonal, Solar and QBO Effects

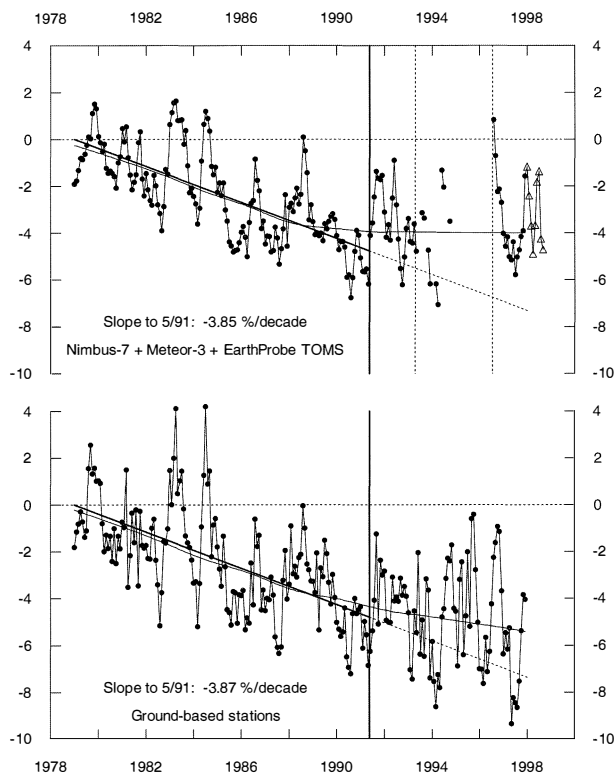


**Figure 4-16.** Deviations in total ozone, area weighted over 25°S-60°S. Calculations of deviations were done as in Figure 4-12, including adjustment for solar and QBO effects. The solid straight line represents the least squares fit to the deviations up to 5/91, and is extended as a dotted line through 12/97. The thin smoother lines are from a loess local regression fit; the fit does not include the 1/98-6/98 TOMS data (triangles).

in Section 4.2. Trends have been estimated using the statistical model documented in Section 4.4.2. In the lower section of the table are shown trend results using regional series constructed as averages of the ground-based stations in each region. The stations represented by the former-USSR regions used filter, not Dobson/Brewer, instruments.

The individual-station seasonal total ozone trends from Table 4-4 are plotted versus latitude in Figure 4-17. Zonal-average trends are overlaid on the individual station results and are also tabulated in Table 4-5, together with zonal average trends over the longer period 1/64-12/97 (trends are from 1/70 using a “hockey stick”

ramp function with a level baseline over 1/64-12/69 and a linear ramp beginning 1/70). The zonal-average ground-based trends 1/79-12/97 are shown again in Figure 4-18 in comparison with TOMS trends.

Seasonal trends have also been calculated from a monthly trend model (Section 4.4.2) for TOMS zonal-mean total ozone using, without any additional calibration adjustments, data from Nimbus-7 over 1/79-4/93, Meteor-3 over 5/93-11/94 where enough data are available to compute a zonal mean, and Earth Probe over 8/96-12/97. These trends are given in Table 4-6 in 5° latitude zones, and plotted in Figure 4-18 (with the ground-based station zonal-mean trends for comparison).

Both the ground-based station trends and TOMS zonal trends exhibit the now-familiar pattern (e.g., WMO, 1992, 1995; Harris *et al.*, 1997) with the following features: (a) small, statistically non-significant trends in equatorial regions (20°S-20°N) in all seasons and year round; (b) large, statistically significant negative trends in both hemispheres in mid and high latitudes; (c) in the Northern Hemisphere, much larger (more negative) trends in the winter and spring seasons (December-January-February, March-April-May), about -3 to -6%/decade, than in summer and fall (June-July-August, September-October-November), about -1 to -3%/decade; (d) in the Southern Hemisphere high latitudes, very large negative trends in winter (June-July-August), up to -6%/decade, and, especially, spring (September-October-November), up to -10%/decade, due to the influence of the Antarctic ozone hole.

The impact of the negative trend increases in the 1980s over the 1970s, or “trend acceleration,” noted in the previous Assessment (WMO, 1995; Harris *et al.*, 1997) can be seen from the results in Table 4-6, where trends over the period 1/79-12/97 are larger in mid and high latitudes than those over the longer period, 1/70-12/97 (data from 1/64), especially in winter/spring. Very low ozone levels in late 1991 through mid-1993 (e.g., Bojkov *et al.*, 1993; Gleason *et al.*, 1993) may affect the trend estimations (WMO, 1995; Harris *et al.*, 1997), although the effect is not very strong in comparison with the error induced by the natural ozone variability, and inclusion of an additional 4 years or more of data beyond that time lessens the impact still further. Trends may be reduced by the inclusion of data after 1994, as described earlier. Table 4-7 shows the results of linear trend calculations over different periods starting in January 1979 and ending from December 1991 to December 1997 with 1-year increments. In northern midlatitude

## OZONE TRENDS

**Table 4-4. Total ozone trend estimates for individual stations and regions.** Seasonal and annual trend estimates by station/region are shown for the period January 1979 through December 1997. The first and the last months of observations are shown if they are different from January 1964 and December 1997 (read 68-08 as August 1968). For regions, an approximate mean latitude is indicated. For stations marked by the asterisk see discussion in Section 4.2. For all other stations the data available from the World Ozone Data Centre were used. The June-August Antarctic trend is based on a very limited number of moon observations and is not reliable.

Station/Region	Latitude	Year-Month		Trend (%/decade $\pm 2\sigma$ )				Year
		First	Last	Dec-Feb	Mar-May	Jun-Aug	Sep-Nov	
<i>Individual Stations</i>								
St. Petersburg	60.0°N	68-08		-7.4 $\pm$ 4.0	-6.6 $\pm$ 2.7	-4.1 $\pm$ 1.9	-3.7 $\pm$ 2.2	-5.6 $\pm$ 1.7
Churchill	58.8°N	64-12		-6.2 $\pm$ 4.1	-4.0 $\pm$ 2.4	-4.5 $\pm$ 1.8	-4.2 $\pm$ 2.9	-4.8 $\pm$ 1.6
Edmonton	53.6°N			-3.0 $\pm$ 3.1	-5.5 $\pm$ 2.4	-4.2 $\pm$ 2.0	-2.2 $\pm$ 2.5	-3.8 $\pm$ 1.5
Goose Bay	53.3°N			-3.0 $\pm$ 3.6	-3.8 $\pm$ 3.1	-4.3 $\pm$ 2.3	-3.0 $\pm$ 2.5	-3.5 $\pm$ 1.8
Potsdam	52.4°N			-4.1 $\pm$ 3.7	-6.6 $\pm$ 3.0	-2.3 $\pm$ 2.1	-1.6 $\pm$ 2.4	-3.8 $\pm$ 1.7
Belsk	51.8°N			-6.0 $\pm$ 3.4	-5.6 $\pm$ 2.6	-3.1 $\pm$ 1.9	-1.1 $\pm$ 2.2	-4.1 $\pm$ 1.6
Bracknell/Camborne	51.4°N			-3.6 $\pm$ 3.6	-7.0 $\pm$ 2.7	-3.2 $\pm$ 1.7	-1.2 $\pm$ 2.6	-4.0 $\pm$ 1.5
Uccle	50.8°N	71-07		-4.9 $\pm$ 3.4	-7.8 $\pm$ 2.7	-2.2 $\pm$ 1.7	-1.8 $\pm$ 2.5	-4.4 $\pm$ 1.5
Hradec Kralove	50.2°N			-5.2 $\pm$ 3.4	-6.3 $\pm$ 2.3	-3.9 $\pm$ 1.7	-1.0 $\pm$ 2.0	-4.3 $\pm$ 1.4
Hohenpeissenberg	47.8°N	68-05		-6.0 $\pm$ 3.3	-7.2 $\pm$ 3.1	-2.8 $\pm$ 1.6	-1.4 $\pm$ 2.2	-4.6 $\pm$ 1.6
Caribou	46.9°N			-3.4 $\pm$ 3.4	-4.4 $\pm$ 2.5	-3.0 $\pm$ 1.6	-2.2 $\pm$ 2.3	-3.3 $\pm$ 1.5
Bismarck	46.8°N			-2.0 $\pm$ 2.5	-4.6 $\pm$ 2.3	-2.0 $\pm$ 1.4	-2.0 $\pm$ 1.7	-2.7 $\pm$ 1.2
Arosa	46.8°N			-4.4 $\pm$ 2.8	-5.9 $\pm$ 2.6	-1.7 $\pm$ 1.4	-0.8 $\pm$ 1.9	-3.4 $\pm$ 1.4
Sestola*	44.2°N	76-11		-4.1 $\pm$ 3.7	-7.4 $\pm$ 3.3	-3.5 $\pm$ 1.9	-1.7 $\pm$ 2.4	-4.4 $\pm$ 1.7
Haute Province	43.9°N	83-09		-4.7 $\pm$ 5.4	-9.2 $\pm$ 4.0	-1.7 $\pm$ 3.0	-0.4 $\pm$ 2.7	-4.4 $\pm$ 2.3
Toronto*	43.8°N			-2.8 $\pm$ 3.1	-4.2 $\pm$ 2.4	-2.4 $\pm$ 1.6	-0.3 $\pm$ 2.3	-2.5 $\pm$ 1.4
Sapporo	43.1°N			-5.5 $\pm$ 2.4	-5.1 $\pm$ 2.3	-4.0 $\pm$ 2.1	-2.7 $\pm$ 1.8	-4.5 $\pm$ 1.4
Vigna Di Valle	42.1°N		97-02	-7.8 $\pm$ 3.1	-7.6 $\pm$ 3.6	-3.7 $\pm$ 2.2	-3.4 $\pm$ 2.3	-5.8 $\pm$ 1.8
Boulder	40.0°N			-2.1 $\pm$ 2.3	-5.9 $\pm$ 2.5	-2.8 $\pm$ 1.3	-1.4 $\pm$ 1.7	-3.2 $\pm$ 1.2
Xianghe	39.8°N	79-01		-2.7 $\pm$ 2.1	-3.9 $\pm$ 2.4	-1.3 $\pm$ 1.9	-0.2 $\pm$ 1.7	-2.1 $\pm$ 1.3
Lisbon	38.8°N	67-08		-0.7 $\pm$ 2.4	-5.9 $\pm$ 2.2	-2.9 $\pm$ 1.6	-0.7 $\pm$ 1.8	-2.7 $\pm$ 1.1
Wallops Island	37.9°N	67-06		-3.9 $\pm$ 3.1	-5.0 $\pm$ 2.6	-2.9 $\pm$ 1.6	-1.5 $\pm$ 2.0	-3.4 $\pm$ 1.4
Nashville	36.3°N			-3.2 $\pm$ 2.7	-4.8 $\pm$ 3.0	-2.4 $\pm$ 1.8	-1.3 $\pm$ 2.1	-3.0 $\pm$ 1.5
Tateno	36.1°N			-2.3 $\pm$ 2.8	-1.9 $\pm$ 2.4	-1.3 $\pm$ 1.7	0.1 $\pm$ 1.6	-1.4 $\pm$ 1.3
Kagoshima*	31.6°N			-2.1 $\pm$ 2.4	-1.7 $\pm$ 2.0	-0.7 $\pm$ 1.6	1.0 $\pm$ 1.6	-0.9 $\pm$ 1.2
Quetta	30.2°N	69-08		-4.3 $\pm$ 2.4	-2.8 $\pm$ 2.9	-1.5 $\pm$ 2.2	-0.9 $\pm$ 1.9	-2.4 $\pm$ 1.8
Cairo	30.1°N	74-11		-1.6 $\pm$ 2.6	-2.3 $\pm$ 2.3	-1.9 $\pm$ 1.2	-1.3 $\pm$ 1.3	-1.8 $\pm$ 1.2
New Delhi	28.6°N	75-01		-1.9 $\pm$ 2.1	-1.4 $\pm$ 2.3	-0.3 $\pm$ 1.9	0.5 $\pm$ 1.3	-0.8 $\pm$ 1.4
Naha	26.2°N	74-04		-1.4 $\pm$ 2.2	-1.4 $\pm$ 1.9	0.2 $\pm$ 1.3	0.5 $\pm$ 1.4	-0.5 $\pm$ 1.1
Varanasi	25.5°N	75-01	97-08	-2.8 $\pm$ 2.2	-2.8 $\pm$ 2.0	-2.8 $\pm$ 1.3	-2.0 $\pm$ 1.4	-2.6 $\pm$ 1.1
Kunming	25.0°N	80-01		-0.5 $\pm$ 2.3	-1.0 $\pm$ 2.3	0.7 $\pm$ 1.6	-0.4 $\pm$ 1.4	-0.3 $\pm$ 1.2
Mauna Loa	19.5°N			-1.5 $\pm$ 2.4	-2.2 $\pm$ 2.1	0.0 $\pm$ 1.6	0.2 $\pm$ 1.4	-0.9 $\pm$ 1.3
Kodaikanal	10.2°N	76-08		0.6 $\pm$ 1.7	-1.0 $\pm$ 1.5	-1.8 $\pm$ 1.8	-1.5 $\pm$ 1.7	-1.0 $\pm$ 1.1
Singapore	1.3°N	79-02		1.2 $\pm$ 1.6	1.1 $\pm$ 1.7	-0.4 $\pm$ 1.9	0.0 $\pm$ 1.6	0.4 $\pm$ 1.3
Nairobi*	4.7°S	84-04		-1.2 $\pm$ 2.5	0.9 $\pm$ 2.1	-1.4 $\pm$ 2.3	-0.8 $\pm$ 2.4	-0.6 $\pm$ 1.4
Natal	5.8°S	78-12		0.8 $\pm$ 1.6	1.4 $\pm$ 1.7	-1.4 $\pm$ 1.5	-0.3 $\pm$ 1.5	0.1 $\pm$ 1.1
Samoa	14.3°S	76-01		-1.6 $\pm$ 1.4	-1.6 $\pm$ 1.3	-1.8 $\pm$ 1.8	-1.0 $\pm$ 1.7	-1.5 $\pm$ 1.1

Table 4-4, continued.

Station/Region	Latitude	Year-Month		Trend (%/decade $\pm 2\sigma$ )				
		First	Last	Dec–Feb	Mar–May	Jun–Aug	Sep–Nov	Year
Cachoeira-Paulista	22.7°S	74-05		-1.4 $\pm$ 1.7	-1.5 $\pm$ 1.7	-3.4 $\pm$ 2.1	-2.0 $\pm$ 1.6	-2.1 $\pm$ 1.2
Brisbane*	27.5°S			-1.3 $\pm$ 1.4	-2.2 $\pm$ 1.3	-2.1 $\pm$ 1.7	-1.6 $\pm$ 1.4	-1.8 $\pm$ 0.9
Perth	32.0°S	69-03		-1.6 $\pm$ 1.4	-1.5 $\pm$ 1.5	-1.9 $\pm$ 1.9	-1.9 $\pm$ 1.4	-1.7 $\pm$ 0.9
Buenos Aires*	34.6°S	65-10		-0.9 $\pm$ 2.0	-1.3 $\pm$ 1.8	-3.4 $\pm$ 2.1	-0.7 $\pm$ 2.2	-1.6 $\pm$ 1.3
Melbourne	38.0°S			-2.1 $\pm$ 1.3	-2.5 $\pm$ 1.2	-3.4 $\pm$ 1.6	-1.9 $\pm$ 1.4	-2.5 $\pm$ 0.8
Lauder/Invercargill	45.0°S	70-07		-4.0 $\pm$ 2.1	-3.1 $\pm$ 1.7	-2.5 $\pm$ 2.5	-2.7 $\pm$ 2.1	-3.0 $\pm$ 1.3
Macquarie Island*	54.5°S			-4.6 $\pm$ 2.2	-1.9 $\pm$ 2.3	-4.3 $\pm$ 2.8	-2.9 $\pm$ 3.0	-3.4 $\pm$ 1.7
<i>Regions</i>								
Arctic	65°N			-7.9 $\pm$ 2.7	-7.7 $\pm$ 2.6	-2.5 $\pm$ 1.5	-3.6 $\pm$ 1.4	-5.7 $\pm$ 1.6
Western Siberia	56°N	73-01		-5.0 $\pm$ 3.0	-7.2 $\pm$ 3.1	-2.1 $\pm$ 1.6	-2.7 $\pm$ 1.7	-4.5 $\pm$ 1.5
Eastern Siberia & Far East	53°N	73-01		-5.7 $\pm$ 2.5	-7.1 $\pm$ 2.7	-3.2 $\pm$ 2.1	-3.8 $\pm$ 1.9	-5.1 $\pm$ 1.6
European USSR	52°N	73-01		-5.0 $\pm$ 2.9	-5.3 $\pm$ 2.6	-2.3 $\pm$ 1.3	-1.1 $\pm$ 1.6	-3.6 $\pm$ 1.3
Dobson Europe	49°N			-5.2 $\pm$ 2.8	-6.6 $\pm$ 2.4	-3.0 $\pm$ 1.5	-1.4 $\pm$ 1.9	-4.3 $\pm$ 1.4
North America	46°N			-3.6 $\pm$ 2.0	-4.8 $\pm$ 1.9	-3.3 $\pm$ 1.2	-2.2 $\pm$ 1.3	-3.5 $\pm$ 1.1
Central Asia	42°N	73-01		-3.3 $\pm$ 2.2	-3.3 $\pm$ 2.5	-2.1 $\pm$ 1.8	-1.1 $\pm$ 1.6	-2.5 $\pm$ 1.4
Australia & New Zealand	39°S			-2.7 $\pm$ 1.1	-2.4 $\pm$ 1.0	-3.1 $\pm$ 1.4	-2.3 $\pm$ 1.6	-2.6 $\pm$ 0.9
Antarctica	75°S			-6.3 $\pm$ 1.9	-2.4 $\pm$ 3.2	-6.5 $\pm$ 4.3	-20 $\pm$ 4.0	-8.9 $\pm$ 2.0

winter, the estimated trend ending 1993 is 2.6% stronger than the trend ending 1997. In contrast with the Northern Hemisphere, in the Southern Hemisphere the effect of the 1993 anomaly seems negligible. Figure 4-16 indicates a much lower impact at that time in the Southern Hemisphere than in the Northern Hemisphere (Figure 4-14). Moreover, southern midlatitude trends tend to actually slow down. The trend estimates ending in 1990 and 1991 were more negative than trends finishing in the years after.

A puzzling result was shown in the last Assessment (WMO, 1995, Tables 1-2 and 1-3), where for the period of 1979-1994 the June-August trend over southern midlatitudes (30-55°S) was estimated at  $(-3.6 \pm 1.7)\%$ /decade from ground-based data and  $(-7.5 \pm 2.5)\%$ /decade for the SBUV-SBUV/2 record; i.e., SBUV data show almost twice the decline (Fioletov *et al.*, 1998b). It is especially strange, because direct comparisons of the ground-based and SBUV data show only 1-2% differences, and there are no such large discrepancies in trends in the Northern Hemisphere (WMO, 1995). The

SBUV-SBUV/2 trend reported in WMO (1995) at 55°S for June-August ( $-10.7\%$ /decade) is much stronger than the ozone trends during the corresponding winter months in northern middle and polar latitudes and comparable with the sub-Antarctic trend ( $-13.6\%$  at 65°S) during “ozone hole” months (September-November). Hollandsworth *et al.* (1995b) found that due to the NOAA-11 orbit some of the data in the Southern Hemisphere are missing, and these gaps should be accounted for when interpreting the trend results. The statistical model used in their paper was less sensitive to errors and gaps in data than the model used by WMO (1995), and the estimated trends were closer to trends for the Dobson data (about 8%/decade in June-August at 60°S).

For a possible explanation of the difference between Dobson and SBUV-SBUV/2 total ozone trends one should look at the combination of SBUV-SBUV/2 instrument and/or algorithm errors for high zenith angles ( $>83^\circ$ ) and specific features of the orbit of the NOAA-11 satellite, on which the SBUV/2 instrument was operated in 1989-1994 as discussed by Fioletov *et al.* (1998a).

## OZONE TRENDS

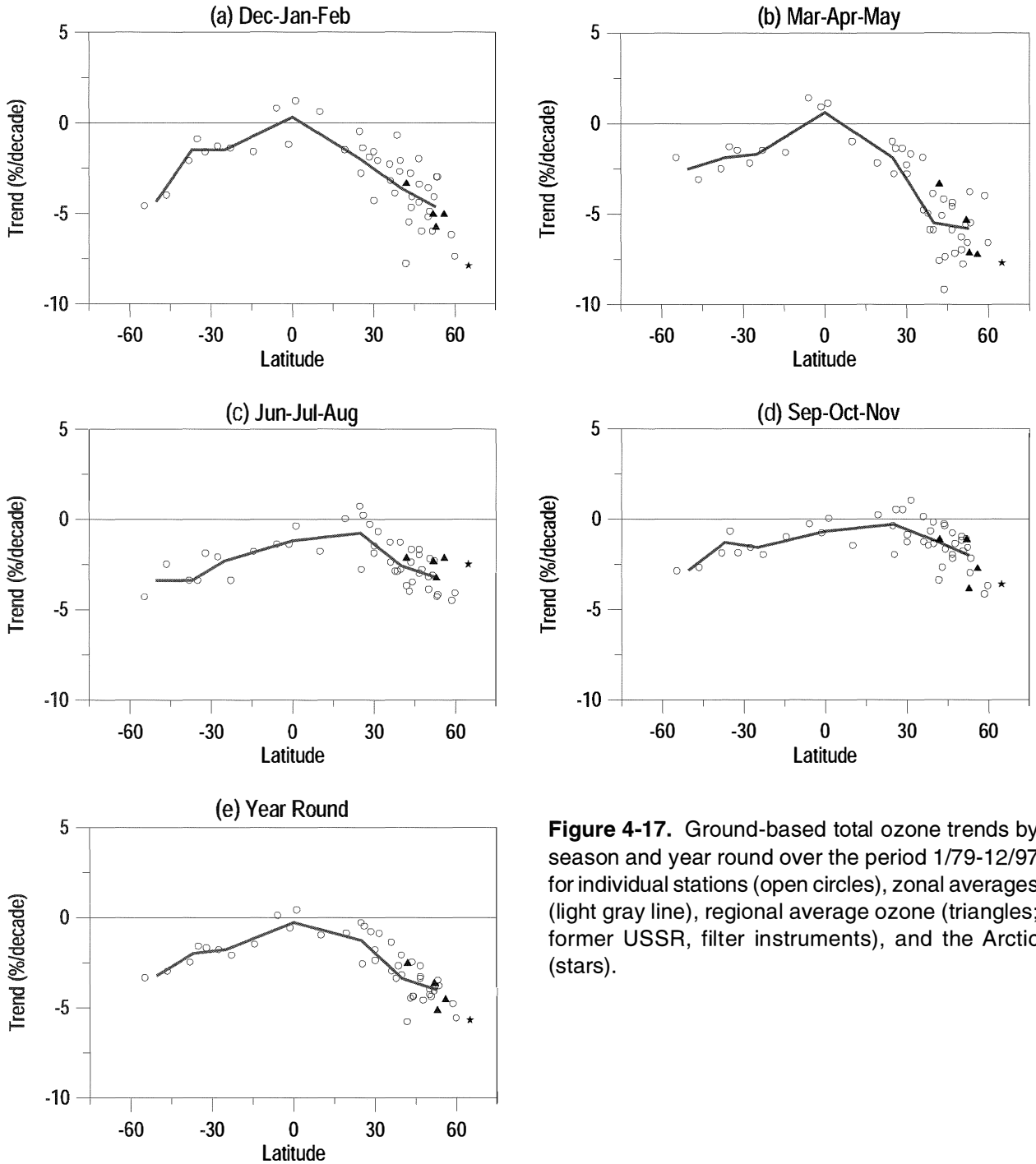


**Figure 4-17.** Ground-based total ozone trends by season and year round over the period 1/79-12/97 for individual stations (open circles), zonal averages (light gray line), regional average ozone (triangles; former USSR, filter instruments), and the Arctic (stars).

In southern midlatitudes only about 5% of the SBUV-SBUV/2 data have such errors, but they are enough to obtain the observed difference in total ozone trends. The high-zenith-angle error introduces up to 5%/decade errors in austral winter total ozone trends in southern high

latitudes, and accounting for this error changes the SBUV-SBUV/2 trend estimations there from 9-11%/decade to ~5%/decade.

The current satellite analysis using TOMS data shows good agreement between the ground-based zonal-

**Table 4-5. Trends over different latitudinal belts calculated from individual station trends.** Tabled numbers are averages of individual trends within latitudinal zones, with two standard errors. The errors demonstrate how scattered the trend estimations are for the stations within the region, but not the effect of ozone variability on the trends, and thus do not truly represent the total uncertainty in the zonal average trend. For the longer period, only stations with records started prior to August 1976 have been used.

Zone	Number of stations	Trend (%/decade)					Year
		Dec–Feb	Mar–May	Jun–Aug	Sep–Nov		
<i>Data from January 1979 through December 1997</i>							
45°–60°N	13	-4.6 ±0.9	-5.8 ±0.7	-3.2 ±0.5	-2.0 ±0.6	-4.0 ±0.4	
35°–45°N	11	-3.6 ±1.2	-5.5 ±1.2	-2.6 ±0.6	-1.2 ±0.6	-3.4 ±0.8	
14°–35°N	8	-2.0 ±0.8	-1.9 ±0.5	-0.8 ±0.8	-0.3 ±0.7	-1.3 ±0.6	
13°S–13°N	4	0.3 ±1.0	0.6 ±1.1	-1.2 ±0.6	-0.7 ±0.7	-0.3 ±0.6	
14°S–34°S	4	-1.5 ±0.1	-1.7 ±0.3	-2.3 ±0.8	-1.6 ±0.4	-1.8 ±0.2	
34°S–45°S	2	-1.5 ±1.2	-1.9 ±1.2	-3.4 ±0.1	-1.3 ±1.2	-2.0 ±0.9	
45°S–55°S	2	-4.3 ±0.6	-2.5 ±1.2	-3.4 ±1.8	-2.8 ±0.2	-3.2 ±0.4	
<i>Data from January 1964 through December 1997 (Trends from January 1970)</i>							
45°–60°N	13	-3.6 ±0.6	-3.5 ±0.4	-1.7 ±0.3	-1.4 ±0.3	-2.7 ±0.2	
35°–45°N	8	-2.3 ±0.8	-2.6 ±0.5	-1.3 ±0.5	-0.8 ±0.6	-1.8 ±0.5	
14°–35°N	7	-1.7 ±0.5	-1.4 ±0.5	-0.9 ±0.8	-0.5 ±0.6	-1.1 ±0.5	
13°S–13°N	1	0.3	-0.9	-1.8	-1.6	-1.0	
14°S–34°S	4	-1.7 ±0.2	-1.7 ±0.5	-2.2 ±0.4	-1.6 ±0.5	-1.8 ±0.3	
34°S–45°S	2	-2.0 ±0.5	-1.8 ±0.1	-2.8 ±1.2	-1.5 ±0.2	-2.0 ±0.3	
45°S–55°S	2	-3.5 ±0.7	-2.8 ±0.7	-3.4 ±0.2	-2.9 ±0.3	-3.2 ±0.1	

average trends and trends from the TOMS zonal means (Figure 4-18). In southern midlatitudes the June-July-August TOMS trends are about 1.5%/decade less negative, but this is not significant given the scarcity of ground-based stations at those latitudes.

The regional trends given in Table 4-4 show some variation among regions at the same latitude, e.g., among North America, Europe, Siberia, etc. The regional differences can be seen in more detail in Figure 4-19, which shows seasonal trends from a gridded monthly trend analysis of TOMS total ozone in each 5° latitude (65°S to 65°N) by 10° longitude block. Average trends along a latitude zone follow the zonal trends of Figure 4-18 (or Table 4-6), but some substantial longitudinal differences can also be seen, verifying the regional differences noted in Table 4-4. In particular, there are extremely negative trends over Siberia in spring and large negative trends over Europe in winter and spring. North America shows relatively smaller trends in winter/spring than the former regions. Similar results were shown by Stolarski *et al.* (1992). Again, there was little change over equatorial regions.

#### 4.5.2 Changes in the Northern Hemisphere: Middle and Polar Latitudes

Since the 1994 Assessment (WMO, 1995), the total ozone amount at middle and polar latitudes in the Northern Hemisphere was, in general, from 7 to 10% below the long-term average of 1957-1975. Compared with the summer and autumn seasons, the ozone deficiency in the winter and spring seasons was more than twice as strong. In the last few years, new record-low ozone values of below 250 DU were observed. From mid-January, through February and March (early April in 1997), over continental-scale regions, e.g., over Siberia (1995), over Northern Europe-Western Siberia and the adjacent part of the Arctic (1996), and over the Canadian Arctic and Central Siberia (1997), a monthly-mean ozone deficiency exceeding 25-35% was observed (Bojkov *et al.*, 1995a, 1997; Fioletov *et al.*, 1998b; Newman *et al.*, 1997; Goutail and Pommereau, 1997; WMO, 1996, 1997). The lower stratosphere inside the Arctic vortex showed low ozone mixing ratios of ~1 ppm in the winter/springs of 1995, 1996, and 1997 (Manney

OZONE TRENDS

TOMS and Ground-based Zonal Trends 1/79 to 12/97

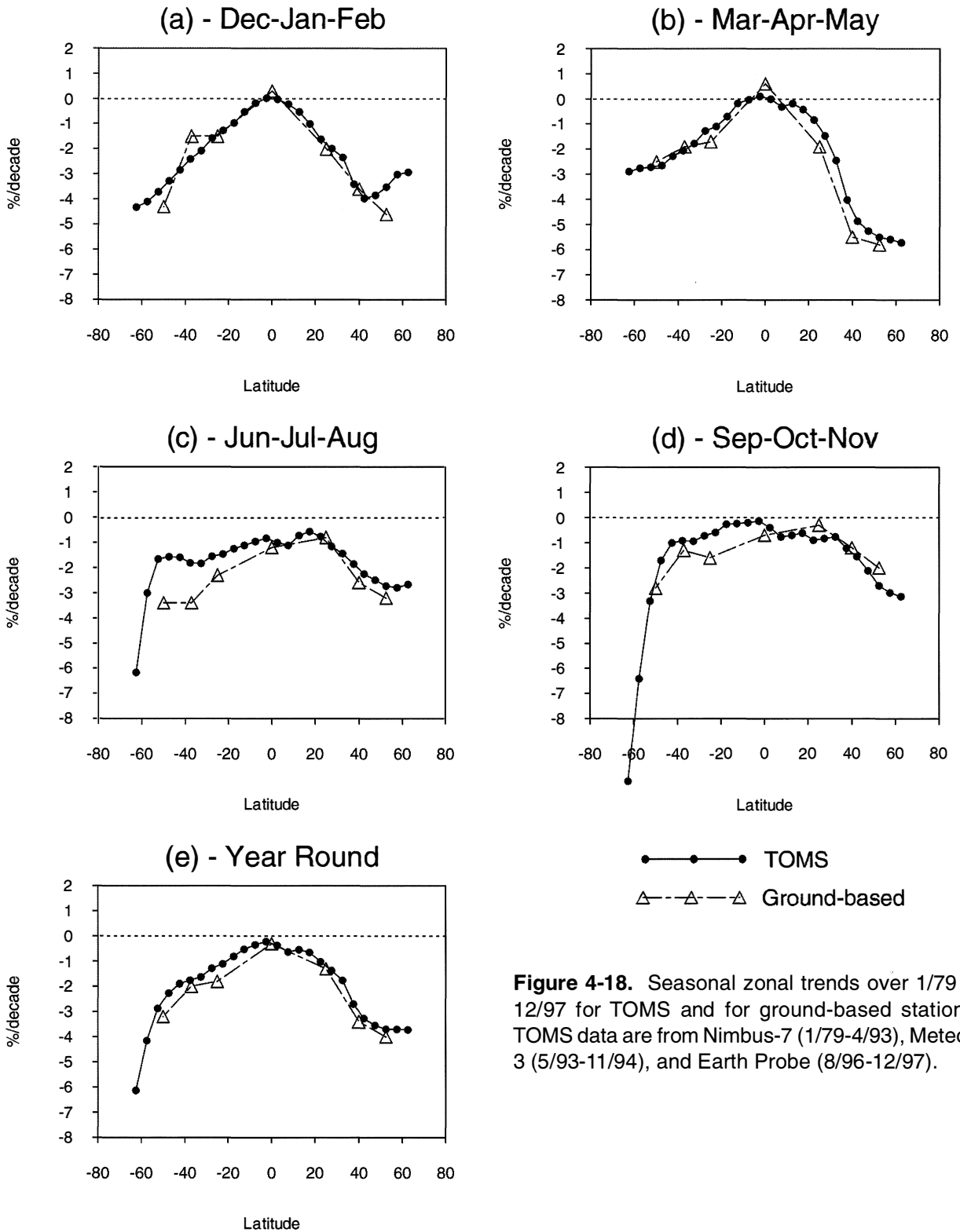


**Figure 4-18.** Seasonal zonal trends over 1/79 to 12/97 for TOMS and for ground-based stations. TOMS data are from Nimbus-7 (1/79-4/93), Meteor-3 (5/93-11/94), and Earth Probe (8/96-12/97).

**Table 4-6. Seasonal total ozone trends in %/decade from Nimbus-7 + Meteor-3 + Earth Probe TOMS over the period January 1979–December 1997, in 5° latitude zones.**

Zone	DJF	2 $\sigma$	MAM	2 $\sigma$	JJA	2 $\sigma$	SON	2 $\sigma$	Year	2 $\sigma$
62.5°N	-2.9	3.1	-5.7	2.5	-2.7	1.3	-3.1	1.2	-3.7	1.7
57.5°N	-3.0	2.7	-5.6	2.3	-2.8	1.4	-3.0	1.3	-3.7	1.6
52.5°N	-3.5	2.5	-5.5	2.2	-2.7	1.3	-2.7	1.2	-3.7	1.5
47.5°N	-3.8	2.4	-5.3	2.0	-2.5	1.2	-2.1	1.3	-3.5	1.4
42.5°N	-4.0	2.5	-4.9	2.1	-2.2	1.2	-1.6	1.3	-3.3	1.5
37.5°N	-3.4	2.8	-4.0	2.5	-1.9	1.3	-1.2	1.5	-2.7	1.8
32.5°N	-2.3	2.6	-2.4	2.6	-1.4	1.3	-0.8	1.6	-1.8	1.9
27.5°N	-2.0	2.3	-1.5	2.6	-1.1	1.4	-0.8	1.3	-1.4	1.7
22.5°N	-1.6	2.1	-0.8	2.3	-0.8	1.3	-0.9	1.2	-1.0	1.5
17.5°N	-1.0	1.9	-0.4	1.9	-0.6	1.2	-0.6	1.1	-0.6	1.3
12.5°N	-0.5	1.5	-0.2	1.5	-0.7	1.2	-0.7	1.2	-0.5	1.2
7.5°N	-0.2	1.5	-0.3	1.8	-1.1	1.1	-0.8	1.2	-0.6	1.2
2.5°N	0.0	1.9	0.0	2.2	-1.0	1.3	-0.4	1.7	-0.4	1.6
2.5°S	0.0	1.6	0.1	2.1	-0.8	1.4	-0.1	1.7	-0.2	1.5
7.5°S	-0.2	1.0	0.0	1.5	-1.0	1.2	-0.2	1.0	-0.3	1.0
12.5°S	-0.5	1.1	-0.2	1.2	-1.1	1.6	-0.3	1.0	-0.5	1.0
17.5°S	-1.0	0.9	-0.7	1.3	-1.2	2.1	-0.3	1.5	-0.8	1.2
22.5°S	-1.3	1.0	-1.1	1.4	-1.5	2.3	-0.6	1.5	-1.1	1.4
27.5°S	-1.6	1.0	-1.3	1.3	-1.5	2.1	-0.7	1.4	-1.3	1.3
32.5°S	-2.1	1.0	-1.8	1.2	-1.8	2.0	-0.9	1.5	-1.6	1.1
37.5°S	-2.4	1.1	-2.1	1.2	-1.8	2.1	-0.9	1.6	-1.8	1.2
42.5°S	-2.8	1.2	-2.3	1.3	-1.6	2.2	-1.0	1.7	-1.9	1.3
47.5°S	-3.3	1.3	-2.6	1.5	-1.6	2.1	-1.7	2.0	-2.3	1.4
52.5°S	-3.7	1.4	-2.7	1.6	-1.7	2.4	-3.3	2.3	-2.9	1.6
57.5°S	-4.1	1.5	-2.8	1.8	-3.0	2.2	-6.4	2.8	-4.2	1.8
62.5°S	-4.3	1.5	-2.9	1.8	-6.2	2.1	-10.5	3.7	-6.1	1.9

*et al.*, 1996a,b, 1997). A chemical ozone loss between 100 and 140 DU has been estimated in the Arctic for each winter/spring since 1989, except in 1998 (Müller *et al.*, 1998; Proffitt *et al.*, 1990, 1993). In the 1997/1998 winter/spring season when the lower stratosphere temperatures were mainly above normal, the ozone levels were only 4 to 7% below the long-term averages.

Relevant studies on ozone chemical losses detected over the Arctic and adjacent upper midlatitudes include: Bojkov, 1988; Hofmann and Deshler, 1991; McKenna *et al.*, 1990; Koike *et al.*, 1991; WMO, 1992; Kyrö *et al.*, 1992; Proffitt *et al.*, 1990, 1993; Larsen *et al.*, 1994; Bojkov *et al.*, 1995a, 1998b; Donovan *et al.*, 1995; von der Gathen *et al.*, 1995; Manney *et al.*, 1995, 1996a,b, 1997; Bojkov and Fioletov, 1997; Dorokhov and Potapova, 1998; Müller *et al.*, 1996, 1997a,b, 1998;

Hansen *et al.*, 1997; Rex *et al.*, 1997; Tsvetkova *et al.*, 1997; Goutail and Pommereau, 1997; Goutail *et al.*, 1997; Knudsen *et al.*, 1998; Yushkov *et al.*, 1998. International campaigns (the Airborne Arctic Stratospheric Expedition (AASE); the European Arctic Stratospheric Ozone Expedition (EASOE); the Second European Stratospheric Arctic and Midlatitude Experiment (SESAME); the Polar Ozone and Aerosol Measurement (POAM) experiment; Match studies) and new satellite-borne experiments (e.g., HALOE and MLS on UARS) have provided evidence of chemically induced ozone loss in the Arctic vortex and adjacent upper midlatitudes, from 25 to 40% of the total ozone. In the spring seasons of 1993, 1995, and 1996, and in late 1997, the ozone deficiency in the Arctic reached, and on few occasions surpassed, the levels of ozone loss observed in the Antarctic

## OZONE TRENDS

**Table 4-7. Total ozone trends over different time intervals for 35-60°N and 35-60°S latitudinal belts (% per decade).** Trends were calculated as averages of individual station trends.

	1/70*- 12/97	1/79- 12/91	1/79- 12/92	1/79- 12/93	1/79- 12/94	1/79- 12/95	1/79- 12/96	1/79- 12/97	1/79-12/97 without 1992, 1993
<i>35°-60°N</i>									
DJF	-3.1	-4.2	-5.6	-6.7	-5.2	-4.9	-4.4	-4.1	-3.1
MAM	-3.2	-4.3	-5.2	-6.5	-6.0	-6.0	-5.7	-5.7	-5.0
JJA	-1.6	-1.8	-2.8	-3.3	-3.4	-3.4	-3.3	-2.9	-2.5
SON	-1.2	-0.4	-1.7	-1.5	-1.5	-1.5	-1.7	-1.6	-1.3
Year	-2.3	-2.8	-3.9	-4.7	-4.2	-4.1	-3.9	-3.7	-3.1
<i>35°-60°S</i>									
DJF	-2.8	-5.6	-5.0	-4.5	-3.8	-3.3	-3.0	-2.9	-2.8
MAM	-2.3	-3.5	-3.2	-2.9	-2.9	-2.3	-2.3	-2.2	-2.2
JJA	-3.1	-5.0	-4.7	-4.2	-4.0	-3.5	-3.1	-3.4	-3.3
SON	-2.2	-3.7	-3.3	-3.2	-2.5	-2.1	-1.6	-2.0	-1.8
Year	-2.6	-4.4	-4.1	-3.7	-3.3	-2.8	-2.5	-2.6	-2.5

\* Data from January 1964.

spring in the early 1990s (e.g., Müller *et al.*, 1997a,b, 1998; Bojkov *et al.*, 1998a; Goutail and Pommereau, 1997). These major ozone losses are related not only to the increasing chlorine loading in the stratosphere but also to the unusually low stratospheric winter/spring temperatures (e.g., see Pawson and Naujokat (1997); Chapter 5 of this Assessment).

Although negative deviations exceeding 150 DU were common for days and sometimes weeks in the northern middle and polar latitudes during most of the springs in the 1990s, ozone hole values of below 220 DU were not observed (except as one-day events in the winter/springs of the 1990s). This is related to the very high background spring-season ozone (~420-450 DU) in the 1960s and early 1970s. Compared with the Antarctic mean values of earlier decades, the winter/spring averages in the northern latitudes were always 100 to 130 DU higher (e.g., Bojkov, 1986, 1988; Stolarski *et al.*, 1997).

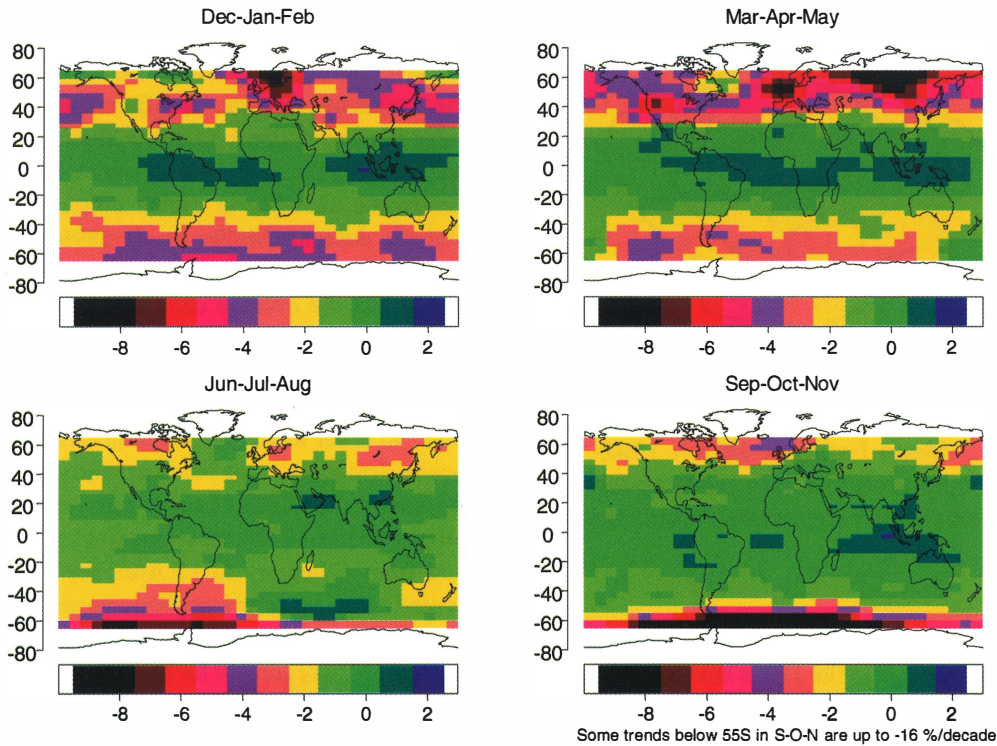
### 4.5.2.1 TRENDS AND VARIABILITY

The ozone decline in the Northern mid and polar latitudes can be assessed from the calculated ozone trends in the previous section (4.5.1). In percent per decade the decline in the Arctic region is more than 2 times stronger during the winter/spring (-7.8) than during the fall

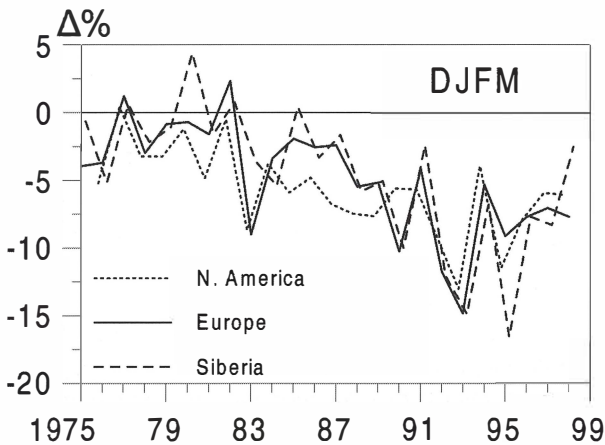
(-3.6) or the summer (-3.5). In the upper midlatitudes (50°-65°N) on the average the trends in the winter/spring are -4.4 and in summer/fall -2.8% /decade. However, from Table 4-5 and Figure 4-19 it is clear that there are substantial regional differences. The spring trends over Siberia are stronger than -7%, and over Europe close to -7%, but over North America they are only about -5%/decade. Summer trends are much more uniform (about -3%/decade).

Figure 4-20 shows the seasonal (December-January-February-March) area-averaged total ozone departures from the pre-1976 mean values between 45 and 65° N over three continental-size regions. In general the winter/spring departures are negative, exceeding the 2 $\sigma$  levels, at least over two of the regions for the past 10 years except in 1991 and 1994. Depending on the position of the polar vortex and its expansion south of 65°N, the February-March negative ozone deviations have extreme values over Siberia of -21% in 1996, -17% in 1995, and -14% in 1993. A number of recent studies (e.g., Hood and Zaff, 1995; McCormack and Hood, 1997; Peters and Entzian, 1998) show that close to half of the longitudinal differences in the ozone trends are probably related to decadal variations in the structure of the quasi-stationary planetary (Rossby) waves. It should be recalled that Stolarski *et al.* (1992) already have demon-

Seasonal Trends 1/79 to 12/97 from TOMS



**Figure 4-19.** TOMS trends in percent per decade (Nimbus-7 + Meteor-3 + Earth Probe) over the period 1/79-12/97 in 5° latitude × 10° longitude blocks (latitudes 65°S-65°N).



**Figure 4-20.** Area-averaged (45°N-65°N) total ozone departures (in %) from the long-term pre-1976 averages over Europe, North America, and Siberia, for the winter/spring (DJFM) seasons, 1975-1998, calculated from ground-based total ozone measurements. The 2-sigma deviation of the natural seasonal variability in the pre-1976 period was less than 6%.

stated the existence of significant longitudinal differences in the ozone trends, which are also seen on Figure 4-20. The regional fluctuations are mostly related to the specifics of the stratospheric circulation and temperature conditions, as discussed for example by Bekoryukov *et al.* (1997); Bojkov *et al.* (1998b); Hood *et al.* (1997); and others.

The major contributions to the winter/spring seasonal negative deviations are during February and March, when the height of the sun above the horizon is rapidly increasing. The mean total ozone departures from the long-term averages for February-March 1992-1997 over the Northern Hemisphere are plotted in Figure 4-21. Over this 2-month-long period, deviations larger than -12% (in excess of 2σ) dominate, with highest deviations stronger than -20% (i.e., >3σ) for the Arctic and most of Siberia. A measure of the unusually strong decline observed during the 1990s over the polar and midlatitudes is provided by the frequency of days with ozone values deviating below the long-term mean by more than 2σ during the winter/spring season, as discussed by Bojkov *et al.* (1998b) and in WMO (1997).

## OZONE TRENDS

Departures (%) for the mean February-March 1992-1997

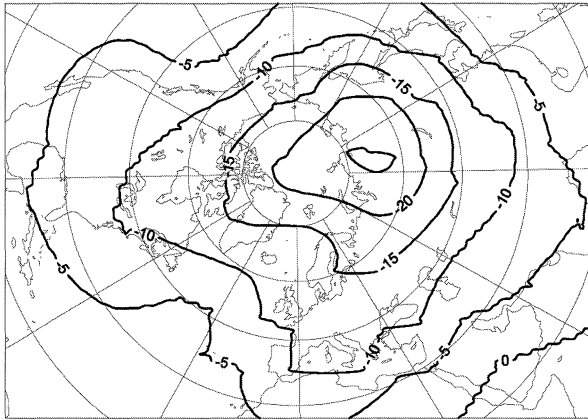


**Figure 4-21.** Mean February-March 1992-1997 total ozone departures (%) from the long-term average in the Northern Hemisphere. (Updated from Bojkov *et al.*, 1998b.)

Except for the 1990/91, 1993/94, and 1997/98 seasons, all other winter/springs in the 1990s have days with deviations 6 to 10 times their pre-1976 averages. The bulk of the winter/spring ozone deficiency within the Arctic polar vortex appears mostly in the lower stratosphere, similar to the ozone depletion during the austral spring in Antarctica (see also Section 4.5.3 and Chapter 7).

### 4.5.2.2 ESTIMATING THE OZONE MASS DEFICIENCY

One approach to detecting the lower stratospheric ozone loss is the Match analysis (von der Gathen *et al.*, 1995; Rex *et al.*, 1997). The ozone loss rates in an ensemble of air parcels were determined from ozonesonde data obtained by a coordinated launch strategy. Through statistical analysis, ozone loss rates in winter and early spring, inside the vortex, could be determined as a function of time and altitude, and ultimately estimates of the loss in column ozone were made. For the winter/spring of 1994/95, a chemical ozone loss of 127 DU in the Arctic vortex was calculated. (See also Chapter 7.)

Manney *et al.* (1997) and Goutail and Pommereau (1997) estimated the chemical ozone loss in the lower stratosphere based on MLS and Système d'Analyse par Observation Zénithale (SAOZ) observations. The cumulative depletion in the vortex based on six SAOZ stations was estimated to reach 30-40% in 1993, 1995, and 1996 and 25-30% in 1997 for the winter/spring season. These numbers are only slightly different from the esti-

mates of the ozone-mass deficiencies given below. Tsvetkova *et al.* (1997), using ozone soundings at Yakutsk, estimated that the ozone loss rate in the 13-19 km layer during the spring of 1995 reached 0.4%/day of the total ozone amount. A different approach is to consider the correlation between a chemically inert tracer and ozone in the Arctic vortex over winter and spring to determine changes in ozone concentrations due to diabatic descent (Müller *et al.*, 1996, 1997a,b, 1998). Using this technique, Müller *et al.* (1997a,b, 1998) estimated that the average ozone loss in the lower stratosphere (12-21 km) during the winter/springs of 1992 through 1996 ranged between 102 DU in 1994 to 140 DU in 1996.

In order to get precise information on the overall ozone changes over the Northern mid and polar latitudes, Bojkov *et al.* (1998a) carried out a comparison of the long-term pre-1976 total ozone field, with data for each day from 1 January to 15 April for 1979-1998. The spread of the polar stratospheric vortex was determined through potential vorticity analysis on the 475-K potential temperature surface for each day for the last 10 years (1989-1998) and compared with the gridded ozone-change analysis. All calculations were carried out for the entire sunlit surface poleward of 35°N.

Figure 4-22 presents the ozone mass deficiency ( $O_3MD$ ) poleward from 35°N within the -10% and -15% contours and corresponding areas for the 1 January-15 April period. These two contours were selected in order to explore the morphology of negative ozone deviations, which generally exceed the natural variability ( $\sim 2\sigma$  and  $3\sigma$ , respectively). It shows substantial interannual variability and a clear increase of  $O_3MD$ , especially during 1993 and 1995. In those 2 years the integrated  $O_3MD$  within the -10% ozone-deviations contour exceeded 12000 Mt over an integrated surface of  $\sim 8000 \times 10^6 \text{ km}^2$  for 105 days. The seasonally integrated average  $O_3MD$  for the 1990s is  $\sim 7800 \text{ Mt}$ , which is nearly 3 times larger than the average ( $\sim 2800 \text{ Mt}$ ) in the years up to the mid-1980s. It should be noted that the contributions to the overall  $O_3MD$  (for 35°N) from regions with even stronger deficiencies (-15% contour) also increased from  $\sim 55\%$  up to the mid-1980s to an average of  $\sim 70\%$  in the 1990s, with the highest values exceeding 75% in 1993, 1995, 1996, and 1997.

The overall increase of ozone deficiency within the -10% contours is not a result of any redistribution (an increase of ozone) within the +10% contours in the middle and polar latitudes of the Northern Hemisphere.

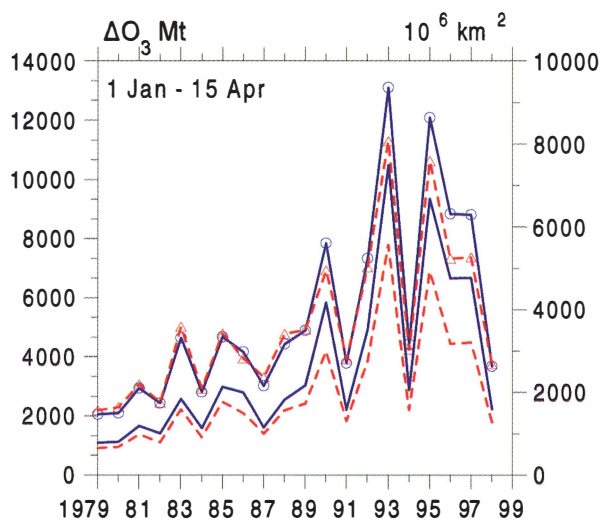


**Figure 4-22.** Ozone mass deficiency integrated over the period 1 January to 15 April, expressed in Mt, inside the -10% contour (continuous line with circles) and the -15% contour (continuous line alone), poleward from 35°N, 1979-1998. The dashed lines show, for each year, the surface area of the -10% contour (with triangles) together with the -15% contour (dashed lines alone) expressed in  $10^6 \text{ km}^2$ .

The fraction of the -10% contour area from the entire area poleward from 35°N has grown from less than 20% in the early-1980s to ~50% for the 1990s, with the highest values (>70%) in 1993 and 1995. At the same time the area covered by positive deviation >+10% has declined from ~10% in the early 1980s to a negligible ~3% in the 1990s.

#### 4.5.2.3 COMPARISONS WITH O<sub>3</sub>MD IN THE SOUTHERN HEMISPHERE

Figure 4-23 shows the O<sub>3</sub>MD (in Mt) within the -10% contours integrated over equal 105-day-long periods poleward from 35°N and 35°S. The periods of 1 January to 15 April and 1 September to 15 December are when major ozone declines have occurred, in the respective north and south polar regions. During the 1980s the average of the 105-day integrated O<sub>3</sub>MD was ~6000 Mt over the southern latitudes versus ~3500 Mt over the northern latitudes (the latter O<sub>3</sub>MD was ~42% smaller). During the 1990s, however, in the northern latitudes, a substantial increase in O<sub>3</sub>MD was observed, up to an

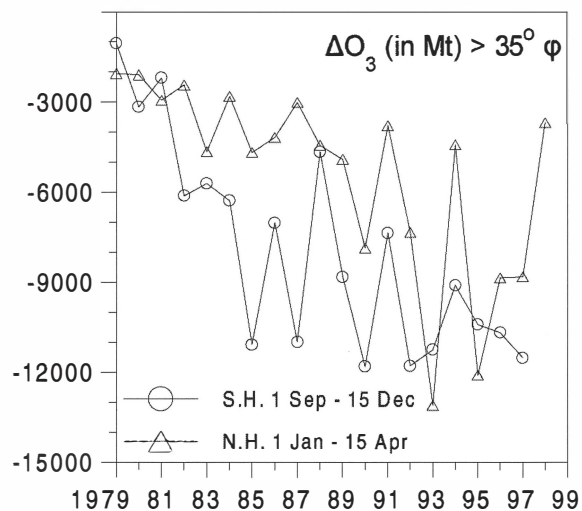


**Figure 4-23.** Ozone mass deficiency (in Mt) integrated over 105 days, inside the -10% contour: (1) north of 35°N, over the period 1 January to 15 April (diamonds), and (2) south of 35°S over the period 1 September to 15 December (circles), for 1979-1998.

average of ~7800 Mt vs. ~10500 Mt over the southern latitudes (the northern O<sub>3</sub>MD was now only 26% smaller). Furthermore, in two particular seasons (1993 and 1995), the overall O<sub>3</sub>MD in the northern latitudes >35°N exceeded the O<sub>3</sub>MD over the corresponding southern latitudes.

The differences between the two hemispheres are better understood if one looks at two specific latitudinal belts. During the 1990s over the middle latitudes from 35° to 50° the average O<sub>3</sub>MD was ~2700 Mt over the northern and only ~1650 Mt over the same southern latitudes. Over the upper middle and polar latitudes, >60°, the average O<sub>3</sub>MD was ~5900 Mt over the southern and only ~3100 Mt over the northern region. This shows that, although for the entire region poleward from 35°, on a molecule-per-molecule basis, the O<sub>3</sub>MD over the Southern Hemisphere exceeds the O<sub>3</sub>MD over the Northern Hemisphere, this difference is due to the severe ozone deficiency over Antarctica. However, over the southern middle latitudes the O<sub>3</sub>MD is much less (~39%) than over the northern 35°-50° belt.

## OZONE TRENDS

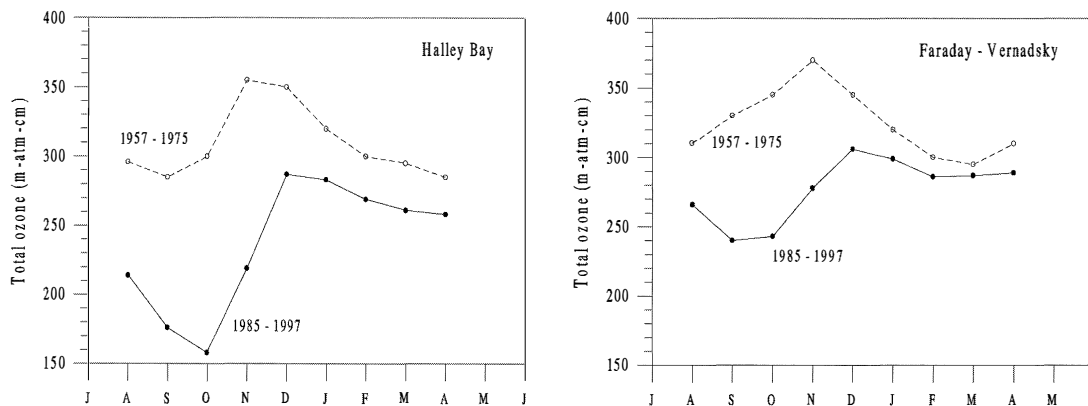


**Figure 4-24.** Comparison of the monthly means at Halley Bay and Faraday-Vernadsky for the periods 1957-1975 and 1985-1997 (plotted using data from the British Antarctic Survey).

### 4.5.3 Changes in Antarctica

Antarctic ozone observations from all ground-based and satellite-borne instruments show that the austral springtime ozone depletion has continued since the time of the last ozone Assessment in 1994 (e.g., Gernandt *et al.*, 1996, 1998; Hofmann *et al.*, 1997; Jones and Shanklin, 1995; Uchino *et al.*, 1998). The last 6 years have been most severely affected. The monthly total ozone in September and October was between 40 and 55% below the pre-ozone-hole values, with up to 70% deficiency in short time periods lasting a week or so. In the lower stratosphere, between 12 and 20 km, the ozone content was 60% below the pre-ozone-hole values in September, ~90% below in October, and ~80% below in November. The major change in the annual course of the total ozone over Antarctica in the last 13 years (1985-1997) compared with the 1957-1975 period is shown in Figure 4-24. The monthly means for September-October-November have been reduced by 37 to 47% at Halley and by 25 to 30% at Faraday-Vernadsky. The date of the annual ozone maximum has changed from November to December. Additional characteristics of the ozone hole for each year since 1979, shown in Figure 4-25, are (a) greatest surface area for a day, (b) lowest ozone value for the season, (c) date of disappearance of values <220 DU, and (d) the 105-day integrated ozone mass deficiency ( $O_3MD$ ) within the ozone hole area.

The maximum spread of the ozone hole, which started to exceed 10 million km<sup>2</sup> only in the mid-1980s, was above 21 million km<sup>2</sup> for the last 6 years. The low-

est ozone values registered, usually at the end of September and/or early October, have fallen from ~200 DU in the early 1980s to ~150 DU in the mid-1980s and down to ~100 DU in the 1990s. The  $O_3MD$  from the Antarctic pre-1976 values, within the -10% contours poleward of 60°S, when integrated for the 1 September-15 December (105-day) period of each year using gridded ozone values estimated from TOMS (1979-1997), SBUV (1994 and 1995), and a few ground-based observations, show that the average for the last six austral springs was ~3800 Mt. The date of disappearance of the ozone hole is very closely related to the breakdown of the polar stratospheric vortex. The delay of the springtime stratospheric warming by about a month over Syowa during the last 10-15 years was shown by Chubachi (1997). An increasing continuity of the days with values less than 220 DU was observed from early to mid-November in most of the 1980s, and up to early December in most of the 1990s.

It is well established that the total ozone loss is caused by depletion in the lower stratosphere (e.g., WMO, 1995). Hofmann *et al.* (1997), using South Pole soundings, determined that for the 9-year interval (from 1986 to 1995), in the 12-20 km layer, the ozone loss rate has increased from 2 to 3.3 DU/day, or about 65%. This increase in the ozone loss rate is in agreement with the estimated stratospheric halogen concentrations increase (~2.4 to 3.3 ppb) (Solomon, 1990). Figure 4-26 shows the ozone profile at Syowa (~69°S) on 6 October 1997 as well as the average ozone profile from all October soundings from 1968 to 1980. In 1997, almost all the

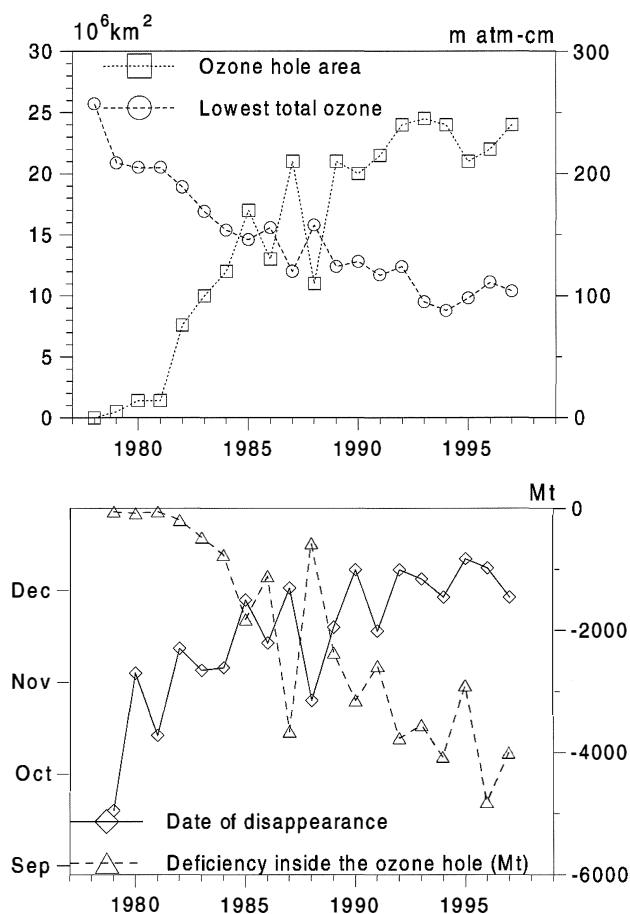


**Figure 4-25.** Evolution of the Antarctic ozone hole (defined by values below 220 DU) based on satellite and ground-based data for the period 1 September-15 December of each year. Upper panel: Maximum day-area covered by ozone hole values (squares; in millions  $\text{km}^2$ ); minimum total column ozone measured each year (circles). Lower panel: ozone mass deficiency from pre-1975 values integrated for 105 days (1 September-15 December) (triangles; in Mt); date of disappearance of the ozone hole values (diamonds). (From Uchino *et al.*, 1998.)

ozone in the 100-50 hPa layer (~15-19 km) was destroyed. Over the Neumayer and South Pole stations, springtime ozone depletion has been especially severe since 1992, with near-complete ozone loss from ~14 to 18 km (see Gernandt *et al.*, 1996, 1998; Hofmann *et al.*, 1997).

The ozone loss in the 12-20 km layer is representative of the severity of the ozone-depletion process in

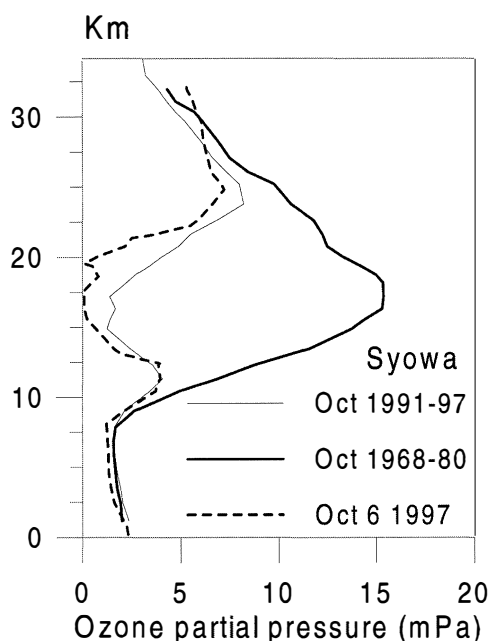


**Figure 4-26.** Vertical profile of ozone over Syowa on 6 October 1997 compared to the long-term average for October 1968-1980 and the average for October 1991-1997.

Antarctica (e.g., Gernandt *et al.*, 1996, 1998; Hofmann *et al.*, 1997). Figure 4-27 gives the ozone content in the 12-20 km layer for Syowa (1968-1997), South Pole (1968, 1970, 1971, 1986-1997), and Forster-Neumayer (1984-1997) based on monthly means for the 3 austral spring months. The drastic decline of the ozone content in the last 6-7 years in September (~60%), in October (~90%), and in November (~80%) compared to the pre-ozone-hole years is demonstrated in all three records and discussed in more detail by Hofmann *et al.* (1997) and Uchino *et al.* (1998).

A vertical cross section of the ozone partial pressure for 1993-1997 over Neumayer station (70°S) produced by the Alfred Wegener Institute for Polar and Marine Research (AWI) (P. von der Gathen, private communication, 1998) is shown in Figure 4-28. It illustrates the rapid decline of lower stratospheric ozone starting at the end of July-early August, from ~160 nb to lower than 10 nb at the end of September and early October. It also shows that later in November the increase of ozone starts above 25 km and slowly propagates downward (Gernandt *et al.*, 1996, 1998). The year-to-year changes of monthly mean ozone partial pressure at 30, 50, 70, 100, and 150 hPa in October over Syowa since 1968 show strong

## OZONE TRENDS

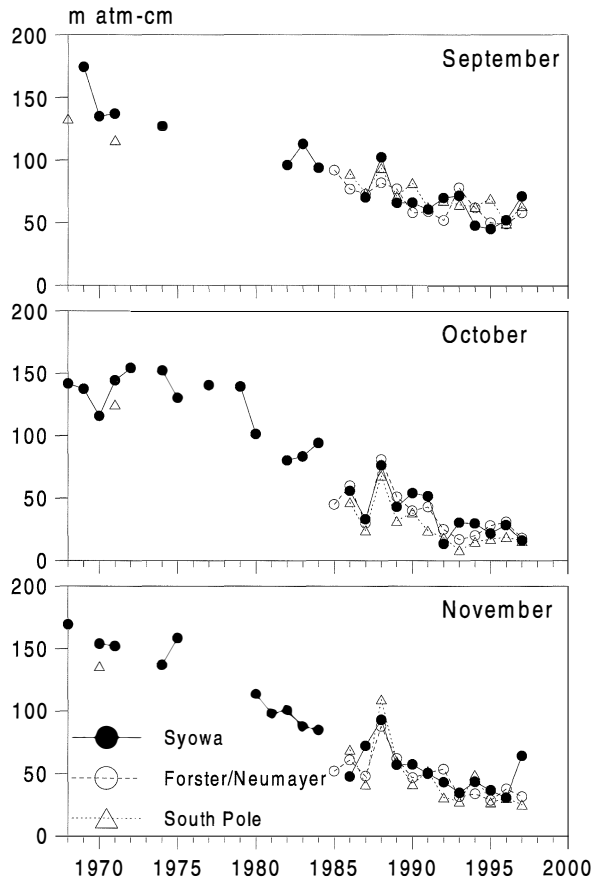


**Figure 4-27.** Change of the ozone content in the 12-20 km layer in September-October-November plotted with data from Syowa by the Japan Meteorological Agency (1968-1997), from South Pole by NOAA (1968, 1970, 1971, and 1986-1997), and from Forster-Neumayer by Alfred Wegener Institute (1984-1997), showing the drastic decline of the ozone in the lower stratosphere during the last years.

negative ozone trends for each layer since the end of the 1970s. The ozone at 100 hPa (~16 km) and 70 hPa (~18 km) has been almost completely depleted for the entire month of October since 1992 (Uchino *et al.*, 1998). Similar findings for the ozone changes over the South Pole are presented by Hofmann *et al.* (1997).

Figure 4-29 summarizes the observed change of ozone and temperature over Antarctica using the entire Syowa ozonesonde record since 1968. The coincidence in location of the region of severe ozone decline with the region of major temperature decline can be clearly seen. The largest values of the temperature change seem

to lag, by about 2 weeks, the occurrence of the maximum ozone decline. The ozone decline over the southern polar latitudes started to be especially strong in the second half of the 1980s. Despite the year-to-year variations, the ozone decline seems to have reached its highest values during most of the 1990s. One indirect confirmation of this is that the fraction of the -10% contour area from the entire surface area poleward from 35°S has grown from about 20% in 1979-1984 to an average of above 50% for the 1990s, or it has increased by ~2.5 times. At the same time the area covered by positive ozone deviations >+10% has actually declined to less than 5% of the surface area poleward from 35°S during the 1990s.

### 4.6 LONG-TERM CHANGES IN VERTICAL PROFILES

A general theme of WMO (1998) is a focus on the revised SAGE data, as this is the only long-term dataset that provides global measurements in the lower stratosphere. Three time periods, 1970-1996, 1980-1996, and 1984-1996, are of interest (the SPARC/IOC report was put in final form during mid-1997 and used data only through the end of 1996). The first time period covers the entire length of the available record from the ground-based observations. The second period encompasses the period of satellite records and, in addition, avoids the problem of merging the Brewer-Mast sonde data with the ECC sonde data at the Canadian stations. Finally, the last period is that for which SAGE II data are available, thus avoiding the issue of treating the gap in the SAGE I to SAGE II data and possible lower-stratospheric altitude registration errors in the SAGE I data.

#### 4.6.1 Upper Stratosphere

Upper stratospheric time series from three measurement systems have been analyzed. These are the SAGE, Umkehr, and SBUV. Figure 4-30 shows time series at 40 km for northern midlatitudes from each of these systems. All three show a general decline over this period, with a more rapid decline between 1980 and 1984 followed by a relatively flat period between 1984 and 1991. The Umkehr and SAGE systems then show a more rapid decrease after 1991. The SBUV system does not show this last decrease, which has been traced to an apparent drift in the NOAA-11 SBUV/2 instrument with time (WMO, 1998). When the upper stratospheric data

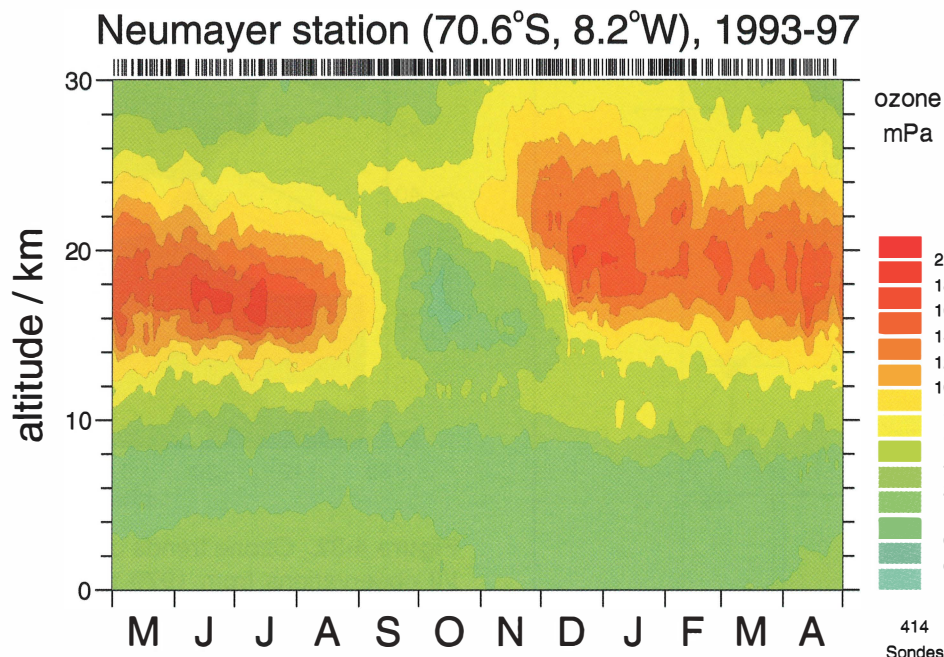


**Figure 4-28.** Average annual cross section of the ozone partial pressure over Neumayer (70°S) for the period 1993-1997, demonstrating the steep decline with the appearance of the sun in August and nearly complete disappearance of the ozone in the lower stratosphere in September-October. Short vertical lines at the top of the panel denote occurrences of sonde launches.

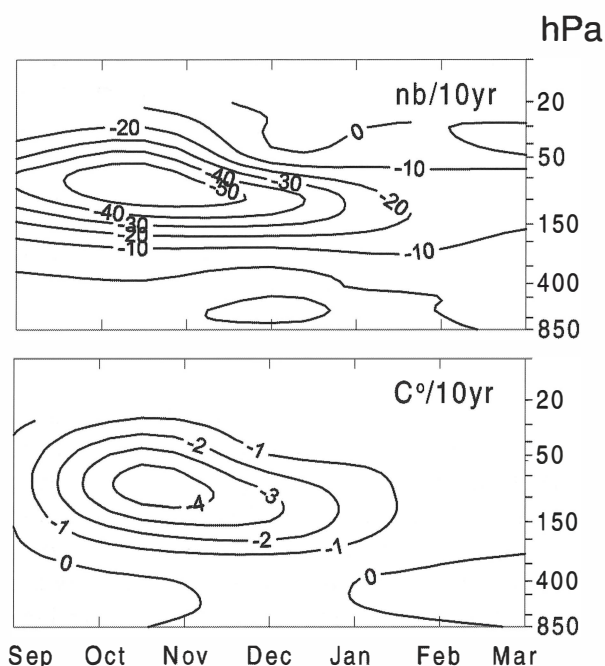


**Figure 4-29.** Annual vertical cross section of the ozone and temperature trends over Syowa (1968-1997). All stratospheric-level trends are significant at the two-sigma level.

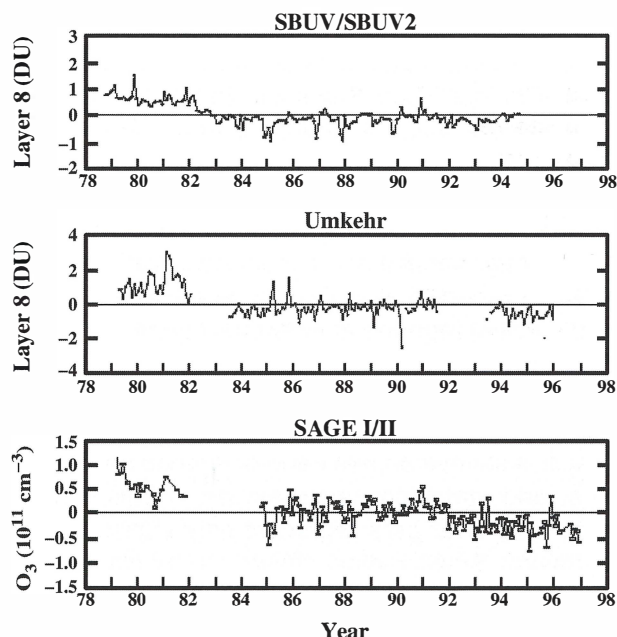


**Figure 4-30.** Monthly time series (deseasonalized) for layer 8 from the Umkehr and SBUV datasets compared with a similar series at 40 km from the SAGE dataset. (From WMO, 1998.)

## OZONE TRENDS

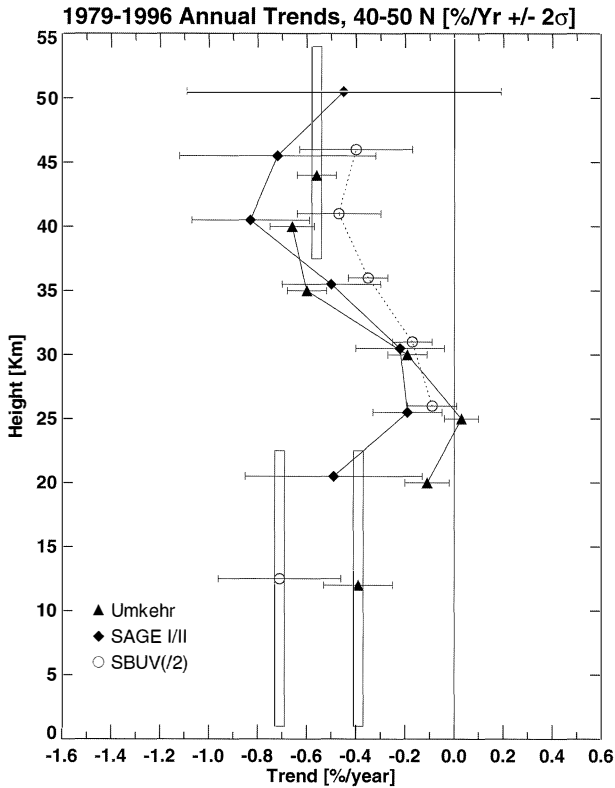


**Figure 4-31.** Ozone trends (%/yr) for 40-50°N over the period 1979-1996 calculated from the following measurement systems: three Dobson/Umkehr stations (Boulder, Haute Provence, and Belsk) reported at individual layers 4 through 8 (triangles), layers 1+2+3+4 (plotted as a vertical bar from ~1 to 22 km with a triangle), and layers 8+9+10 (plotted as a vertical bar from ~37 to 54 km with a triangle); SAGE I/II average sunrise and sunset observations (diamonds) reported at individual layers 4-10; SBUV (/2) (circles) reported at individual layers 5 through 9 and layer 1+2+3+4. All error bars are 95% confidence intervals of the trend. SAGE I/II error bars represent SAGE I altitude-correction uncertainties, SAGE II sunrise/sunset trend difference uncertainties, and statistical uncertainties. Umkehr and SBUV(/2) error bars represent only statistical uncertainty. Small vertical offsets are for clarity only (e.g., all values plotted near 30 km represent layer-6 results). (From WMO, 1998.)

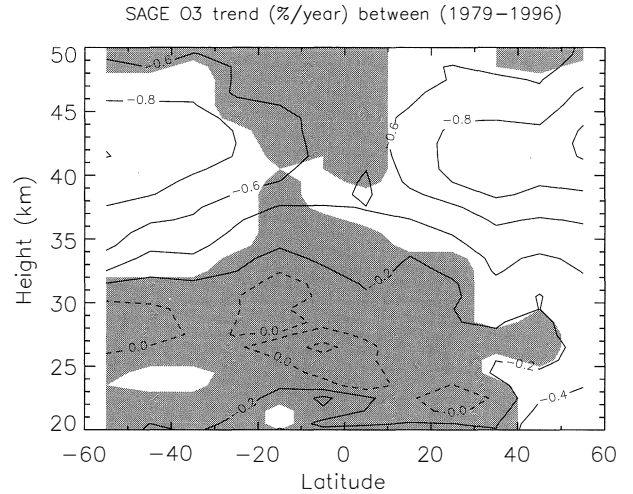


**Figure 4-32.** Ozone trends calculated from SAGE I/II observations from 1979 to 1996 expressed in %/year of the midpoint of the time series (1987). Results are contoured from calculations done in 5° latitude bands and 1-km altitude intervals. Contours differ by 0.2%/year with the dashed contours indicating zero or positive trend. The shaded area indicates where the trends do not differ from zero within 95% confidence limits. The estimate of uncertainty contains terms due to the SAGE I reference height correction and the SAGE II sunrise-sunset trend differences. (From WMO, 1998.)

are fit to a standard statistical model, negative trends are found throughout the region, with statistically significant peak values of -5 to -8%/decade at 40-45 km altitude (Figure 4-31). There is good agreement between SAGE I/II and Umkehr. The SBUV-SBUV/2 combined record shows less negative trends principally because of the lack of decline in that record after 1991. Because of the potential drift problems with the present version (6.1.2) of the NOAA-11 SBUV2 data, less confidence should be placed on the trends from the combined SBUV-SBUV/2 record.

Figure 4-32 shows the annual-average trend over the time period of 1979 through 1996 from SAGE I/II as a function of altitude and latitude. The peak negative trend is strongest at high latitudes, with a maximum negative trend of nearly 1%/yr occurring between 40 and 45 km altitude. The maximum negative trend in the equatorial region is a little less than 0.6%/yr. There is no significant interhemispheric difference in upper stratospheric trends. This contrasts with earlier results based

on SBUV (WMO, 1995). The earlier SBUV asymmetry was not statistically significant and has mostly disappeared with the extension of the dataset. The trend in layer 8 (around 40-km altitude or near the peak trend value) exhibits a seasonal variation with a maximum negative trend in both hemispheres during late winter (Figure 4-33). The seasonal variation in the trend in each hemisphere is nearly a factor of 2, ranging from -0.6%/yr to more than -1%/yr. The equatorial trend is not statistically significant except for the period from about April through July.

### 4.6.2 Lower Stratosphere

Previous evaluations have demonstrated that significant trends also occur in the lower stratosphere (altitudes between about 10 and 30 km). As we will see below, a second peak occurs in the percentage trend in the lower stratosphere. Because of the higher ozone density in the lower stratosphere, this second peak is responsible for most of the trend observed in the column amount of ozone. The primary trend instruments in this region are sondes (ground up to 27 km) and SAGE (SAGE I from 20 km up and SAGE II from 15 km up).

Two groups, Logan and Megretskaja (LM, Harvard University) and Tiao *et al.* (University of Chicago), carried out analyses of the sonde data. They used different methods to screen the sonde data and arrived at somewhat different trend results, which will be shown below.

Tiao *et al.* used a more stringent selection criterion for the so-called “correction factor” deduced for a sonde measurement. After applying this more-stringent criterion, Tiao *et al.* then used uncorrected data. Logan and Megretskaja allowed more data to pass the screening by adopting a less stringent criterion for correction factors, and then used the corrected data. This resulted in a time

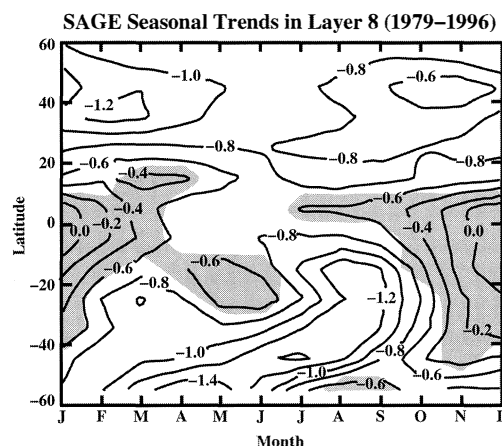


**Figure 4-33.** Seasonal variation of ozone trends in layer 8 (in %/year) calculated from SAGE I/II (1979-1996) for latitudes 55°S to 55°N. Non-shaded areas indicate 95% confidence intervals that include SAGE I altitude correction, SAGE II sunrise-sunset trend differences, and statistical uncertainties. (From WMO, 1998.)

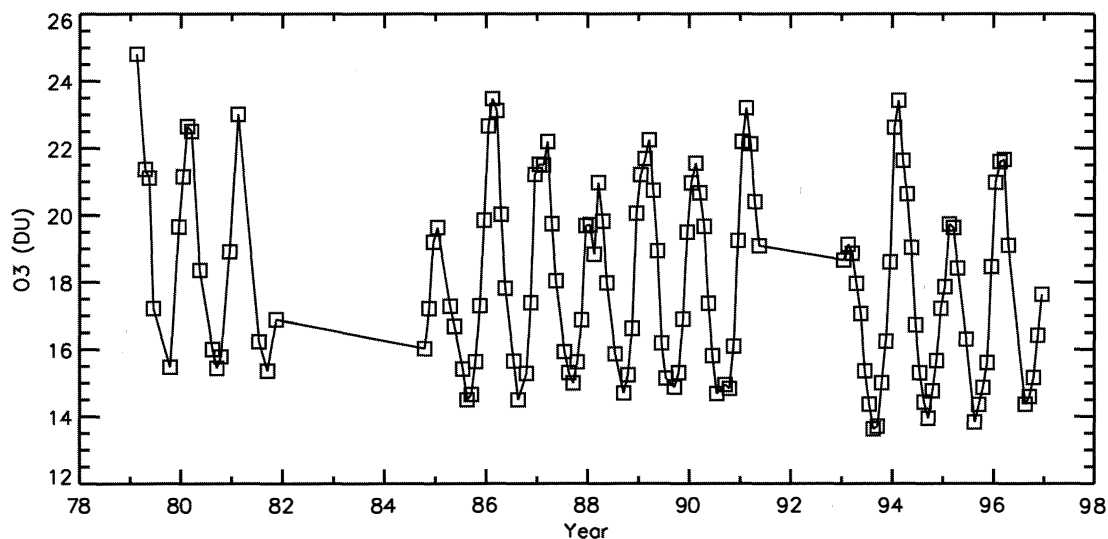


**Figure 4-34.** SAGE I/II monthly mean ozone measurements between 45°N and 50°N integrated from 20 to 21 km altitude in Dobson units. (From WMO, 1998.)

## OZONE TRENDS

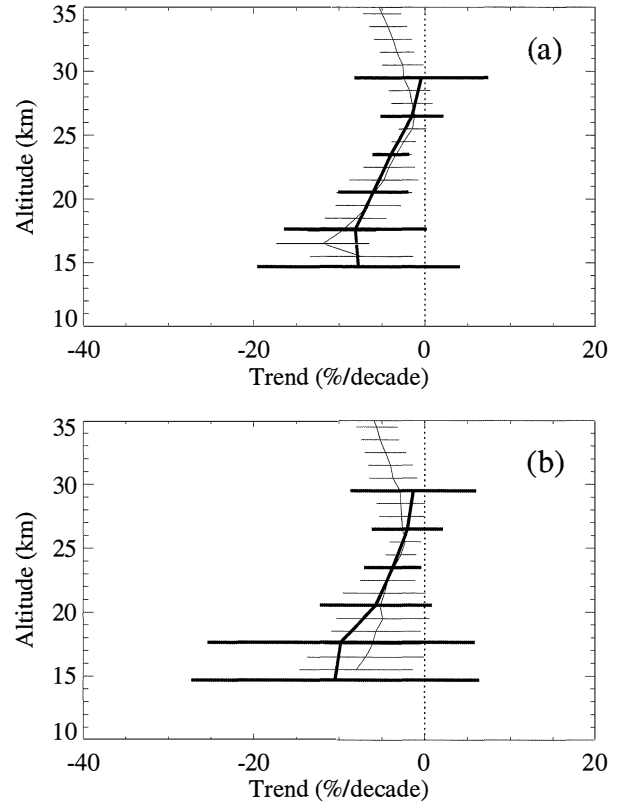
series with significantly more data points. The results of the two analyses are in agreement on major points but do have some important differences, some of which will be shown below.

Figure 4-34 shows a time series from the SAGE I/II measurements integrated between 40 and 45°N latitudes and 20 and 21 km altitudes. The series is dominated by seasonal cycles, but a trend can also be seen in the data. A problem pointed out in previous Assessments (e.g., WMO, 1995) is the disagreement between trends derived from sondes and SAGE in the lower stratosphere. With the reanalyzed sonde data and the new version of SAGE data, this disagreement no longer exists. Figure 4-35 shows the average ozonesonde trend derived from seven stations at northern midlatitudes compared with those derived from SAGE for the zonal mean between 45 and 50°N latitudes as a function of altitude. The comparison now shows excellent agreement.

Figure 4-36 shows the trends derived from nine separate stations as a function of altitude. The analyses of both LM and Tiao *et al.* are shown. While the details of the two analyses are different, both reach the conclusion that the trends are negative over the region of the lower stratosphere at all stations. The trends near 100 mb (~17 km) range from about -3%/decade to -10%/decade and are statistically significant at all stations. The trends decrease at higher altitudes and are near zero at 20 mb. The trends in the troposphere are much more widely varying from station to station (see Chapter 8 for a discussion of tropospheric ozone trends).

Figure 4-37 shows the combined calculated trends for the time period from 1970 through 1996 from eight sonde stations as a function of altitude for four seasons. The results from both the LM and Tiao *et al.* analyses are shown. Both indicate that the trends are not a function of season above about 70 mb and in the troposphere. The seasonal dependence of ozone trends appears to be confined to the region between about 10 and 20 km altitude. The two analyses get a somewhat different seasonality in the 10-20 km region. When the stations are divided up by region, some interesting differences appear. In Figure 4-38, the trends calculated by LM for 1970-1996 are shown for the four seasons for three combined European stations and three combined Canadian stations. The Canadian stations show a seasonal variation that is quite different from that seen at the European stations and extends over a larger altitude range.

The trends shown for the lower stratosphere thus



**Figure 4-35.** Average ozonesonde trends for Uccle, Hohenpeissenberg, Payerne, Edmonton, Goose Bay, Boulder, and Sapporo (40-53°N) for the time periods (a) 1980-1996 and (b) 1984-1996, in percent/decade (darker lines). These are compared to (a) trends for SAGE I/II and (b) trends for SAGE II alone for 45-50°N (lighter lines). The SAGE trends were analyzed at 1-km intervals, and the ozonesonde trends have been expressed as a function of altitude using the 1976 standard, midlatitude atmosphere. The 2-sigma error bars are given. (From WMO, 1998.)

far have been for the time period starting in 1970. The SAGE data begin in 1979 with SAGE I and resume again in 1984 with SAGE II. The SPARC/IOC report showed calculations of the trend from sondes over the time period of 1970-1996 compared with those for 1980-1996 (see also Chapter 8 of this report). Only minor differences were seen in the stratosphere. We can use the SAGE measurements to give us a global picture of the trends since 1979. These trends, which extend from 20-km altitude upward, were shown in Figure 4-32. For the

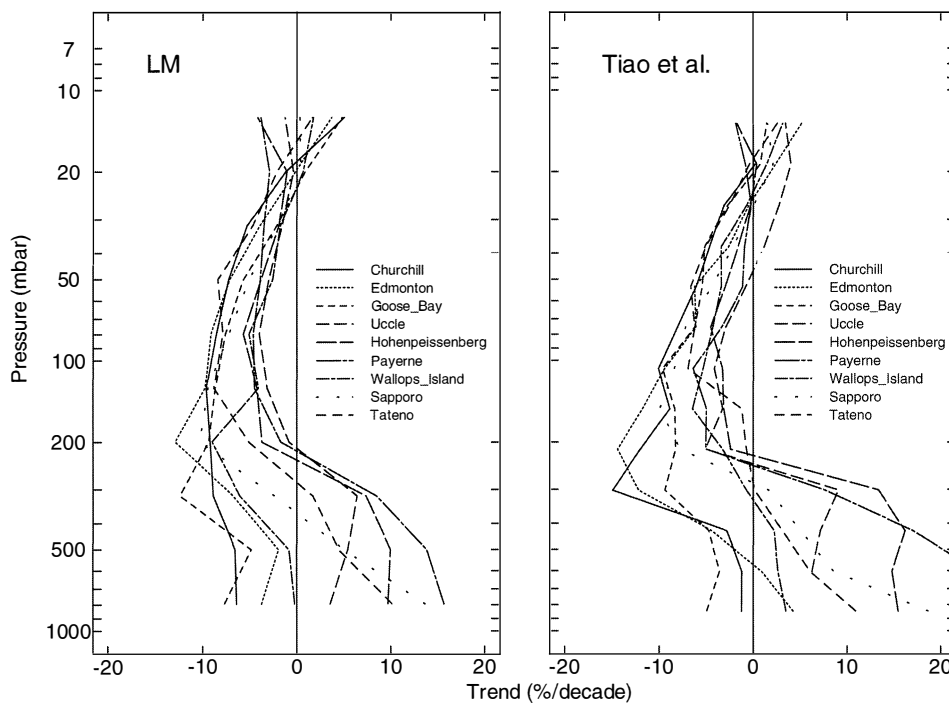


**Figure 4-36.** Annual ozone trends for individual sonde stations located between 59°N and 36°N for the period 1970-1996: LM results (left), and Tiao *et al.* results (right). (Modified from a figure in WMO, 1998.)

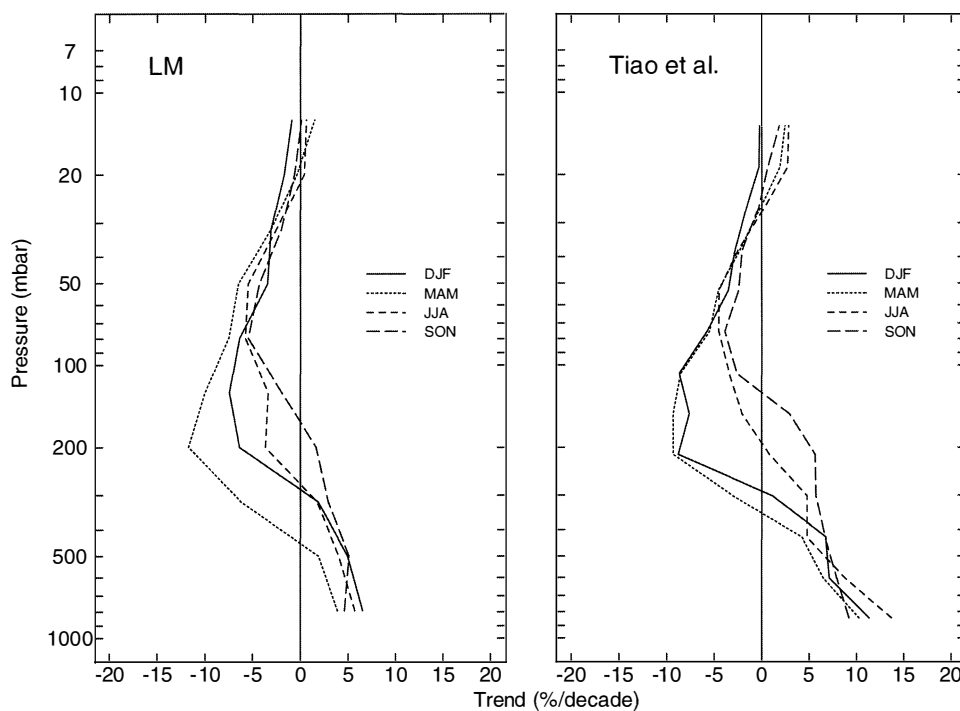


**Figure 4-37.** Seasonal-mean profiles of ozone trends (% for eight sonde stations located between 59°N and 36°N: LM results (left), and Tiao *et al.* results (right). (Modified from a figure in WMO, 1998.)

## OZONE TRENDS

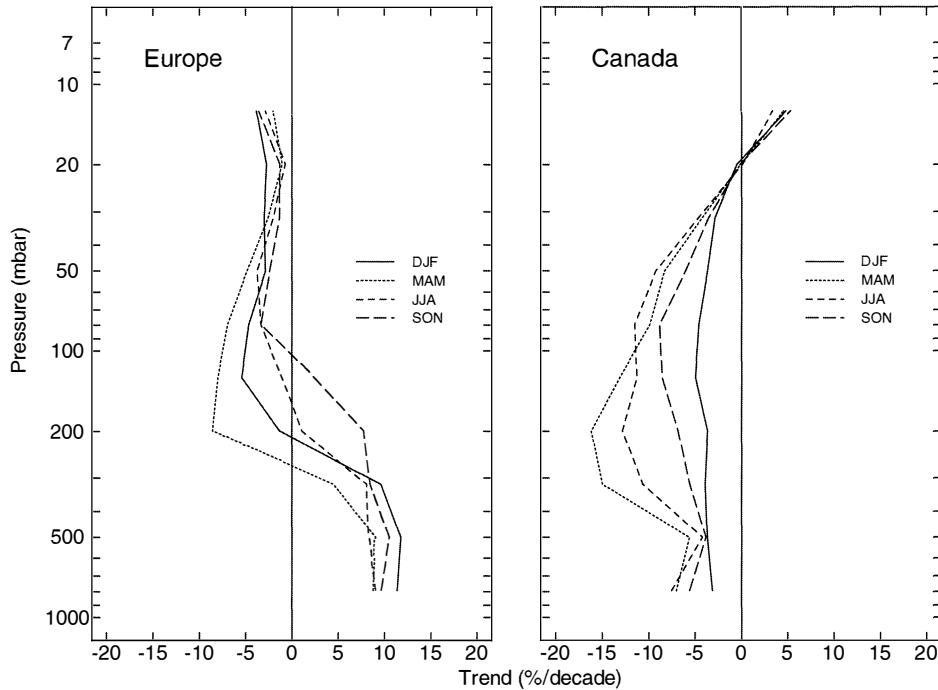


**Figure 4-38.** Seasonal mean profiles of ozone trend for three European stations, 48-51°N (left) and three Canadian stations, 53-59°N (right); LM results. (Modified from a figure in WMO, 1998.)

shorter time period from 1984 through 1996 where SAGE II data are available, the record can be extended down to 15 km. The resulting annually averaged trend is shown in Figure 4-39 as a function of altitude and latitude. The northern midlatitude negative peak in the trend, previously shown in Figure 4-32, is apparent. At southern midlatitudes, no such peak in the negative trend is seen, and the trends are in fact slightly positive. Note that between 15 and 20 km altitude, the trends shown are mostly statistically not different from zero. This is because of the shortness of the record, the variability of ozone, and the sampling frequency.

### 4.6.3 Combined Trends

The SPARC/IOC (WMO, 1998) report made a first attempt at combining the trends and uncertainties (including both statistical and systematic) estimated from all available measurement systems. This was done only for northern midlatitudes, where sufficient measurements from multiple systems are available. The calculations are all for the trend since 1979. The combination of the trends was done by using the following prescription. First, trends and statistical uncertainties were determined for each instrument or station. Then instrumental un-

certainties were estimated for each instrument. These were limited to those uncertainties that would result in potential drift errors in the data. Thus, cross section errors were not counted in this estimate because they would be constant in time. Next, the statistical and instrumental errors were combined by taking the root sum of their squares.

The trends for the sonde stations were then averaged by taking a weighted mean of their results at each altitude. The weighting factor was one over the square of the combined estimated standard error. The uncertainty in the averaged trend over all of the stations was determined in two ways. One was to combine the uncertainties deduced from each sonde station. The other was to calculate the standard error of the mean for the individually determined trends. This second method gave the largest estimate of uncertainty for 20 km and below and was used in all subsequent calculations.

Trends as a function of altitude were derived for each of the four measurement systems and their uncertainties were estimated according to the above description. These were then combined into a single trend as a function of altitude by using a weighted mean of the individual trends and a weighted mean of the individual

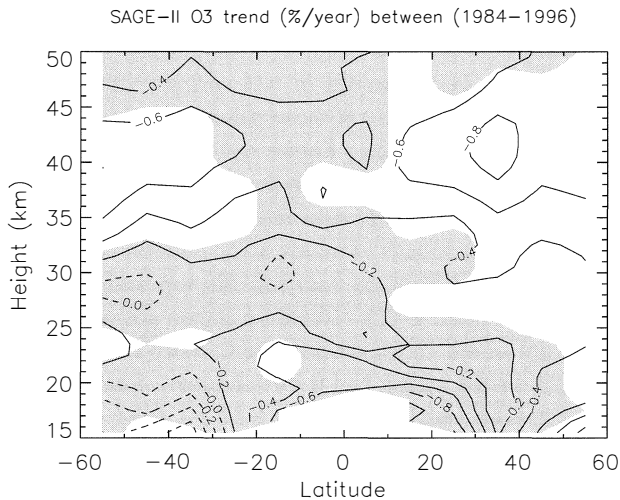


**Figure 4-39.** Annual trends for SAGE II only for the time period 1984 to 1996. (From WMO, 1998.) The shaded area indicates where the trends do not differ from zero within 95% confidence limits.

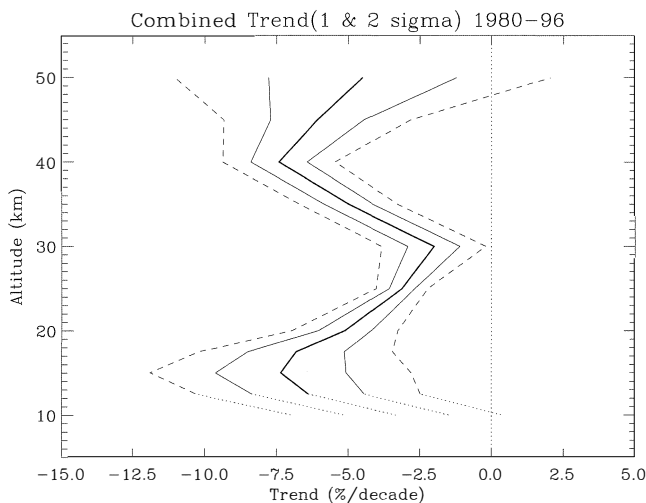


**Figure 4-40.** Estimate of the mean trend using all four measurement systems at northern midlatitudes (heavy solid line). Combined uncertainties are also shown as 1 sigma (light solid line) and 2 sigma (dashed line). Combined trends and uncertainties are extended down to 10 km as shown by the light dotted lines. The results below 15 km are a mixture of tropospheric and stratospheric trends and the exact numbers should be viewed with caution. Combined trends have not been extended lower into the troposphere because the small sample of sonde stations have an additional unquantified uncertainty concerning their representativeness of mean trends. (From WMO, 1998.)

uncertainties at each altitude where more than one system made measurements. This procedure results in a single trend estimate as a function of altitude for the northern midlatitude data. The trend estimate is weighted at each altitude toward the result from the system that had the smallest combined statistical and instrumental drift uncertainties. The result is shown in Figure 4-40.

The estimated trend for the upper stratosphere peaks at  $(-7.4 \pm 2.0)\%$ /decade at 40 km. This result is dominated by the SAGE data which have the smallest estimated uncertainty. At 20 km, the trend is from the combined SAGE, sonde, and Umkehr results. Below 20 km, the trend estimate comes from sondes alone. The lower stratospheric trend shows a maximum negative value of  $(-7.3 \pm 4.6)\%$ /decade at 15 km. The minimum trend between these peaks is  $(-2.0 \pm 1.8)\%$ /decade at 30 km, which is just statistically significant at the 95% confidence level. Thus, at northern midlatitudes, a statistically significant negative trend is found at all altitudes between 12 and 45 km.

#### 4.6.4 Consistency between Total Ozone and Vertical Profile Trends

It is clear from the preceding sections that our ozone trend assessment capabilities have increased in recent years. One particular concern highlighted by WMO (1995) was the disagreement found between the TOMS-based total ozone trends and vertically integrated profile trends derived from sonde and SAGE I and II data. This now appears to have been largely resolved.

In WMO (1998), column ozone trends derived from TOMS data were compared to the integrated ozone profile trends derived from SAGE I/II and from ozonesonde data, in order to determine the consistency between the independent results. Figure 4-41 (a direct reproduction of Figure 3.49 in WMO (1998)) shows the first results of this analysis. Figure 4-41 (top) shows the TOMS column ozone trends as a function of latitude and season. The data show negative trends in NH midlatitudes during late-winter/spring; the March-April values of about -24 DU/decade correspond to percentage changes of about -6%/decade. There are smaller magnitude midlatitude trends in the SH (about -10 DU/decade) and no significant trends in the tropics. The trends in column ozone over 20-55 km derived from SAGE I/II data are shown in Figure 4-41 (middle panel). Significant negative trends of order -4 to -8 DU/decade are observed in NH midlatitudes throughout most of the year (with a maximum in April-May near 50°N) and in

## OZONE TRENDS

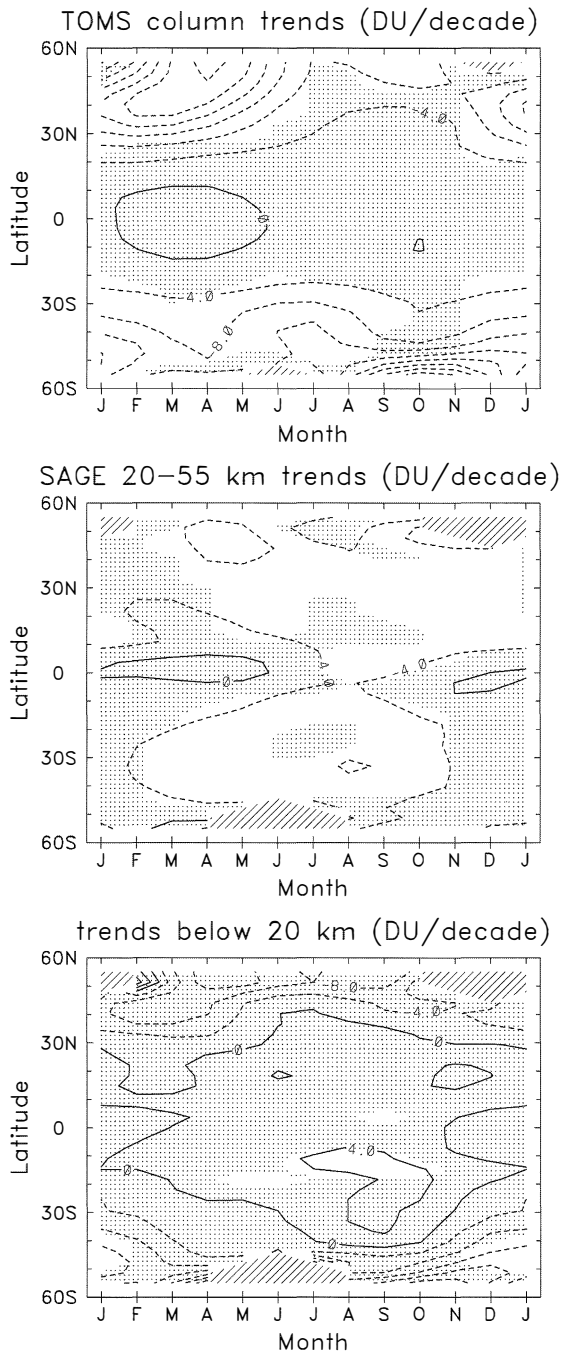


**Figure 4-41.** Top panel: Seasonal and latitudinal variation of trends in column ozone from TOMS. Middle panel: Seasonal and latitudinal variation of trends in column integral of SAGE from 20 to 55 km. Bottom panel: Seasonal and latitudinal variations of trends in TOMS minus SAGE (i.e., column ozone below 20 km). The contour interval for all panels is 4 DU/decade. Statistically insignificant  $2\sigma$  trends are shaded. (From WMO, 1998.)

SH midlatitudes during winter. Significant trends are not observed near the equator. Comparison with the much larger TOMS trends in NH spring midlatitudes suggests that a majority of these column trends occur at altitudes below 20 km. Figure 4-41 (bottom) shows trends in the difference between the TOMS column ozone data and the SAGE I/II data integrated from 20 to 55 km. This corresponds to trends in the column below 20 km (i.e., the difference between the top and middle frames of Figure 4-41). Negative trends are observed poleward of  $40^\circ$  in each hemisphere; there are relative maxima in NH spring and in SH summer. Small positive trends are seen in the tropics ( $\sim 30^\circ\text{N}$ - $30^\circ\text{S}$ ); because of the small background (seasonal) values in the tropics below 20 km, these latter trends equate to a relatively high percentage ( $\sim 5$ - $10\%$ /decade).

## REFERENCES

- Ancellet, G., and M. Beekmann, Evidence for changes in the ozone concentration in the free troposphere over southern France from 1976-1995, *Atmos. Environ.*, *31*, 2835-2851, 1997.
- Angell, J.K., Estimated impacts of Agung, El Chichón, and Pinatubo volcanic eruptions on global and regional total ozone after adjustment for the QBO, *Geophys. Res. Lett.*, *24*, 647-650, 1997.
- Angreji, P.D., Reevaluation of total ozone measurements with Dobson spectrophotometer at Mt. Abu/Ahmedabad during 1951-1985, *Scientific Rep. ISRO-PRL-SR-34-89*, Indian Space Research Organization, Bangalore, 1989.
- Atkinson, R.J., and R.A. Plumb, Three-dimensional ozone transport during ozone hole break-up in December 1987, *J. Geophys. Res.*, *102*, 1451-1466, 1997.
- Basher, R.E., *Survey of WMO-Sponsored Dobson Spectrophotometer Intercomparisons*, World Meteorological Organization Global Ozone Research and Monitoring Project—Report No. 19, Geneva, 1995.
- Bekoryukov, V.I., I.V. Bugaeva, G.R. Zakharov, B.M. Kiryushov, G.M. Kruchenitskii, and D.A. Tarasenko, Influence of atmospheric centres of action on total ozone in Siberia, *Meteorol. Gidrol.*, No. 7, 33-39, 1997.

- Bhartia, P.K., R.D. McPeters, C.L. Mateer, L.E. Flynn, and C. Wellemeyer, Algorithm for the estimation of vertical ozone profiles from the backscattered ultraviolet technique, *J. Geophys. Res.*, *101*, 18793-18806, 1996.
- Bojkov, R.D., The 1979-85 ozone decline in the Antarctic as reflected in ground based observations, *Geophys. Res. Lett.*, *13*, 1236-1239, 1986.
- Bojkov, R.D., The 1983 and 1985 anomalies in ozone distribution in perspective, *Mon. Wea. Rev.*, *115*, 2187-2201, 1987.
- Bojkov, R.D., Ozone variations in the northern polar region, *Meteorol. Atmos. Phys.*, *38*, 117-130, 1988.
- Bojkov, R.D., and V. Fioletov, Changes of the lower stratospheric ozone over Europe and Canada, *J. Geophys. Res.*, *102*, 1337-1347, 1997.
- Bojkov, R.D., and V. Fioletov, Latitudinal and regional total ozone trends from quality controlled ground-based data, in *Atmospheric Ozone: Proceedings of the XVIII Quadrennial Ozone Symposium*, L'Aquila, Italy, 12-21 September 1996, edited by R.D. Bojkov and G. Visconti, pp. 13-16, Parco Scientifico e Tecnologico d'Abruzzo, L'Aquila, Italy, 1998.
- Bojkov, R.D., C. Mateer, and A. Hanson, Comparison of ground-based and Total Ozone Mapping Spectrometer measurements used in assessing the performance of the global ozone observing system, *J. Geophys. Res.*, *93*, 9525-9533, 1988.
- Bojkov, R.D., L. Bishop, W.J. Hill, G.C. Reinsel, and G.C. Tiao, A statistical trend analysis of revised Dobson total ozone data over the Northern Hemisphere, *J. Geophys. Res.*, *95*, 9785-9807, 1990.
- Bojkov, R.D., C.S. Zerefos, D.S. Balis, I.C. Ziomas, and A.F. Bais, Record low total ozone during northern winters of 1992 and 1993, *Geophys. Res. Lett.*, *20*, 1351-1354, 1993.
- Bojkov, R.D., V.E. Fioletov, and A.M. Shalamjansky, Total ozone changes over Eurasia since 1973 based on reevaluated filter ozonometer data, *J. Geophys. Res.*, *99*, 22985-22999, 1994.
- Bojkov, R.D., V.E. Fioletov, D.S. Balis, C.S. Zerefos, T.V. Kadygrova, and A.M. Shalamjansky, Further ozone decline during the Northern Hemisphere winter-spring of 1994-1995 and the new record low ozone over Siberia, *Geophys. Res. Lett.*, *22*, 2729-2732, 1995a.
- Bojkov, R.D., L. Bishop, and V.E. Fioletov, Total ozone trends from quality controlled ground-based data (1964-1994), *J. Geophys. Res.*, *100*, 25867-25876, 1995b.
- Bojkov, R.D., D.S. Balis, C.S. Zerefos, K. Tourpali, M. Tzortziou, and T.V. Kadygrova, An update of ozone changes in the Northern Hemisphere through April 1997, in *Report on the Fourth European Symposium on Stratospheric Ozone Research*, Schliersee, Bavaria, September 1997, pp.185-189, 1997.
- Bojkov, R.D., D.S. Balis, and C.S. Zerefos, Characteristics of the ozone decline in the northern polar and middle latitudes during the winter-spring, *Meteorol. Atmos. Phys.*, in press, 1998a.
- Bojkov, R.D., D.S. Balis, C.S. Zerefos, and K. Tourpali, Northern Hemisphere winter-spring ozone changes in 1990-1996, in *Atmospheric Ozone: Proceedings of the XVIII Quadrennial Ozone Symposium*, L'Aquila, Italy, 12-21 September 1996, edited by R.D. Bojkov and G. Visconti, pp. 251-254, Parco Scientifico e Tecnologico d'Abruzzo, L'Aquila, Italy, 1998b.
- Box, G.E.P., G.M. Jenkins, and G.C. Reinsel, *Time Series Analysis: Forecasting and Control*, 3<sup>rd</sup> ed., Prentice Hall, Englewood Cliffs, N.J., 1994.
- Brasseur, G.P., The response of the middle atmosphere to long-term and short-term solar variability: A two dimensional model, *J. Geophys. Res.*, *98*, 23079-23090, 1993.
- Brasseur, G., and C. Granier, Mount Pinatubo aerosols, chlorofluocarbons, and ozone depletion, *Science*, *257*, 1239-1242, 1992.
- Chandra, S., and R.D. McPeters, The solar cycle variation of ozone in the stratosphere inferred from Nimbus 7 and NOAA 11 satellites, *J. Geophys. Res.*, *99*, 20665-20671, 1994.
- Chernikov, A.A., Yu.A. Borisov, A.M. Zvyagintsev, G.M. Kruchenitskii, S.P. Perov, N.S. Sidorenkov, and O.V. Stasyuk, The 1997-1998 El Niño influence on the Earth's ozone layer, *Meteorol. Hidrol.*, No. 3, 104-110, 1998.
- Chesters, D., and A.C. Neuendorffer, Comparison between TOMS, TOVS and Dobson observations: Satellite and surface view of total column ozone, *Paleogeogr. Paleoclimatol. Paleocol.*, *90*, 61-73, 1991.

## OZONE TRENDS

- Chubachi S., Annual variation of total ozone at Syowa Station, Antarctica, *J. Geophys. Res.*, *107*, 1349-1354, 1997.
- Cunnold, D.M., H. Wang, W. Chu, and L. Froidevaux, Comparisons between SAGE II and MLS ozone measurements and aliasing of SAGE II ozone trends in the lower stratosphere, *J. Geophys. Res.*, *101*, 10061-10075, 1996.
- Dave, J.V., and C.L. Mateer, A preliminary study on the possibility of estimating total atmospheric ozone from satellite measurements, *J. Atmos. Sci.*, *24*, 414-427, 1967.
- Dobson, G.M.B., A.W. Brewer, and B.M. Cwilong, Meteorology of the lower stratosphere, *Proc. Roy. Meteorol. Soc. London*, *A185*, 144-175, 1946.
- Donovan, D.P., J.C. Bird, J.A. Whiteway, T.J. Duck, S.R. Pal, and A.I. Carwell, Lidar observations of stratospheric ozone and aerosol above the Canadian high Arctic during the 1994-95 winter, *Geophys. Res. Lett.*, *22*, 3489-3492, 1995.
- Dorokhov, V.M., and T.E. Potapova, Variation of total ozone and NO<sub>2</sub> at polar latitudes in eastern sector of the Arctic, in *Atmospheric Ozone: Proceedings of the XVIII Quadrennial Ozone Symposium*, L'Aquila, Italy, 12-21 September 1996, edited by R.D. Bojkov and G. Visconti, pp. 201-204, Parco Scientifico e Tecnologico d'Abruzzo, L'Aquila, Italy, 1998.
- Fioletov, V.E., J.B. Kerr, E.W. Hare, G. Labow, and R. McPeters, An assessment of the world ground-based total ozone network performance from the comparison with satellite data, *J. Geophys. Res.*, submitted, 1998a.
- Fioletov, V.E., R.D. Bojkov, P.K. Bhartia, R. McPeters, A.J. Miller, and W. Planet, Total ozone trends derived from Solar Backscatter Ultraviolet (SBUV) and SBUV/2 measurements, in *Atmospheric Ozone: Proceedings of the XVIII Quadrennial Ozone Symposium*, L'Aquila, Italy, 12-21 September 1996, edited by R.D. Bojkov and G. Visconti, pp. 37-40, Parco Scientifico e Tecnologico d'Abruzzo, L'Aquila, Italy, 1998b.
- Fleig, A.J., R.D. McPeters, P.K. Bhartia, B.M. Schlesinger, R.P. Cebula, K.R. Klenk, S.L. Taylor, and D.F. Heath, *Nimbus 7 Solar Backscatter Ultraviolet (SBUV) Ozone Products User's Guide*, NASA Ref. Publ. 1234, National Aeronautics and Space Administration, Washington, D.C., 1990.
- Gernandt, H., A. Herber, P. von der Gathen, M. Rex, A. Rinke, S. Wessel, and S. Kaneto, Variability of ozone and aerosols in the polar stratosphere, *Mem. Natl. Inst. Polar Res., Spec. Issue*, *51*, 189-215, 1996.
- Gernandt, H., P. von der Gathen, A. Herber, and S. Kaneto, Interannual ozone changes in the lower and middle stratosphere above the Antarctic in spring, in *Atmospheric Ozone: Proceedings of the XVIII Quadrennial Ozone Symposium*, L'Aquila, Italy, 12-21 September 1996, edited by R.D. Bojkov and G. Visconti, pp. 205-208, Parco Scientifico e Tecnologico d'Abruzzo, L'Aquila, Italy, 1998.
- Gleason, J.F., and R.D. McPeters, Corrections to the Nimbus 7 Solar Backscatter Ultraviolet data on the "nonsync" period (February 1987 to June 1990), *J. Geophys. Res.*, *100*, 16873-16877, 1995.
- Gleason, J.F., P.K. Bhartia, J.R. Herman, R. McPeters, P. Newman, R.S. Stolarski, L. Flynn, G. Labow, D. Larko, C. Seftor, C. Wellemeyer, W.D. Komhyr, A.J. Miller, and W. Planet, Record low global ozone in 1992, *Science*, *260*, 523-526, 1993.
- Goutail, F., and J.P. Pommereau, Ozone loss: The northern polar picture, in *Report on the Fourth European Symposium on Stratospheric Ozone Research*, Schliersee, Bavaria, September 1997, pp. 273-276, 1997.
- Goutail, F.J., J.P. Pommereau, F. Lefèvre, E. Kyrö, M. Rummukainen, P. Ericksen, S.B. Andersen, B.-A. Kaastad-Hoiskar, G. Breathen, V. Dorokhov, and V. Khattatov, Total ozone reduction in the Arctic vortex during the winters of 1995/96 and 1996/97, in *Report on the Fourth European Symposium on Stratospheric Ozone Research*, Schliersee, Bavaria, September 1997, pp. 277-280, 1997.
- Gustin, G.P., S.A. Sokolenko, B.G. Dudko, and V.V. Lagutina, Ozonometer M-124 (in Russian), *Tr. Glav. Geofiz. Obs.*, *499*, 60-67, 1985.
- Hansen, G., T. Svenoe, M.P. Chipperfield, A. Dahlback, and U.P. Hoppe, Evidence of substantial ozone depletion in winter 1995/96 over northern Norway, *Geophys. Res. Lett.*, *24*, 799-802, 1997.
- Harris, N.R.P., G. Ancellet, L. Bishop, D.J. Hofmann, J.B. Kerr, R.D. McPeters, M. Préndez, W.J. Randel, J. Staehelin, B.H. Subbaraya, A. Volz-Thomas, J. Zawodny, and C.S. Zerefos, Trends in stratospheric and free tropospheric ozone, *J. Geophys. Res.*, *102*, 1571-1590, 1997.

- Hasebe, F., Quasi-biennial oscillations of ozone and diabatic circulation in the equatorial stratosphere, *J. Atmos. Sci.*, *51*, 729-745, 1994.
- Heath, D.F., C.L. Mateer, and A.J. Krueger, The Nimbus-4 backscatter ultraviolet atmospheric ozone experiment, *Pure Appl. Geophys.*, *106-108*, 1238-1253, 1973.
- Heath, D.F., A.J. Krueger, H.A. Roeder, and B.D. Henderson, The Solar Backscatter Ultraviolet and Total Ozone Mapping Spectrometer (SBUV/TOMS) for Nimbus G, *Opt. Eng.*, *14*, 323-331, 1975.
- Herman, J.R., P.K. Bhartia, A.J. Krueger, R.D. McPeters, C.G. Wellemeyer, C.J. Seftor, G. Jaross, B. Schlesinger, O. Torres, G. Labow, W. Byerly, S.L. Taylor, T. Swissler, R.P. Cebula, and X. Gu, *Meteor 3 Total Ozone Mapping Spectrometer (TOMS) Data Protocol User's Guide*, NASA Ref. Publ. 1393, 1996.
- Hilsenrath, E., D.E. Williams, R.T. Caffrey, R.P. Cebula, and S.J. Hynes, Calibration and radiometric stability of the Shuttle Solar Backscatter Ultraviolet (SSBUV) experiment, *Metrologia*, *30*, 243-248, 1993.
- Hofmann, D.J., and T. Deshler, Evidence from balloon measurements for chemical depletion of stratospheric ozone in the Arctic winter of 1989-90, *Nature*, *349*, 300-305, 1991.
- Hofmann, D.J., and S. Solomon, Ozone destruction through heterogeneous chemistry following the eruption of El Chichón, *J. Geophys. Res.*, *94*, 5029-5041, 1989.
- Hofmann, D.J., S.J. Oltmans, J.M. Harris, B.J. Johnson, and J.A. Lathrop, Ten years of ozonesonde measurements at the South Pole: Implications for recovery of spring time Antarctic ozone, *J. Geophys. Res.*, *102*, 8931-8943, 1997.
- Hollandsworth, S.M., K.P. Bowman, and R.D. McPeters, Observational study of the quasi-biennial oscillation in ozone, *J. Geophys. Res.*, *100*, 7347-7361, 1995a.
- Hollandsworth, S.M., R.D. McPeters, L.E. Flynn, W. Planet, A.J. Miller, and C. Chandra, Ozone trends deduced from combined Nimbus 7 SBUV and NOAA 11 SBUV/2 data, *Geophys. Res. Lett.*, *22*, 905-908, 1995b.
- Hood, L.L., The solar cycle variation of total ozone: Dynamical forcing in the lower stratosphere, *J. Geophys. Res.*, *102*, 1355-1369, 1997.
- Hood, L.L., and D.A. Zaff, Lower stratospheric stationary waves and the longitude dependence of ozone trends in winter, *J. Geophys. Res.*, *100*, 25791-25800, 1995.
- Hood, L.L., J.P. McCormack, and K. Labitzke, An investigation of dynamical contributions to mid-latitude ozone trends in winter, *J. Geophys. Res.*, *102*, 13079-13093, 1997.
- Jackman, C.H., E.L. Fleming, S. Chandra, D.B. Considine, and J.E. Rosenfield, Past, present, and future modelled ozone trends with comparisons to observed trends, *J. Geophys. Res.*, *101*, 28753-28767, 1996.
- Jones, A.E., and J.D. Shanklin, Continued decline of total ozone over Halley, Antarctica, since 1985, *Nature*, *376*, 409-411, 1995.
- Kayano, M.T., Principal modes of the total ozone on the Southern Oscillation timescale and related temperature variations, *J. Geophys. Res.*, *102*, 25797-25806, 1997.
- Kerr, J.B., I.A. Asbridge, and W.F.J. Evans, Intercomparison of total ozone measured by the Brewer and Dobson spectrophotometers at Toronto, *J. Geophys. Res.*, *93*, 11129-11140, 1988.
- Kerr, J.B., C.T. McElroy, and D.W. Wardle, The Brewer instrument calibration centre 1984-1996, in *Atmospheric Ozone: Proceedings of the XVIII Quadrennial Ozone Symposium*, L'Aquila, Italy, 12-21 September 1996, edited by R.D. Bojkov and G. Visconti, pp. 915-918, Parco Scientifico e Tecnologico d'Abruzzo, L'Aquila, Italy, 1998.
- Knudsen, B.M., N. Larsen, I.S. Mikkelsen, J.-J. Morcrette, G.O. Braathen, E. Kyrö, H. Fast, H. Gernandt, H. Kanzawa, H. Nakane, V. Dorokhov, V. Yushkov, G. Hansen, M. Gil, and R.J. Shearman, Ozone depletion in and below the Arctic vortex for 1997, *Geophys. Res. Lett.*, *25*, 627-630, 1998.
- Köhler, U., and H. Claude, Homogenized ozone record at Hohenpeissenberg, in *Atmospheric Ozone: Proceedings of the XVIII Quadrennial Ozone Symposium*, L'Aquila, Italy, 12-21 September 1996, edited by R.D. Bojkov and G. Visconti, pp. 57-60, Parco Scientifico e Tecnologico d'Abruzzo, L'Aquila, Italy, 1998.
- Koike, M., Y. Kondo, M. Hayashi, Y. Iwasake, P.A. Newman, M. Helten, and P. Amedieu, Depletion of Arctic ozone in the winter 1990, *Geophys. Res. Lett.*, *18*, 791-794, 1991.

## OZONE TRENDS

- Komhyr, W.D., R.D. Grass, R.D. Evans, R.K. Leonard, D.M. Quincy, D.J. Hofmann, and G.L. Koenig, Unprecedented 1993 ozone decrease over the United States from Dobson spectrophotometer observations, *Geophys. Res. Lett.*, *21*, 201-204, 1994.
- Krueger, A.J., D.F. Heath, and C.L. Mateer, Variations in the stratospheric ozone field inferred from Nimbus satellite observations, *Pure Appl. Geophys.*, *106-108*, 1254-1263, 1973.
- Kyrö, E., P. Taalas, T.S. Jorgensen, B. Knudsen, F. Stordal, G. Braathen, A. Dahlback, R. Neuber, B.C. Krüger, V. Dorokhov, V.A. Yushkov, V.V. Rudakov, and A. Torres, Analysis of the ozone soundings made during the first quarter of 1989 in the Arctic, *J. Geophys. Res.*, *97*, 8083-8091, 1992.
- Labitzke, K., and H. van Loon, The signal of the 11-year sunspot cycle in the upper troposphere-lower stratosphere, *Space Sci. Rev.*, *80*, 393-410, 1997.
- Lapworth, A., *Report of Re-evaluation of Total Ozone Data from the U.K. Dobson Network for the Last Decade*, U.K. Meteorological Office, Bracknell, 1991.
- Larsen, N., B. Knudsen, I.S. Mikkelsen, T.S. Jorgensen, and P. Eriksen, Ozone depletion in the Arctic stratosphere in early 1993, *Geophys. Res. Lett.*, *21*, 1611-1614, 1994.
- Lehmann, P., D.J. Karoly, P.A. Newman, T.S. Clarkson, and W.A. Matthews, Long-term winter total ozone changes at Macquarie Island, *Geophys. Res. Lett.*, *19*, 1459-1462, 1992.
- Manney, G.L., L. Froidevaux, J.W. Waters, J.C. Gille, R.W. Zurek, J.B. Kummer, J.L. Mergenthaler, A.E. Roch, A. O'Neill, and R. Swinbank, Formation of low-ozone pockets in the middle stratospheric anticyclone during winter, *J. Geophys. Res.*, *100*, 13939-13950, 1995.
- Manney, G.L., L. Froidevaux, J.W. Waters, M.L. Santee, W.G. Read, D.A. Flower, R.F. Jarnot, and R.W. Zurek, Arctic ozone depletion observed by UARS MLS during the 1994-95 winter, *Geophys. Res. Lett.*, *23*, 85-88, 1996a.
- Manney, G.L., L. Froidevaux, M.L. Santee, J.W. Waters, and R.W. Zurek, Polar vortex conditions during the 1995-1996 Arctic winter, *Geophys. Res. Lett.*, *23*, 3203-3206, 1996b.
- Manney, G.L., L. Froidevaux, M.L. Santee, R.W. Zurek, and J.W. Waters, MLS observations of Arctic ozone loss in 1996-1997, *Geophys. Res. Lett.*, *24*, 2697-2700, 1997.
- Mateer, C.L., and J.J. DeLuisi, A new Umkehr inversion algorithm, *J. Atmos. Terr. Phys.*, *54*, 537-556, 1992.
- McCormack, J.P., and L.L. Hood, The frequency and size of ozone "mini-hole" events at northern mid-latitudes in February, *Geophys. Res. Lett.*, *24*, 2647-2650, 1997.
- McCormack, J.P., L.L. Hood, R. Nagatani, A.J. Miller, W.G. Planet, and R.D. McPeters, Approximate separation of volcanic and 11-year signals in the SBUV-SBUV/2 total ozone record over the 1970-1995 period, *Geophys. Res. Lett.*, *24*, 2729-2732, 1997.
- McKenna, D.S., R.L. Jones, L.R. Poole, S. Solomon, D.W. Fahey, K.K. Kelly, M.H. Proffitt, W.H. Brune, M. Loewenstein, and K.R. Chan, Calculations of ozone destruction during the 1988/89 Arctic winter, *Geophys. Res. Lett.*, *17*, 553-556, 1990.
- McPeters, R.D., and G.J. Labow, An assessment of the accuracy of 14.5 years of Nimbus 7 TOMS Version 7 ozone data by comparison with the Dobson Network, *Geophys. Res. Lett.*, *23*, 3695-3698, 1996.
- McPeters, R.D., P.K. Bhartia, A.J. Krueger, J.R. Herman, B. Schlesinger, C.G. Wellemeyer, C.J. Seftor, G. Jaross, S.L. Taylor, T. Swissler, O. Torres, G. Labow, W. Byerly, and R.P. Cebula, *Nimbus 7 Total Ozone Mapping Spectrometer (TOMS) Data Protocol User's Guide*, NASA Ref. Publ. 1384, National Aeronautics and Space Administration, Washington, D.C., 1996.
- Meetham, A.R., The correlation of the amount of ozone with other characteristics of the atmosphere, *Quart. J. Roy. Meteorol. Soc.*, *63*, 289-307, 1937.
- Müller, R., P.J. Crutzen, J.-U. Groöb, C. Brühl, J.M. Russell III, and A.F. Tuck, Chlorine activation and ozone depletion in the Arctic vortex: Observations by HALOE on UARS, *J. Geophys. Res.*, *101*, 12531-12554, 1996.
- Müller, R., J.-U. Groöb, D.S. McKenna, P.J. Crutzen, C. Brühl, J.M. Russell III, and A.F. Tuck, HALOE observations of the vertical structure of chemical ozone depletion in the Arctic vortex during winter and early spring 1996-1997, *Geophys. Res. Lett.*, *24*, 2717-2720, 1997a.
- Müller, R., P.J. Crutzen, J.-U. Groöb, C. Brühl, J.M. Russell III, H. Gernandt, D.S. McKenna, and A.F. Tuck, Severe chemical ozone loss in the Arctic during the winter of 1995-96, *Nature*, *389*, 709-712, 1997b.

- Müller, R., P.J. Crutzen, J.-U. Groö, C. Brühl, H. Gernandt, J.M. Russell III, and A.F. Tuck, Chlorine activation and ozone depletion in the Arctic stratospheric vortex during the first five winters of HALOE observations on the UARS, in *Atmospheric Ozone: Proceedings of the XVIII Quadrennial Ozone Symposium*, L'Aquila, Italy, 12-21 September 1996, edited by R.D. Bojkov and G. Visconti, pp. 225-229, Parco Scientifico e Tecnologico d'Abruzzo, L'Aquila, Italy, 1998.
- Neuendorffer, A.C., The decline in polar stratospheric ozone as observed by NOAA infrared satellites, in *Atmospheric Ozone, Proc. SPIE*, 2047, 100-113, 1993.
- Neuendorffer, A.C., Ozone monitoring with TIROS-N operational vertical sounders, *J. Geophys. Res.*, 101, 18807-18828, 1996.
- Newman, P., J.F. Gleason, R.D. McPeters, and R.S. Stolarski, Anomalous low ozone over the Arctic, *Geophys. Res. Lett.*, 24, 2689-2692, 1997.
- Pawson, S., and B. Naujokat, Trends in daily wintertime temperatures in the northern stratosphere, *Geophys. Res. Lett.*, 24, 575-578, 1997.
- Peters, D., and G. Entzian, On the longitude-dependent total ozone trend over the Atlantic-European region in boreal winter months, in *Atmospheric Ozone: Proceedings of the XVIII Quadrennial Ozone Symposium*, L'Aquila, Italy, 12-21 September 1996, edited by R.D. Bojkov and G. Visconti, pp. 69-72, Parco Scientifico e Tecnologico d'Abruzzo, L'Aquila, Italy, 1998.
- Plumb, R.A., and R.C. Bell, A model of the quasi-biennial oscillation on an equatorial beta-plane, *Quart. J. Roy. Meteorol. Soc.*, 108, 335-352, 1982.
- Portmann, R.W., S. Solomon, R.R. Garcia, L.W. Thomason, L.R. Poole, and M.P. McCormick, Role of aerosol variations in anthropogenic ozone depletion in the polar regions, *J. Geophys. Res.*, 101, 22991-23006, 1996.
- Proffitt, M.H., J.J. Margitan, K.K. Kelly, M. Lowenstein, J.R. Podolske, and K.R. Chan, Ozone loss in the Arctic polar vortex inferred from high-altitude aircraft measurements, *Nature*, 347, 31-36, 1990.
- Proffitt, M.H., K. Aikin, J.J. Margitan, M. Lowenstein, J.R. Podolske, A. Weaver, K.R. Chan, H. Fast, and J.W. Elkins, Ozone loss inside the northern polar vortex during the 1991-1992 winter, *Science*, 261, 1150-1154, 1993.
- Randel, W.J., and J.B. Cobb, Coherent variations of monthly mean total ozone and lower stratospheric temperature, *J. Geophys. Res.*, 99, 5433-5447, 1994.
- Randel, W.J., and F. Wu, Isolation of the ozone QBO in SAGE II data by singular-value decomposition, *J. Atmos. Sci.*, 53, 2546-2559, 1996.
- Randel, W.J., F. Wu, J.M. Russell III, J.W. Waters, and L. Froidevaux, Ozone and temperature changes in the stratosphere following the eruption of Mount Pinatubo, *J. Geophys. Res.*, 100, 16753-16764, 1995.
- Reed, R.J., The present status of the 26 month oscillation, *Bull. Am. Meteorol. Soc.*, 46, 374-387, 1965.
- Rex, M.R., N.R.P. Harris, P. von der Gathen, R. Lehmann, G.O. Braathen, E. Reimer, A. Beck, M.P. Chipperfield, R. Alfier, M. Allaart, F. O'Connor, H. Dier, V. Dorokhov, H. Fast, M. Gil, E. Kyrö, Z. Litynska, I.S. Mikkelsen, M.G. Molyneux, H. Nakane, J. Notholt, M. Rummukainen, P. Viatte, and J. Wenger, Prolonged stratospheric ozone loss in the 1995-96 Arctic winter, *Nature*, 389, 835-838, 1997.
- Russell, J.M. III, L.L. Gordley, J.H. Park, S.R. Drayson, D.H. Hesketh, R.J. Cicerone, A.F. Tuck, J.E. Frederick, J.E. Harries, and P.J. Crutzen, The Halogen Occultation Experiment, *J. Geophys. Res.*, 98, 10777-10797, 1993.
- Sahai, Y., V.W.J.H. Kirchoff, R.D. McPeters, F. Zamorano, C. Casicca, and N.R. Teixeira, Total ozone trends in Brazilian stations, in *Atmospheric Ozone: Proceedings of the XVIII Quadrennial Ozone Symposium*, L'Aquila, Italy, 12-21 September 1996, edited by R.D. Bojkov and G. Visconti, pp. 73-76, Parco Scientifico e Tecnologico d'Abruzzo, L'Aquila, Italy, 1998.
- Shiotani, M., Annual, quasi-biennial and El Niño-Southern Oscillation time scale variations in equatorial total ozone, *J. Geophys. Res.*, 97, 7625-7633, 1992.
- Solomon, S., Progress towards a quantitative understanding of Antarctic ozone depletion, *Nature*, 347, 347-354, 1990.
- Solomon, S., R.W. Portmann, R.R. Garcia, L.W. Thomason, L.R. Poole, and M.P. McCormick, The role of aerosol trends and variability in anthropogenic ozone depletion at northern midlatitudes, *J. Geophys. Res.*, 101, 6713-6727, 1996.

## OZONE TRENDS

- Stahelin, J., A. Renaud, J. Bader, R. McPeters, P. Viatte, B. Hoeffler, V. Bugnion, M. Giroud, and H. Schill, Total ozone series at Arosa (Switzerland): Homogenization and data comparison, *J. Geophys. Res.*, *103*, 5827-5841, 1998a.
- Stahelin, J., R. Kegel, and N.R.P. Harris, Trend analysis of the homogenized ozone series of Arosa (Switzerland), 1926-1996, *J. Geophys. Res.*, *103*, 8389-8399, 1998b.
- Stolarski, R., R.D. Bojkov, L. Bishop, C. Zerefos, J. Stahelin, and J. Zawodny, Measured trends in stratospheric ozone, *Science*, *256*, 343-349, 1992.
- Stolarski, R.S., G.J. Labow, and R.D. McPeters, Spring-time Antarctic total ozone measurements in the early 1970's from the BUV instrument on Nimbus 4, *Geophys. Res. Lett.*, *24*, 591-594, 1997.
- Trepte, C.R., and M.H. Hitchman, Tropical stratospheric circulation deduced from satellite aerosol data, *Nature*, *355*, 626-628, 1992.
- Tsvetkova, N.D., V.A. Yushkov, V.M. Dorokhov, and I.G. Zaitsev, Some results of measurements of vertical ozone distribution over Yakutsk during the 1995-96 winter/spring season, *Meteorol. Gidrol.*, *9*, 45-51, 1997.
- Uchino, O., R.D. Bojkov, D.S. Balis, K. Akagi, M. Hayashi, and R. Kajiwara, Essential characteristics of the Antarctic ozone decline, *Geophys. Res. Lett.*, submitted, 1998.
- von der Gathen, P., M. Rex, N.R.P. Harris, D. Lucic, G.M. Knudsen, G.O. Braathen, H. De Backer, R. Fabian, H. Fast, M. Gil, E. Kyrö, I.S. Mikkelsen, M. Rummukainen, J. Stähelin, and C. Varotsos, Observational evidence for chemical ozone depletion over the Arctic in winter 1991-92, *Nature*, *375*, 131-134, 1995.
- Wallace, J.M., and D.S. Gutzler, Teleconnections in the geopotential height field during the north hemisphere winter, *Mon. Wea. Rev.*, *109*, 784-812, 1981.
- Wang, H.J., D.M. Cunnold, and X. Bao, A critical analysis of SAGE ozone trends, *J. Geophys. Res.*, *101*, 12495-12514, 1996.
- Wege, K., and H. Claude, Über Zusammenhänge zwischen stratosphärischem Ozon und meteorologischen Parametern mit Folgerungen für die Zeiträume nach den Ausbrüchen von Chichón und Pinatubo, *Meteorol. Z.*, *6*, 73-87, 1997.
- WMO (World Meteorological Organization), *Report of the Meeting of Experts on Assessment of Performance Characteristics of Various Ozone Observing Systems*, Boulder, Colo., U.S., 28 July-2 August, 1980, Global Ozone Research and Monitoring Project—Report No. 9, Geneva, 1980.
- WMO (World Meteorological Organization), *Report of the International Ozone Trends Panel: 1988*, Global Ozone Research and Monitoring Project—Report No. 18, Geneva, 1990a.
- WMO (World Meteorological Organization), *Scientific Assessment of Stratospheric Ozone: 1989*, Global Ozone Research and Monitoring Project—Report No. 20, Geneva, 1990b.
- WMO (World Meteorological Organization), *Scientific Assessment of Ozone Depletion: 1991*, Global Ozone Research and Monitoring Project—Report No. 25, Geneva, 1992.
- WMO (World Meteorological Organization), *Handbook for Ozone Data Reevaluation*, Global Ozone Research and Monitoring Project—Report No. 29, Geneva, 1993.
- WMO (World Meteorological Organization), *Scientific Assessment of Ozone Depletion: 1994*, Global Ozone Research and Monitoring Project—Report No. 37, Geneva, 1995.
- WMO (World Meteorological Organization), *Atlas of GO3OS Total Ozone Maps for the Northern Hemisphere Winter-Spring of 1993-1994 and 1994-1995*, Global Ozone Research and Monitoring Project—Report No. 38, edited by R.D. Bojkov, and C.S. Zerefos, Geneva, 1996.
- WMO (World Meteorological Organization), *Atlas of GO3OS Total Ozone Maps for the Northern Hemisphere Winter-Spring of 1995-1996, 1996-1997*, Global Ozone Research and Monitoring Project—Report No. 39, edited by R.D. Bojkov and C.S. Zerefos, Geneva, 1997.
- WMO (World Meteorological Organization), *SPARC/IOC/GAW Assessment of Trends in the Vertical Distribution of Ozone*, edited by N. Harris, R. Hudson, and C. Phillips, SPARC Report No. 1, World Meteorological Organization Global Ozone Research and Monitoring Project—Report No. 43, Geneva, 1998.
- Yang, H., and K.K. Tung, On the phase propagation of extratropical ozone quasi-biennial oscillation in observational data, *J. Geophys. Res.*, *100*, 9091-9100, 1995.

- Yushkov, V., V. Dorokhov, V. Khattatov, A. Lukyanov, I. Zaitcev, N. Zvetkova, H. Nakane, H. Akiyoshi, and T. Ogawa, Evidence of ozone depletion over Yakutsk, Eastern Siberia, in 1995, in *Atmospheric Ozone: Proceedings of the XVIII Quadrennial Ozone Symposium*, L'Aquila, Italy, 12-21 September 1996, edited by R.D. Bojkov and G. Visconti, pp. 241-244, Parco Scientifico e Tecnologico d'Abruzzo, L'Aquila, Italy, 1998.
- Zerefos, C.S., A.F. Bais, T.C. Ziomias, and R.D. Bojkov, On the relative importance of quasi-biennial oscillation and El Niño/Southern Oscillation in the revised Dobson total ozone records, *J. Geophys. Res.*, 97, 10135-10144, 1992.
- Zerefos, C.S., K. Tourpali, and A.F. Bais, Further studies on possible volcanic signal to the ozone layer, *J. Geophys. Res.*, 99, 25741-25746, 1994.
- Zerefos, C.S., K. Tourpali, and A.F. Bais, Recent volcanic signals in the ozone layer, in *The Mount Pinatubo Eruption: Effect on the Atmosphere and Climate*, NATO ASI Series I, Vol. 142, edited by G. Fiocco, D. Fua, and G. Visconti, pp. 211-216, Springer-Verlag, Berlin, 1996.
- Zerefos, C.S., K. Tourpali, B.R. Bojkov, D.S. Balis, B. Rognerud, and I.S.A. Isaksen, Solar activity-total column ozone relationships: Observations and model studies with heterogeneous chemistry, *J. Geophys. Res.*, 102, 1561-1569, 1997.
- Zerefos, C.S., K. Tourpali, I.S.A. Isaksen, B. Rognerud, B.R. Bojkov, and C.J.E. Schuurmans, The solar output and total ozone, in *Atmospheric Ozone: Proceedings of the XVIII Quadrennial Ozone Symposium*, L'Aquila, Italy, 12-21 September 1996, edited by R.D. Bojkov and G. Visconti, pp. 279-282, Parco Scientifico e Tecnologico d'Abruzzo, L'Aquila, Italy, 1998.
- Ziemke, J.R., S. Chandra, R.D. McPeters, and P.A. Newman, Dynamical proxies of column ozone with applications to global trend models, *J. Geophys. Res.*, 102, 6117-6129, 1997.